let. - vol. 48 (2002) št. - no.

STROJNIŠKI VESTNIK

JOURNAL OF MECHANICAL ENGINEERING

strani - pages 243 - 300

ISSN 0039-2480 . Stroj V . STJVAX

cena 800 SIT

1. Tokovne razmere v avtomobilski lakirnici: numerična in eksperimentalna analiza
lo Conditions in an Automotive Spray-Paint Chamber: Numerical and Experimental Analyses

2. Računski model za preračun upogibne trdnosti zobnikov
A Computational Model for Calculating the ending-Load Capacity of ears

3. Naprava s pnevmatično aktivno površino: Tehnike krmiljenja lege togih objektov s povratno zvezo in brez nje
A Pneumatic Active-Surface Device: Open- and Closed-loop Control-Positioning Techni ues for Rigid Objects

4. Prispevek k obvladovanju neuravnoteženosti krempljastih polov alternatorjev
A Contribution to the Unbalance Control of Cla Poles for Automotive Alternators

9 770039 248001

© Strojniški vestnik 48(2002)5,243
Mesečnik
ISSN 0039-2480

© Journal of Mechanical Engineering 48(2002)5,243
Published monthly
ISSN 0039-2480

Vsebina
Contents

Strojniški vestnik - Journal of Mechanical Engineering
letnik - volume 48, (2002), številka - number 5

Razprave

Marn, J., Žunič, Z., Ramak, M., Ternik, P.: Tokovne razmere v avtomobilski lakirnici: numerična in eksperimentalna analiza 244

Glodež, S., Flašker, J., Jelaska, D., Kramberger, J.: Računski model za preračun upogibne trdnosti zobnikov 257

Uran, S., Šafarič, R.: Naprava s pnevmatično aktivno površino: Tehnike krmiljenja lege togih objektov s povratno zvezo in brez nje 267

Nastran, M., Krušič, V., Boltežar, M.: Prispevek k obvladovanju neuravnoteženosti krempljastih polov alternatorjev 283

Poročila 295

Strokovna literatura 296

Osebne vesti 298

Navodila avtorjem 299

Papers

Marn, J., Žunič, Z., Ramak, M., Ternik, P.: Flow Conditions in an Automotive Spray-Paint Chamber: Numerical and Experimental Analyses 244

Glodež, S., Flašker, J., Jelaska, D., Kramberger, J.: A Computational Model for Calculating the Bending-Load Capacity of Gears 257

Uran, S., Šafarič, R.: A Pneumatic Active-Surface Device: Open- and Closed-loop Control-Positioning Techniques for Rigid Objects 267

Nastran, M., Krušič, V., Boltežar, M.: A Contribution to the Unbalance Control of Claw Poles for Automotive Alternators 283

Reports 295

Professional Literature 296

Personal Events 298

Instructions for Authors 299

© Strojniški vestnik 48(2002)5,244-256
ISSN 0039-2480
UDK 667.644.3:532.525:519.61/.64
Izvrini znanstveni članek (1.01)

© Journal of Mechanical Engineering 48(2002)5,244-256
ISSN 0039-2480
UDC 667.644.3:532.525:519.61/.64
Original scientific paper (1.01)

Tokovne razmere v avtomobilski lakirnici: numerična in eksperimentalna analiza

Flow Conditions in an Automotive Spray-Paint Chamber: Numerical and Experimental Analyses

Jure Marn - Zoran Žunič - Matjaž Ramšak - Primož Ternik

V prispevku smo analizirali tokovne razmere v avtomobilski lakirni komori. Za reševanje Navier-Stokesovih enačb prostorskega toka nestisljive izotermne tekočine smo uporabili metodo nadzornih prostornin (CFX 5.4). Podrobno smo opisali potek izračuna, uporabljene robne in začetne pogoje, uporabljene metode za stabilizacijo numeričnih nihanj ter druge parametre, pomembne za izračun. Predstavili smo rezultate za ravninski in prostorski primer izračuna. Robni pogoji so bili določeni z meritvami na realni komori in to za primer brez avtomobila in z njim. Filter komore je bil upoštevan kot porozna snov s kvadratno funkcijo upora po podatkih proizvajalca, ki smo jih preverili z lastnimi meritvami padca tlakov.

(Ključne besede: komore lakirne, dinamika tekočin, analize numerične, turbulenca)

This paper deals with the flow analysis around a car in a spray-paint chamber. To solve the Navier-Stokes equations for 3D flow of an incompressible and isothermal fluid we used the control-volume method (CFX 5.4). The numerical procedure, the boundary and initial conditions, the methods used for stabilizing the numerical oscillations as well as the other parameters important for the numerical procedure are described in detail. Results for 2D and 3D calculations are presented. The boundary conditions were determined with measurements in a real chamber with and without a car. The filter in the chamber was considered to be porous matter with a quadratic law of resistance, this is in accordance with the manufacturer's data that were verified with pressure-loss measurements.

(Keywords: spray-paint chamber, fluid dynamic, numerical analysis, turbulence)

0 UVOD IN SPODBUDA ZA DELO

V pričujočem prispevku smo se ukvarjali z analizo toka okoli avtomobila v lakirnici. Med lakiranjem je zelo pomembno, da zrak teče okoli avtomobila kar se da mirno, s čim manjšimi vrtinci, še zlasti pa se želimo izogniti recirkulacijskim conam, kjer bi zaradi pojavov vrtinčenja in zato ponovnega dviga prahu lahko prišlo do usedanja prašnih delcev na sveže pobarvane dele avtomobilske karoserije, s tem pa do napak pri lakiranju.

Analizo bi bilo moč opraviti na dva načina. Pri prvem bi se lahko naslonili na eksperimentalno analizo, pri kateri bi na določene točke v lakirnici postavili dimne vire in opazovali tirnice dimnih delcev skozi lakirnico. Težava pri takem postopku bi bila v omejeni uporabi, saj bi lahko ugotovili recirkulacijske cone le za določen tip vozila in za določene robne pogoje, in v nenatančnosti, saj bi se lahko zgodilo, da bi zgrešili kako recirkulacijsko območje. Drugi način je numerična analiza, pri kateri

0 INTRODUCTION AND MOTIVATION FOR THE WORK

In this paper we have analyzed the flow around a car in a spray-paint chamber. During the process of lacquering it is very important that the air flows around the car as smoothly as possible, generating the smallest eddies possible. However, most importantly, we wish to avoid recirculation zones, where curling and the resulting dust raising could cause the deposition of dust particles on the freshly painted car body, which eventually means a degradation of the paint quality.

An analysis could be performed in two ways. First, we could use an experimental analysis that involved mounting smoke sources at certain points in the lacquer chamber and the observing the path of the smoke particles through the lacquer chamber. The disadvantage of this approach is in its limited application: the recirculating zones can only be observed for a certain type of car and for certain boundary conditions, and there is also the uncertainty that would arise because we could overlook some recirculating

lahko robne pogoje spreminjamo, prav tako tudi geometrijsko obliko. Tak način je preprostejši, ker modeliramo večino geometrijskih parametrov le prvič, nato pa spreminjamo vstopne in izstopne pogoje ter ugotavljamo spremembe.

Poleg želje po določitvi recirkulacijskih območij smo želeli še zlasti prikazati, kako je moč primerno uporabiti sedanja orodja računalniške dinamike tekočin in hkrati eksperimentalno določiti robne pogoje. Prav ti v primeru uveljavljenih orodij, npr. CFX, katerih ovrednotenje in preveritev sta bili že opravljeni, pogosto določajo kakovost rezultatov.

0.1 Opis lakirnice

V obravnavanem primeru gre za lakirnico dolžine 5880 mm, širine 3560 mm in največje višine 2480 mm. Zrak vstopa v lakirnico s stropa in izstopa v okolico skozi talno rešetko dolžine 4000 mm in širine 3000 mm ter nato v kanal na dnu lakirnice. Kanal vodi na prosto skozi izpust zraka prizmatične oblike širine 1000 mm, višine 860 mm in pri vrhu globine 650 mm, pri čemer je izpust zavarovan z izpustno rešetko z žaluzijami. Talna rešetka je prekrita s filtri debeline 50 mm, ki barvi, razpršeni v zraku, preprečujejo izstop v okolico in onesnaženje.

Ventilator in grelnik zraka za to analizo nista bila pomembna, zato njunih tehničnih podatkov ne navajamo.

1 MERITVE

V sami lakirnici smo opravili dvoje vrst meritev, in sicer meritve zaradi določitve robnih pogojev in meritve zaradi določitev snovskih lastnosti filtra. Kakor je bilo že zapisano, je bil končni cilj zastavljene naloge numerična analiza toka okoli avtomobila v lakirnici z željo, da bi določili morebitne recirkulacijske cone. Taka numerična analiza je neprimerno hitrejša in cenejša od meritev v vseh pomembnih točkah okoli avtomobila, poleg tega pa ni nasilna, je pa po naših izkušnjah odvisna zlasti od določitve robnih in začetnih pogojev ter snovskih lastnosti.

1.1 Opis meritev robnih pogojev

V prvem delu raziskav za določitev robnih pogojev smo izvedli meritve hitrosti v osmih točkah ob stropu vstopnega dela, ki so prikazane na sliki 1.

Meritve smo opravili v dveh razporedih, brez avtomobila in z njim, pri čemer nismo pričakovali bistvenih razlik med posameznimi rezultati. Vsako od meritev smo opravili po dvakrat, da bi zmanjšali velikost napak.

Meritve smo opravili z ročnim merilnikom z vročo žičko. Merilnik smo pred izvajanjem meritev

zones. Second, we can take advantage of numerical analysis where we can modify the boundary and initial conditions as well as the geometry. This approach is simpler because we model most of the geometrical parameters only once, and then by modifying the inlet and outlet conditions we can follow the changes.

In addition to determining the recirculating zones we particularly wanted to present the use of existing numerical tools and to experimentally determine the boundary conditions. In the case of well-known programs, in our case CFX, which were validated and verified, it is the boundary conditions that suggest the results' quality.

0.1 Spray-paint chamber

The spray-paint chamber is 5,880 mm in length, 3,560 mm in width and has a maximum height of 2,480 mm. Air enters the chamber from the ceiling and exits through the floor grid which is 4,000 mm in length and 3,000 mm in width, and then flows into the channel below the chamber. The channel leads to the outside through the prismatic opening that is 1,000 mm wide, 860 mm high and 650 mm deep. The outlet is secured with a shuttered grid. The floor grid is covered with a 50-mm-thick filter that prevents the dispersed paint from polluting the environment.

The ventilator and the air heater are not important for this analysis and therefore we do not give any technical specifications for them.

1 MEASUREMENTS

In the spray-paint chamber we performed two kinds of measurements: measurements for determining the boundary conditions and measurements for determining the filter properties. As already stated, we wanted to perform a numerical simulation of the flow around a car in a spray-paint chamber and determine the recirculation zones. A numerical analysis is much faster and cheaper than measurements at all the important points around the car, and more over, it is a non-invasive procedure. We also believe that the numerical analysis plays an important role in determining the boundary and initial conditions as well as the physical properties.

1.1 Description of the boundary-conditions measurement

In the first part of our analysis we measured the velocity at eight points in the inlet region (Figure 1).

The measurements were made with and without a car. We did not expect significant differences for particular results. Each measurement was performed twice in order to reduce the magnitude of the errors.

The measurements were made with a manual hot-wire anemometer. The instrument was calibrated

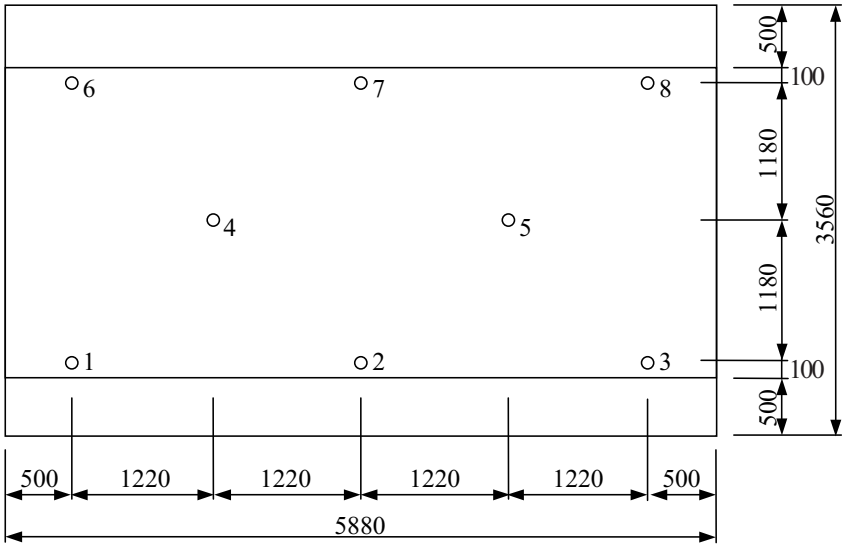

Sl. 1. *Merilne točke v lakirni komori (izmere v mm)*
Fig. 1. *Measurement points in spray-paint chamber (dimensions in mm)*

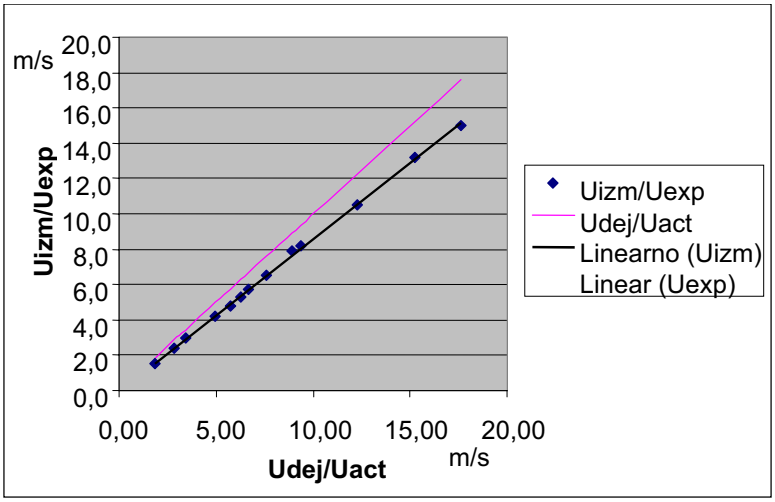

Sl. 2. *Napaka ročnega merilnika hitrosti z vročo nitko glede na primerjalno hitrost*
Fig. 2. *Error of manual hot-wire anemometer according to reference velocity*

umerili na testni progi iz plastičnih cevi premera 120 mm, v katerega smo tlačili zrak skozi cev z uporabo aksialno-radialnega ventilatorja IMP. Proga je opremljena s Pitotovo cevjo, dinamični tlak in padec tlaka pa smo izmerili z manometrom BETZ natančnosti 1 Pa. Meritve smo opravili med 2,1 m/s in 8,0 m/s ter ugotovili natančnost nitke med +1,50% in +4%. Ugotovimo lahko torej, da je v merilnem območju natančnost merilnika +4%, natančnejši rezultati pa so prikazani na sliki 2.

Opravili smo tudi meritve pri vhodu v merilno komoro in ugotovili, da je puščanje zraka iz lakirne komore zanemarljivo, vsekakor pa znotraj merilne negotovosti merilnega instrumenta. Zato smo predpostavili, da ves zrak vstopa pri vrhu in izstopa pri dnu. Prav tako smo predpostavili, da so vrednosti vstopnih hitrosti pri vrhu linearno interpolirane med posameznimi merilnimi točkami.

in a test line made of plastic pipes with a diameter of 120 mm that was fed with air by means of an IMP axial-radial ventilator. The line was equipped with a Pitot pipe, the dynamic pressure and the pressure drop were measured with a BETZ manometer of accuracy 1 Pa. The measurements were performed between 2.1 m/s and 8.0 m/s, and the determined accuracy of a hot wire is between +1.5% and +4%. We can conclude that in the selected measurement range the precision of the data is within +4%. More detailed results are presented in Figure 2.

The measurements at the inlet of the spray-paint chamber indicated that any leakage of air from the spray-paint chamber is negligible and still within the measurement uncertainty of the instrument. We supposed that the air enters at the top and leaves at the bottom. We also assumed that all the values of the inlet velocities at the top are linearly interpolated between the particular measurement points.

1.2 Opis in rezultati meritev padca tlaka skozi filter

Kakor smo že zapisali, je bila talna rešetka prekrita s filtrom debeline 50 mm. V dejanskem primeru je bil uporabljen filter KONUS KOFIL KFS 50, za katerega je proizvajalec v svoji specifikaciji podal tri merilne točke upora v odvisnosti od hitrosti zraka, ki teče skozi filter. Te podatke smo želeli laboratorijsko preveriti. Uporabljena merilna proga je bila enaka tisti, uporabljeni za umerjanje ročnega merilnika hitrosti, na slikah 3 in 4 pa so prikazani rezultati.

1.2 Description and measurements results of the pressure drop through the filter

The lattice was covered with a 50-mm-thick filter. In the real process a KONUS KOFIL KFS 50 filter was used, for which the manufacturer, in its specification, gave three points of resistance depending on the air speed flowing through the filter. These data were experimentally examined. The measurement lane was the same as the one used for calibrating the manual velocity measurer, the results are shown in Figures 3 and 4.

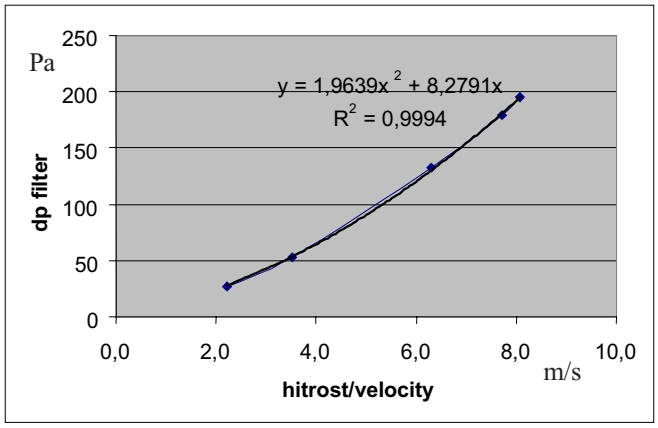

Sl. 3. *Tlačni padec skozi filter kot funkcija hitrosti zraka*
Fig. 3. *Pressure drop through filter as a function of air speed*

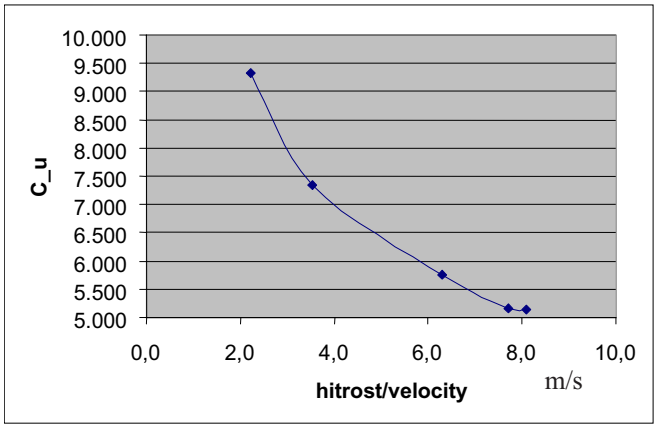

Sl. 4. *Količnik upora filtra kot funkcija hitrosti*
Fig. 4. *Resistance coefficient of filter as a function of velocity*

1.3 Rezultati meritev robnih pogojev na vstopu in izstopu

V postopku izvedbe meritev robnih pogojev na vstopu smo izvedli štiri nize preskusov brez avtomobila in dva niza preskusov z njim v vsaki od točk, da bi zmanjšali vpliv napak. Rezultati so prikazani v preglednicah 1 (brez avtomobila) in 2 (z avtomobilom). V vsaki točki je prikazano tudi odstopanje od srednje vrednosti.

Izmerili smo tudi profil hitrosti na izhodu, a smo imeli zaradi izstopnih žaluzij težave z razlago rezultatov. Lega žaluzij namreč povzroča, da tok zraka periodično

1.3 Results of the boundary conditions during inlet and outlet measurements

When measuring the boundary conditions at the inlet, four sets of experiments with the car and two sets of experiments without the car were performed. The goal was to reduce the influence of experimental errors. The results are shown in Table 1 (without the car) and Table 2 (with the car). For each experimental point the deviation about the mean is also shown.

We have also measured the velocity profiles at the outlet, but the grid shuttles caused problems with the interpretation of the results. The position of

Preglednica 1. *Hitrost zraka v m/s v posamezni merilni točki na vstopu v komoro brez avtomobila*
Table 1. *Air velocity in m/s at a particular measurement point for the chamber inlet without car*

	I	II	III	IV
1	0,32	0,35	0,32	0,35
2	0,28	0,38	0,38	0,28
3	0,40	0,38	0,35	0,40
4	0,38	0,48	0,42	0,42
5	0,28	0,25	0,28	0,30
6	0,38	0,40	0,40	0,35
7	0,40	0,32	0,35	0,40
8	0,38	0,35	0,35	0,35
Povprečje/Average	0,3525	0,3638	0,3563	0,3563
Odstopanje/Deviation	0,0444	0,0463	0,0328	0,0378

Preglednica 2. *Hitrosti zraka v m/s v posamezni merilni točki na vstopu v komoro z avtomobilom*
Table 2. *Air velocity in m/s at a particular measurement point for the chamber inlet with car*

	I	II
1	0,41	0,4
2	0,28	0,4
3	0,42	0,35
4	0,38	0,38
5	0,28	0,28
6	0,32	0,4
7	0,48	0,4
8	0,28	0,35
Povprečje/Average	0,3563	0,3700
Odstopanje/Deviation	0,0663	0,0325

spreminja hitrost, saj žaluzije tok usmerjajo in se za njimi ustvarjajo cone recirkulacije. Tako smo rezultate uporabili zgolj za oceno pravilnosti izračunanega masnega toka zraka na izstopu.

1.4 Merilna negotovost

1.4.1 Osnove za izračun merilne negotovosti

Dinamični tlak na Pitotovi cevi in padec tlaka na filtru merimo z Betzovim manometrom, katerega natančnost je ocenjena na 1Pa. Pri tem je ločljivost skale Betzovega manometra 0,1mm.

Hitrost zraka izračunamo z Bernoullijevo enačbo:

$$v = \sqrt{\frac{2 \cdot p_d}{\rho}} \qquad (1),$$

kjer je:
p_d - dinamični tlak na Pitotovi cevi,
$\rho = 1{,}164\ \mathrm{kg/m^3}$ - gostota zraka pri $T = 20°\mathrm{C}$.

Koeficient upora filtra C_u izračunamo z uporabo izraza za lokalne izgube:

$$C_u = \frac{2 \cdot \Delta p}{\rho \cdot v^2} \qquad (2),$$

kjer je:
Δp - padec tlaka na filtru.

the shuttles causes periodically changing velocities due to the influence of the shuttles on the direction of the flow. Velocity profiles were therefore only used for a verification of the mass flow through the outlet.

1.4 Measurement uncertainty

1.4.1 Basics of measurement uncertainty calculation

The dynamic pressure at the Pitot pipe and pressure drop through the filter are measured with the BETZ manometer. The scale resolution of the BETZ manometer is 0.1 mm.

The air speed is determined from Bernoulli's equation as:

$$v = \sqrt{\frac{2 \cdot p_d}{\rho}} \qquad (1),$$

where:
p_d - dynamic pressure at the Pitot pipe
$\rho = 1.164\ \mathrm{kg/m^3}$ - density of air at $T = 20°\mathrm{C}$.

The resistance coefficient C_u is determined with the equation for local pressure losses:

$$C_u = \frac{2 \cdot \Delta p}{\rho \cdot v^2} \qquad (2),$$

where:
Δp - pressure drop through the filter.

Preglednica 3. *Rezultati meritev*
Table 3. *Results of measurements*

točka point	p_d Pitot (Pa)	Δp filter (Pa)	v Pitot (m/s)	v anem (m/s)	Cu filter
1	2,94	27,41	2,25	2,30	9,33
2	7,34	53,85	3,55	3,60	7,33
3	23,50	135,11	6,35	6,40	5,75
4	35,25	182,10	7,78	8,00	5,17
5	38,67	198,74	8,15	8,40	5,14

1.4.2 Določitev merilne negotovosti

Ker je standardna merilna negotovost posredno merjene veličine:

$$u(y) = \sqrt{\sum_{i=1}^{M} \left(\frac{\partial f}{\partial x_i} \right)^2 \cdot u^2(x_i)} \tag{3}$$

lahko ob upoštevanju, da je $u(\rho) = 0$, zapišemo skupno standardno merilno negotovost hitrosti zraka:

$$u(v) = \sqrt{\left(\frac{\partial v}{p_d} \right)^2 \cdot u^2(p_d)} = \sqrt{\left(\frac{1}{2 \cdot \rho \cdot p_d} \right) \cdot u^2(p_d)} \tag{4}$$

in količnika upora:

$$u(C_u) = \sqrt{\left(\frac{\partial C_u}{\partial \Delta p} \right)^2 \cdot u^2(\Delta p) + \left(\frac{\partial C_u}{\partial v} \right)^2 \cdot u^2(v)} = \sqrt{\left(\frac{2}{\rho \cdot v^2} \right)^2 \cdot u^2(\Delta p) + \left(-\frac{4 \cdot \Delta p}{\rho \cdot v^3} \right)^2 \cdot u^2(v)} \tag{5}.$$

Ker je $u(\Delta p) = u(p_d) = u_B(p_d)$ (meritev izvedena le enkrat), sta posamezni merilni negotovosti:

$$u(v) = \sqrt{\left(\frac{1}{2 \cdot \rho \cdot p_d} \right) \cdot u_B^2(p_d)} \tag{6}$$

in

$$u(C_u) = \sqrt{\left(\frac{2}{\rho \cdot v^2} \right)^2 \cdot u_B^2(\Delta p) + \left(-\frac{4 \cdot \Delta p}{\rho \cdot v^3} \right)^2 \cdot \left(\frac{1}{2 \cdot \rho \cdot p_d} \right) \cdot u_B^2(p_d)}. \tag{7}$$

Merilno negotovost tipa B Betzovega manometra določimo z upoštevanjem njegove natančnosti (1 Pa):

$$u_B'(p_d) = u_B'(\Delta p) = \frac{1Pa}{\sqrt{3}} = 0,577Pa \tag{8}$$

in ločljivosti skale (0,1 mm oz. 0,979 Pa):

$$u_B''(p_d) = u_B''(\Delta p) = \frac{0,979Pa}{\sqrt{3}} = 0,565Pa \tag{9}$$

kot

$$u_B(p_d) = u_B(\Delta p) = \sqrt{u_B'^2(p_d) + u_B''^2(p_d)} = 0,808Pa \tag{10}.$$

Rezultati vseh merilnih točk prikazuje preglednica 4.

Merilna negotovost samih meritev, ki so bili opravljeni na progi, je enaka merilni negotovosti tipa B, ki pa se ujema z merilno negotovostjo instrumenta.

1.4.2 Measurement-uncertainty determination

Considering that the combined standard uncertainty is:

and $u(\rho) = 0$, we can write the combined standard uncertainty of the air speed as:

and the coefficient of resistance as:

Because $u(\Delta p) = u(p_d) = u_B(p_d)$, we can write:

and:

The type B component of measurement uncertainty for the BETZ manometer is determined by considering its accuracy (1 Pa):

and scale resolution (0.1 mm, corresponding to 0.979 Pa):

as:

The results for all experimental points are shown in Table 4.

The measurement uncertainty of the measurements is equal to the type B component of the measurement uncertainty, which coincides with the measurement uncertainty of the instrument.

Preglednica 4. *Merilna negotovost u(v) in u(Cu)*
Table 4. *Measurement uncertainties u(v) and u(Cu)*

točka point	v Pitot (m/s)	u(v) (m/s)	Cu filter	u(Cu)
1	2,25	0,309	9,33	2,56
2	3,55	0,195	7,33	0,81
3	6,35	0,109	5,75	0,20
4	7,78	0,089	5,17	0,12
5	8,15	0,085	5,14	0,11

2 NUMERIČNA ANALIZA

2.1 Vodilne enačbe

Reševali smo splošno znane Reynoldsove povprečene Navier-Stokesove enačbe (RANS) za prostorski tok nestisljive izotermne tekočine:

$$\frac{\partial u_j}{\partial x_j} = 0 \tag{11},$$

$$\rho \frac{\partial u_i}{\partial t} + \rho u_j \frac{\partial u_i}{\partial x_j} = -\frac{\partial p}{\partial x_i} + \frac{\partial}{\partial x_i}\left[\mu \left(\frac{\partial u_i}{\partial x_j} + \frac{\partial u_j}{\partial x_i} \right) - \rho \overline{u_i' u_j'} \right] \tag{12},$$

kjer je u časovno povprečeni hitrostni vektor, x krajevni vektor, p časovno povprečeni tlak, ρ gostota, μ dinamična viskoznost in zadnji člen na desni strani enačbe zveza med hitrostnimi nihanji, ki jo imenujemo tudi Reynoldsov napetostni tenzor.

Za modeliranje Reynoldsovega napetostnega tenzorja uporabimo dvoenačbni model k-ε:

$$-\rho \overline{u_i' u_j'} = \mu_T \left(\frac{\partial u_i}{\partial x_j} + \frac{\partial u_j}{\partial x_i} \right) - \frac{2}{3} \rho \; k \delta_{ij} \tag{13},$$

$$\mu_T = c_\mu \rho \frac{k^2}{\varepsilon} \tag{14},$$

kjer je μ_T dinamična turbulentna viskoznost, k turbulentna kinetična energija, ε stopnja turbulentnega raztrosa, δ_{ij} Kroneckerjeva delta funkcija in c_m empirična konstanta z vrednostjo 0,09.

Za modeliranje izotropnega upora tekočine uporabimo kvadratni zakon upora. Izvirni člen S_M v gibalni enačbi se glasi:

$$S_i = -C_{R1} u_i - C_{R2} |u_i| \; u_i \tag{15},$$

kjer sta C_{R1} in C_{R2} koeficienta upora.

Zraven enačb (11) in (12) dobimo še dve prenosni enačbi za k in ε:

$$\rho \frac{\partial k}{\partial t} + \rho u_j \frac{\partial k}{\partial x_j} = \frac{\partial}{\partial x_j}\left(\mu + \frac{\mu_T}{\sigma_k} \frac{\partial k}{\partial x_j} \right) + P - \rho \varepsilon \tag{16},$$

$$\rho \frac{\partial \varepsilon}{\partial t} + \rho u_j \frac{\partial \varepsilon}{\partial x_j} = \frac{\partial}{\partial x_j}\left(\mu + \frac{\mu_T}{\sigma_\varepsilon} \frac{\partial \varepsilon}{\partial x_j} \right) + c_1 \frac{\varepsilon}{k} P - c_2 \rho \frac{\varepsilon^2}{k} \tag{17},$$

kjer sta σ_k in σ_ε turbulentni Prandtlovi števili za k in ε, c_1 in c_2 pa sta empirični konstanti. V našem primeru so imele konstante vrednost σ_k=1,0; σ_ε=1,3; c_1=1,44 in c_2=1,92.

2 NUMERICAL ANALYSIS

2.1 Leading equations

We were solving the generally known Reynolds' averaged Navier-Stokes equations (RANS) for the 3D flow of incompressible and isothermal flow:

(11), (12),

where u a is time-averaged velocity vector, x is a spatial vector, p is the time-averaged pressure, ρ is the density, μ is the dynamic viscosity and the last term on the right-hand side of the equation is the correlation between the velocity fluctuations, also known as the Reynolds stress tensor.

The Reynolds stress tensor is modeled with a two-equation k-ε model

(13), (14),

where μ_T is the dynamic turbulent viscosity, k is the turbulent kinetic energy, ε is the level of turbulent dissipation, δ_{ij} is Kronecker's delta function and c_m is the empirical constant with a value of 0.09.

The isotropic resistance of the fluid was modeled with the quadratic law of resistance. The source term S_M in the equation of motion is:

(15),

where C_{R1} and C_{R2} are resistance coefficients.

Besides equations (11) and (12) we obtain two transport equations for k and ε:

(16), (17),

where σ_k and σ_ε are turbulent Prandtl's numbers for k and ε, and c_1 and c_2 are empirical constants. In our case the values for the constants were σ_k=1.0, σ_ε=1.3, c_1=1.44 and c_2=1.92.

Člen P imenujemo produkcija in je definiran kot:

$$P = \mu_T \left(\frac{\partial u_i}{\partial x_j} + \frac{\partial u_j}{\partial x_i} \right) \frac{\partial u_i}{\partial x_j} \quad (18).$$

2.2 Postopek reševanja

Zgoraj opisane enačbe so bile po postopku nadzornih prostornin spremenjene v sistem algebrajskih enačb.

Sisteme linearnih enačb smo reševali na delno povezan način, kar pomeni, da so bile v eni iteraciji reševane kontinuitetna in tri gibalne enačbe, nato pa še ločeno enačbi za turbulentno kinetično energijo in turbulentnim raztrosom. Na tak način dosežemo kompromis med številom nelinearnih iteracij in potrebno količino pomnilnika za rešitev sistema enačb.

Za reševanje sistemov linearnih enačb smo uporabili algebrsko večmrežje z dodano popravo. Tako najbolje izkoristimo dejstvo, da diskretizirane enačbe pomenijo ohranitev bilance osnovnih spremenljivk v nadzorni prostornini. Enačbe redke mreže dobimo preprosto z združevanjem posameznih prostornin goste mreže. Z numeričnega vidika je večmrežje učinkovitejše kakor druge metode. Na dani mreži so lahko iterativni rešilniki učinkoviti le pri zmanjševanju napak, ki imajo valovne dolžine velikosti mreže. Slabše se obnesejo pri napakah z valovnimi dolžinami velikostnega reda računskega območja. Metoda večmrežja obide navedeno težavo z navideznim redčenjem osnovne mreže v postopku iterativnega reševanja sistema enačb, reševanjem enačbe za popravo na redki mreži in nato podaljšanje poprave nazaj na fino mrežo. Redka mreža je zmožna gladiti napake nižjih frekvenc kot fina mreža, tako da z nekaj nivoji redčenja osnovne mreže pokrijemo celoten frekvenčni spekter napak, kar ima za posledico boljšo konvergenco.

Za stabilizacijo konvektivnega člena smo uporabili protivetrno metodo prvega reda natančnosti. Zanjo smo se odločili predvsem zaradi njene numerične stabilnosti. Mogoče bi bilo uporabiti tudi višjeredno metodo popravek numerične korekcije, ki pa je zaradi možnega pojava numerične disperzije in večje porabe računalniškega časa nismo uporabili.

Viskozni podsloj, ki nastane ob steni pri turbulentnem toku modeliramo z uporabo posebnih zidnih elementov. V zidnih elementih uporabimo oblikovne funkcije, ki so posebej prirejene, da zajamejo strme spremembe osnovnih spremenljivk v viskoznem podsloju. Te funkcije temeljijo na splošnem "zidnem zakonu" in so odvisne od karakterističnih turbulentnih Reynoldsovih števil. Med iterativnim postopkom reševanja se spreminjajo, da bi čim bolje zajele lokalne razmere.

The term P is called production and is defined as:

2.2 Solving procedure

The above equations were transformed into a system of algebraic equations following the procedure of the control-volume method.

The systems of linear equations were solved in a partially coupled manner. In one iteration the continuity equation and three momentum equations were solved coupled, followed by the equations for turbulent kinetic energy and turbulent dissipation. This is the compromise between the number nonlinear iterations and the amount of computer memory required for solving a system of equations.

The selected system of linear equations was solved using the additive-correction algebraic multigrid method. This approach takes advantage of the fact that the discrete equations are representative of the balance of conserved quantities over a control volume. The coarse-mesh equations can be created by merging the original control volumes to create larger ones. From a numerical standpoint the multigrid approach offers a significant advantage. For a given mesh size, iterative solvers are only efficient at reducing errors that have a wavelength of the order of the mesh spacing. So, while shorter-wavelength errors disappear quite quickly, errors with longer wavelengths can take a very long time to disappear. The multigrid method bypasses this problem by coarsening the virtual mesh spacing during the course of the iterations, solving the equation for the coarse-mesh correction and then prolonging of the correction back to the finer mesh. The coarse-mesh smooths errors with lower frequencies, so with a few levels of coarsening we cover the whole range of error frequencies, which leads to a better convergence.

For stabilization of the convective term we used the upwind method of the first order of accuracy. The main reason for its application was its numerical stability and robustness. It could be possible to use the high-order NAC (numerical advection correction) method but we did not use it because of possible numerical dispersion.

The viscous sublayer that occurs near the wall when the flow is turbulent is modelled by using particular wall elements. In the wall elements we use shape functions that are arranged for the capture of the high primitive variables gradients in the viscous sublayer. These functions are based on a general law-of-the-wall and depend on characteristic turbulent Reynolds numbers. During an iterative procedure they change in order to better capture the local conditions.

Talni filter smo modelirali kot porozno snov s kvadratnim zakonom upora, pri čemer smo konstante modela določili po podatkih proizvajalca filtra.

2.3 Rezultati

2.3.1 Ravninski primer

V primeru ravninskega izračuna smo uporabili 72 846 elementov. Velikost elementov je znašala med 50 in 100 mm. Dobili smo sistem linearnih enačb z 19 872 neznankami. Za reševanje je bilo potrebno 49 MB (MB = 1024×1024 byte) pomnilnika.

Na vstopu smo predpisali vstopno hitrost. To hitrost smo predpisali kot povprečno vrednost v vseh merjenih točkah. Predpisali smo tudi privzete vrednosti turbulentne intenzivnosti ter mešalne dolžine (CFX 5.4). Na izstopu smo predpisali statični tlak. Predpisana natančnost reševanja je znašala 10^{-6} (kvadratna norma ostankov). Rešitev smo dobili po 90 iteracijah, za kar smo porabili 4383 s (73 min 3 s) procesorskega časa na delovni postaji Hewlett-Packard B1000. Na sliki 5 je prikazano diskretizirano območje.

The floor grid with the filter has been modelled as a porous region with the quadratic law of resistance, with the constants calculated using the filter manufacturer's data.

2.3 Results

2.3.1 2D problem

In the 2D calculation 72846 we used elements. The size of each element was between 50 and 100 mm. We were solving a system of linear equations with 19872 unknowns and we used 49 MB (MB=1024×1024 byte) of memory.

At the inlet the inlet velocity was prescribed. We prescribed it as an average value in all the points as discussed above. We also prescribed assumed values for the turbulent intensity and the mixed length (CFX 5.4). At the outlet the static pressure was prescribed. The prescribed numerical accuracy was 10^{-6} (root mean square of residuums). The solution was obtained after 90 iterations and it took 4383 s (73 min 3 s) of processor time on a Hewlett-Packard B1000 work station. Figure 5 shows the discretised area.

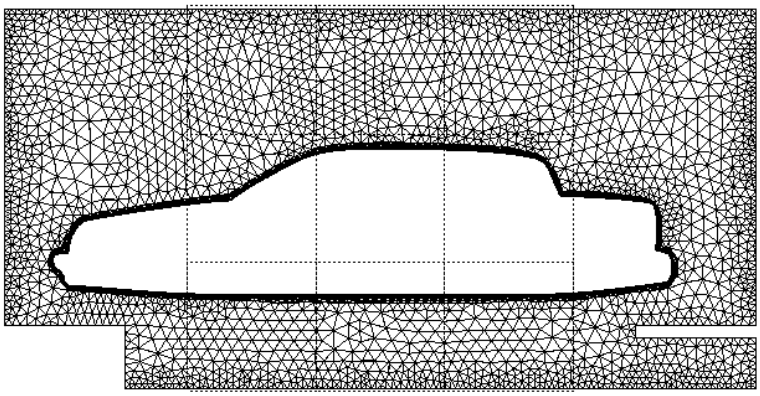

Sl. 5. *Diskretizirano območje*
Fig. 5. *Discretised area*

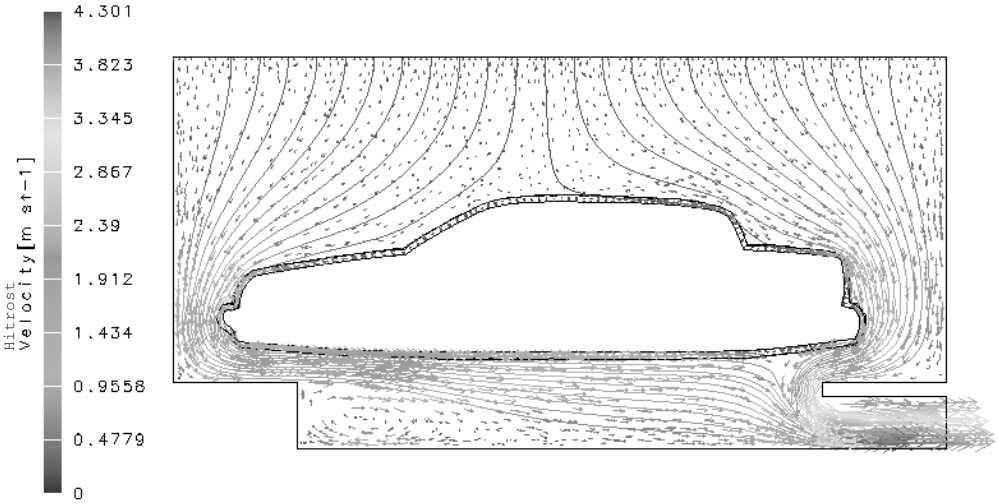

Sl. 6. *Hitrostno polje s tokovnicami*
Fig. 6. *Velocity field with stream lines*

Na sliki 6 je prikazan ravninski model avtomobila s prikazanimi vektorji hitrostnega polja in vrisanimi tokovnicami. Vidimo, da v tem, dvoizmernem primeru ne prihaja do recirkulacijskih območij v okolici avtomobila.

Na sliki 7 je prikazano polje turbulentne kinetične energije. Vidimo, da je stopnja kinetične energije v območju barvanja dokaj majhna, močno pa se poveča v izstopnem kanalu.

2.3.2 Prostorski primer

Na sliki 8 je prikazano diskretizirano območje z vrisanimi ploskovnimi elementi.

Za primere z avtomobili velikosti od 320 cm do 400 cm smo diskretizirali območje s 369620 do 355092 elementi (četverci). Velikost elementov je znašala 80 do 100 mm po površini avtomobila in komore ter 200 mm po območju. Razmerje velikosti med dvema sosednjima elementoma je bilo omejeno na 1.1. Mejno plast smo diskretizirali s tremi plastmi prizmatskih elementov. Za reševanje je bilo potrebno 190 MB pomnilnika.

Figure 6 shows the 2D model of a car with the velocity field vectors and stream lines. It can be seen that for the 2D case there are no recirculating zones.

Figure 7 shows the turbulent kinetic energy field. It can be seen that for the area of the painting it is relatively low but increases significantly in the outlet channel.

2.3.2 3D problem

Figure 8 shows the discretised area with the surface elements.

For cars with lengths between 320 cm and 400 cm the area was discretised with 369620–355092 elements (tetrahedrons). The size of the elements was set to 80–100 mm on the car body and the chamber walls' surface and 200 mm in the domain. The ratio of the size of the neighboring elements was limited to 1.1. The boundary layer was discretised with three layers of prismatic elements. For the solution of the problem 190 MB of computer memory was needed.

Sl. 7. *Turbulentna kinetična energija*
Fig. 7. *Turbulent kinetic energy*

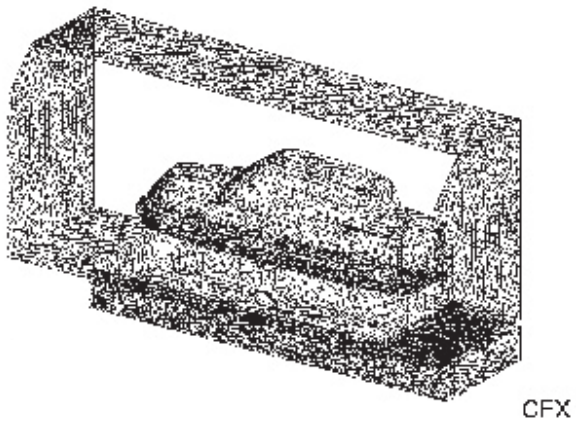

Sl. 8. *Diskretizirano območje prostorskega primera*
Fig. 8. *Discretised area of 3D example*

Na vstopu smo predpisali vstopno hitrost in privzete vrednosti turbulentne intenzivnosti ter mešalne dolžine (CFX 5.4). Na izstopu smo predpisali statični tlak. Zaradi simetričnosti območja smo modelirali samo polovico območja, na simetrijski ploskvi pa smo predpisali simetrijske robne pogoje. Kot začetne pogoje smo predpisali stanje mirovanja v območju ($v_x=v_y=v_z=0$). Predpisana natančnost reševanja je znašala 10^{-4} (kvadratna norma ostankov).

Rešitev smo dobili po 40 iteracijah, za kar smo porabili 7255 s (120 min 55 s) procesorskega časa na delovni postaji Hewlett-Packard B1000.

Na sliki 9 je prikazano hitrostno polje na simetrijski ploskvi in tlačno polje na površini avtomobila.

At the inlet the constant velocity and the default values of the turbulent intensity and the mixing length were prescribed (CFX 5.4). At the outlet the zero static pressure was prescribed. Due to the symmetrical domain only half of the chamber was discretised and symmetrical boundary conditions were prescribed. The initial condition was a zero velocity field ($v_x=v_y=v_z=0$). The prescribed convergence criterion was 10^{-4} (root mean square of residua).

The solution was obtained after 40 iterations and 7255 s (120 min 55 s) of CPU time on a Hewlett-Packard B1000 workstation.

Figure 9 shows the velocity field on a symmetry plane and the pressure field on the car-body surface.

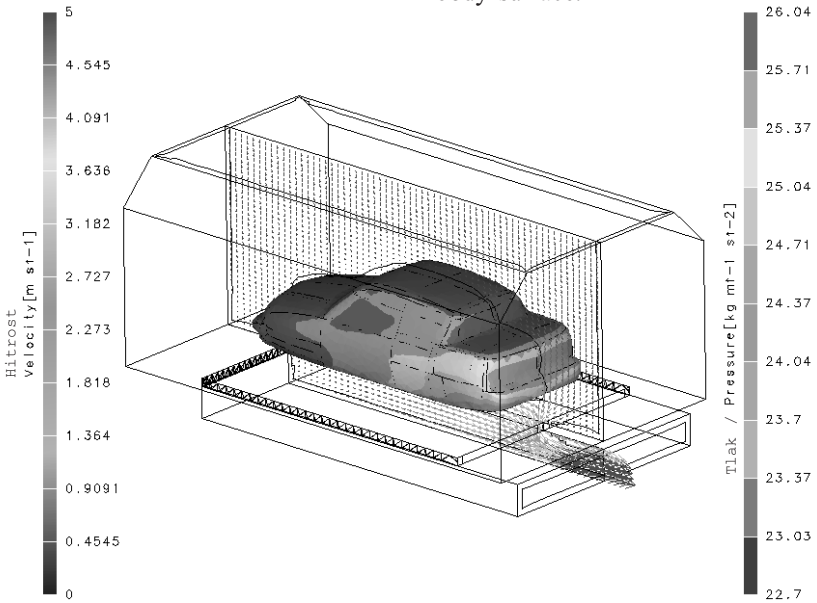

Sl. 9. *Hitrostno polje na simetrali in tlačno polje na površini avtomobila*
Fig. 9. *Velocity field on symmetry line and pressure field on a car*

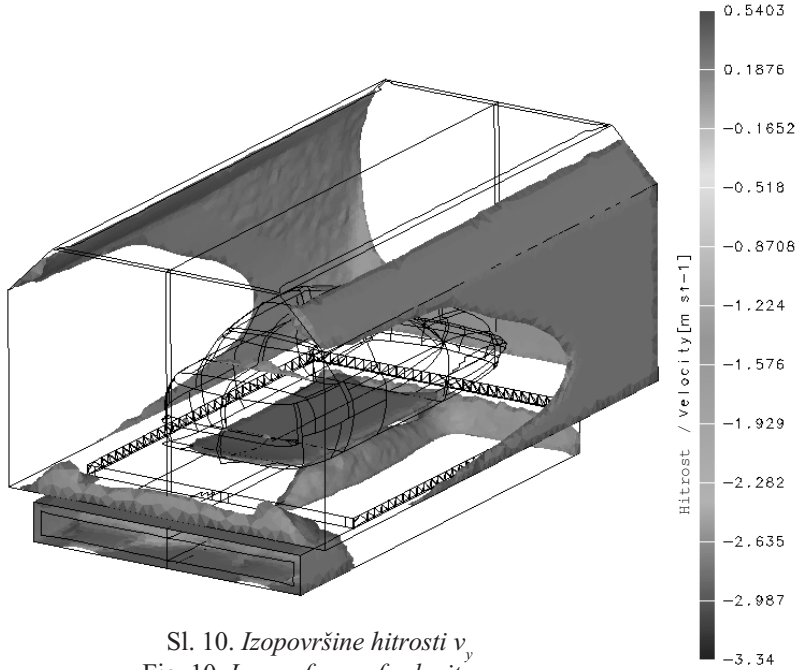

Sl. 10. *Izopovršine hitrosti* v_y
Fig. 10. *Iso-surfaces of velocity* v_y

Na sliki 10 so prikazane izopovršine hitrosti v_y, ki najbolj nazorno pokaže območja, kjer prihaja do povratnega toka (recirkulacij). Vidimo, da v okolici avtomobila ni večjih recirkulacijskih con. Po pričakovanju nastajajo manjši vrtinci v bližini sten in vogalov, kar pa na učinkovitost odvajanja barve v bližini avtomobilov ne vpliva.

Na sliki 11 so prikazane izopovršine turbulentne kinetične energije *k*, ki pove, kje so območja najbolj intenzivnega mešanja toka.

Figure 10 shows the isosurfaces of velocity v_y, which is the most illustrative way of showing zones with a recirculating flow. It can be seen that near the car-body surface no large recirculation zones exist. There are small eddies near the wall bottoms and corners as expected, but this does not have any influence on the efficiency of the painting fog removal.

Figure 11 shows the isosurface of turbulent kinetic energy *k*, which marks the areas of the most intensely mixed flow.

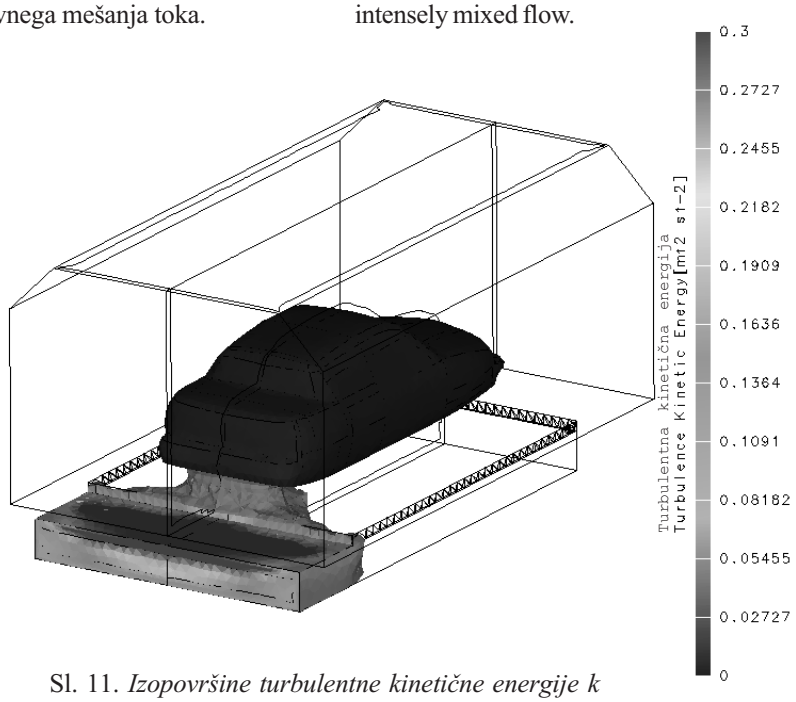

Sl. 11. *Izopovršine turbulentne kinetične energije k*
Fig. 11. *Iso-surfaces of turbulent kinetic energy k*

3 SKLEP

V prikazanem prispevku smo želeli povezati konkretno inženirsko vprašanje z metodološkim postopkom, ki omogoča preprosto spreminjanje vhodnih podatkov ter tako izdelavo variantnih rešitev brez večkratnega merjenja.

Najprej smo postavili računalniški triizmerni model lakirnice, v kateri smo želeli oceniti vpliv tokovnega polja na hrapavost nanesene barve, pri čemer smo hrapavost povezali z možnostjo recirkulacije zračnega toka. Predpostavka je nekoliko konzervativna, saj ni nujno, da vsaka recirkulacija povzroči nanos prašnih delcev, na drugi strani pa je malo verjetno, da bi prašni delci v odsotnosti recirkulacije s pomočjo difuzije napredovali proti toku zraka.

Robne pogoje smo postavili z meritvami. Izračune smo opravili z uporabo računalniškega paketa CFX in ugotovili, da v bližini realnega modela avtomobila recirkulacijskih con ni najti, kar ob upoštevanju prejšnje predpostavke pomeni, da od tega hrapavosti na lakiranih mestih avtomobila ni pričakovati.

Bistven dosežek prikazanega dela ni v končnem rezultatu in odgovoru na vprašanje glede

3 CONCLUSION

This paper deals with an engineering question and the answer based on a methodology involving a simple change of inlet parameters that gives an easy parametric analysis without repeated experiments.

First, a 3D computer model of a spray-paint chamber was built aiming to assess the influence of the fluid field on smoothness of the painted surface or better paint thereof whereas the coarseness of the painted surface was connected to recirculation of air flow. This is arguably a conservative assumption as the recirculation itself does not necessarily mean the deposition of dust particles on the painted surface.

The boundary conditions were set using measurements. The calculations were conducted using the CFX computer code and the results show that no recirculation zones were found, which means that the air flow around the vehicle should not cause the deposition of dust particles on the surface of the painted surfaces.

In itself, the final result was not the goal of this paper. The main task, i.e. showing that engineering

hrapavosti lakiranih mest na vozilu, temveč odgovor na vprašanje, da je tudi za inženirske analize in vprašanja moč uporabiti računalniško tehnologijo brez nepotrebnih poenostavitev ob uporabi meritev samo za natančno določitev robnih pogojev.

questions can be answered without undue simplification taking advantage of computer technology and relying on measurements only for as-realistic boundary conditions as possible, was in our opinion successfully achieved.

4 LITERATURA
4 REFERENCES

[1] CFX 5.4 Users manual (1999) *AEA Technology*.
[2] KOFIL, Prostorska filtracija, prospekt *Konus Konex d.o.o.*
[3] Ramšak, M., P. Ternik, J. Marn (2000) Meritev tlačnega padca za filter KONUS KOFIL KFS 50, Poročilo, Laboratorij za prenosne pojave v trdninah in tekočinah, *Fakulteta za strojništvo, Univerza v Mariboru*.
[4] Žunič, Z. (1997) Numerična obravnava problema aerodinamike vozil, Magistrsko delo, *Fakulteta za strojništvo, Univerza v Mariboru.*

Naslov avtorjev: prof.dr. Jure Marn
mag. Zoran Žunič
mag. Matjaž Ramšak
mag. Primož Ternik
Fakulteta za strojništvo
Univerze v Mariboru
Smetanova 17
2000 Maribor
jure.marn@uni-mb.si
zoran.zunic@uni-mb.si
matjaz.ramsak@uni-mb.si
primoz.ternik@uni-mb.si

Authors' Address: Prof.Dr. Jure Marn
Mag. Zoran Žunič
Mag. Matjaž Ramšak
Mag. Primož Ternik
Faculty of Mechanical Eng.
University of Maribor
Smetanova 17
2000 Maribor, Slovenia
jure.marn@uni-mb.si
zoran.zunic@uni-mb.si
matjaz.ramsak@uni-mb.si
primoz.ternik@uni-mb.si

Prejeto: 23.1.2002
Received:

Sprejeto: 23.5.2002
Accepted:

© Strojniški vestnik 48(2002)5,257-266
ISSN 0039-2480
UDK 621.833:539.388.1:620.178.3
Izvrini znanstveni članek (1.01)

© Journal of Mechanical Engineering 48(2002)5,257-266
ISSN 0039-2480
UDC 621.833:539.388.1:620.178.3
Original scientific paper (1.01)

Računski model za preračun upogibne trdnosti zobnikov

A Computational Model for Calculating the Bending-Load Capacity of Gears

Srečko Glodež - Jože Flašker - Damir Jelaska - Janez Kramberger

V prispevku je predstavljen računski model za določitev dobe trajanja zobnikov glede na trdnost v zobnem korenu. Potek utrujanja, ki vodi do zloma zoba v korenu, sestoji iz nastanka in širjenja utrujenostne razpoke. Za določitev potrebnega števila obremenitvenih ponovitev N_i za nastanek utrujenostne razpoke je uporabljen Coffin-Mansonov zakon, pri katerem je predpostavljeno, da je začetna razpoka locirana na mestu največjih napetosti v zobnem korenu. Za nadaljnje širjene razpoke je uporabljen znani Parisov zakon, pri katerem so potrebne materialne veličine določene poprej na podlagi ustreznih testnih preskušancev. Funkcijska odvisnost med faktorjem intenzivnosti napetosti in dolžino razpoke K=f(a), ki je potrebna za določitev potrebnega števila obremenitvenih ciklov N_p za razširitev razpoke od začetne do kritične dolžine, je izračunana numerično z metodo končnih elementov. Skupno število obremenitvenih ponovitev N za pojav končne poškodbe je vsota $N = N_i + N_p$. Čeprav nekateri vplivi (nehomogeni material, gibanje dislokacij) pri preračunih niso upoštevani, je predstavljen računski model zelo primeren za določitev dobe trajanja zobnikov, saj so tukaj predstavljeni numerični postopki hitrejši in cenejši v primerjavi z eksperimentalnim delom.

(Ključne besede: zobniki, procesi utrujanja, doba življenjska, širjenje razpok)

A computational model for determining the service life of gears with regard to bending fatigue in a gear-tooth root is presented. The fatigue process leading to tooth breakage is divided into the crack-initiation and crack-propagation periods. The Coffin-Manson relationship is used to determine the number of stress cycles, N_i, required for the fatigue crack initiation, where it is assumed that the initial crack is located at the point of the largest stresses in a gear-tooth root. The simple Paris equation is then used for the further simulation of the fatigue crack growth, where the required material parameters have been determined previously with appropriate test specimens. The functional relationship between the stress-intensity factor and the crack length, K=f(a), which is needed for determining the required number of loading cycles, N_p, for a crack propagation from the initial to the critical length, is obtained numerically in the framework of the finite-element method. The total number of stress cycles, N, for the final failure to occur is then a sum $N = N_i + N_p$. Although some influences (non-homogeneous material, travelling of dislocations, etc.) were not taken into account in the computational simulations, the presented model seems to be very suitable for determining the service life of gears because the numerical procedures used here are much faster and cheaper than experimental testing.

(Keywords: gears, bending fatigue, service life, crack propagation)

0 UVOD

Pri zobnikih se lahko zaradi ponavljajoče se obremenitve pri utrujanju pojavita dve poškodbi; jamičenja zobnih bokov in zlom zoba v korenu [1]. V tem prispevku je obravnavan samo zlom zoba v korenu. Predstavljen računski model je uporabljen za preračun upogibne trdnosti v korenu zoba oziroma dobe trajanja zobnika.

Za trdnostni nadzor zobnikov glede na napetost v zobnem korenu se običajno uporabljajo

0 INTRODUCTION

Two kinds of tooth damage can occur on gears under repeated loading due to fatigue: the pitting of gear-tooth flanks and tooth breakage in the tooth root [1]. In this paper only tooth breakage is addressed and the developed computational model is used for calculating the tooth bending strength *i.e.* the service life of the gear tooth root.

Several classical, standardised procedures (DIN, AGMA, ISO, *etc.*) can be used for the approximate

postopki po različnih standardih (DIN, AGMA, ISO itn.). Ti so zasnovani na primerjavi največje upogibne napetosti v zobnem korenu z dopustno upogibno napetostjo [1]. Obe napetosti sta odvisni od številnih vplivnih koeficientov, s katerimi upoštevamo dejanske razmere obratovanja zobnika (dodatne notranje in zunanje dinamične obremenitve, slika nošenja, material zobnika, površinska hrapavost itn.). Omenjeni standardni postopki so zasnovani samo na preskusih na testnih zobniških dvojicah in upoštevajo le zadnjo fazo utrujanja zobnega korena zobnika, to je pojav končne poškodbe.

V splošnem lahko potek nastanka utrujenostnih poškodb na strojnih elementih razdelimo v naslednje faze ([2] do [5]): (1) nastanek mikrorazpoke; (2) širjenje kratke razpoke; (3) širjenje dolge razpoke; in (4) nastanek končne poškodbe. Pri inženirskih analizah sta prvi dve fazi običajno obravnavani kot "faza nastanka razpoke", širjenje dolgih razpok pa kot "faza širjenja razpoke". Čeprav je natančna meja prehoda med nastankom in širjenjem razpoke običajno neznana, v splošnem velja, da pomeni nastanek razpoke pogosto večji delež dobe trajanja, predvsem pri obremenitvi blizu trajne trdnosti materiala (sl. 1). Skupno število obremenitvenih ponovitev N do pojava poškodbe potem določimo kot vsoto obremenitvenih ponovitev N_i za nastanek razpoke in obremenitvenih ponovitev N_p za razširitev razpoke od začetne do kritične dolžine, ko se utrujenostna poškodba tudi dejansko pojavi:

determination of the load capacity of the gear-tooth root. They are commonly based on a comparison of the maximum tooth-root stress with the permissible bending stress [1]. Their determination depends on a number of different coefficients that allow for the appropriate consideration of real working conditions (additional internal and external dynamic forces, contact area of the engaging gears, gear material, surface roughness, *etc*.). The classical procedures are exclusively based on the experimental testing of the reference gears, and they consider only the final stage of the fatigue process in the gear tooth root, *i.e.* the occurrence of final failure.

However, the complete process of fatigue failure of mechanical elements may be divided into the following stages ([2] to [5]): (1) microcrack nucleation; (2) short crack growth; (3) long crack growth; and (4) occurrence of final failure. In engineering applications the first two stages are usually termed as the "crack-initiation period", while long crack growth is termed as the "crack-propagation period". An exact definition of the transition from the initiation to the propagation period is usually not possible. However, the crack-initiation period generally accounts for most of the service life, especially in high-cycle fatigue (HCF), see Figure 1. The total number of stress cycles N, can then be determined from the number of stress cycles N_i, required for the fatigue crack initiation and the number of stress cycles, N_p, required for a crack to propagate from the initial to the critical crack length, when the final failure can be expected to occur:

$$N = N_i + N_p \tag{1}.$$

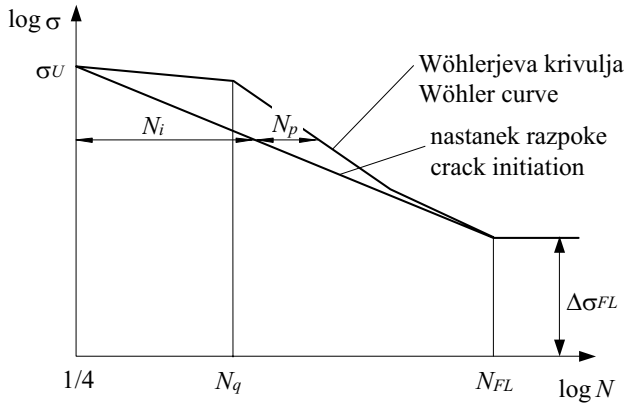

Sl. 1. *Shematska predstavitev dobe trajanja strojnih elementov*
Fig 1. *Schematic representation of the service life of machine elements*

1 NASTANEK UTRUJENOSTNE RAZPOKE

Predstavljen model nastanka utrujenostne razpoke je zasnovan na teoriji mehanike trdnin, pri kateri je predpostavljeno, da je material homogen in izotropen ter brez poškodb in nepravilnosti. V tem primeru so postopki za analize utrujanja materiala običajno zasnovani na Coffin-Mansonovem zakonu, ki podaja razmerje med deformacijami (ε), napetostmi (σ) ter številu ponovitev (N_i) v obliki ([6] in [7]):

1 FATIGUE CRACK INITIATION

The presented model for the fatigue crack initiation is based on the continuum mechanics approach, were it is assumed that the material is homogeneous and isotropic, i.e. without imperfections or damage. Methods for the fatigue analyses are, in that case, usually based on the Coffin-Manson relation between deformations (ε), stresses (σ) and the number of cycles (N_i), which can be described as follows ([6] and [7]):

$$\Delta\varepsilon = \Delta\varepsilon_{el} + \Delta\varepsilon_{pl} = \frac{\sigma'_f}{E} N_i^b + \varepsilon'_f N_i^c \quad (2),$$

kjer so $\Delta\varepsilon$ prirastek skupne ter $\Delta\varepsilon_{el}$ in $\Delta\varepsilon_{pl}$ prirastek elastične ter plastične deformacije pri utrujanju, E modul elastičnosti materiala, σ'_f koeficient trdnosti, ε'_f koeficient žilavosti, b eksponent trdnosti in c eksponent žilavosti materiala. Prirastek deformacije pri utrujanju lahko določimo numerično (običajno po MKE), ali eksperimentalno z merilnimi lističi, ki jih namestimo v zobnem korenu na mestu, kjer pričakujemo nastanek razpoke. Materialne veličine σ'_f, ε'_f, b in c se določijo z ustreznimi preskusi, ločeno za vsak material v odvisnosti od razmerja napetost/deformacija.

V področju obremenitev blizu trajne trdnosti, kateri so v večini primerov izpostavljeni tudi zobniki, je delež plastične deformacije zanemarljivo majhen, tako da se Coffin-Mansonov zakon omeji le na elastični del ([8] in [9]):

where $\Delta\varepsilon$ is the strain increment, $\Delta\varepsilon_{el}$ and $\Delta\varepsilon_{pl}$ are the elastic and plastic strain increment, E is the Young's modulus of the material and σ'_f, ε'_f, b and c are the strength coefficient, ductility coefficient, strength exponent and ductility exponent for crack initiation, respectively. The strain icrement can be obtained numerically (usually by FEM), or by strain-gauge measuring in the area of tooth root, where the crack initiation is expected. The material constants σ'_f, ε'_f, b and c are obtained for each material and stress/strain ratio, from strain controlled tests.

In the HCF region commonly applied for gears, where the plastic strain can be neglected, the Coffin-Manson relation reduces only to the elastic part and so transforms to an equation of the Basquin type ([8] and [9]):

$$(\Delta\sigma)^{k_i} \cdot N_i = C_i \quad (3),$$

kjer so $\Delta\sigma$ prirastek napetosti ter k_i in C_i materialni veličini. Če predpostavimo, da se ujema v točki (N_{FL}; $\Delta\sigma_{FL}$) Wöhlerjeva krivulja s krivuljo nastanka razpoke (celotno dobo trajanja predstavlja v tej točki faza nastanka razpoke), lahko po enačbi (3) določimo število obremenitvenih ponovitev za nastanek razpoke pri poljubni napetosti $\Delta\sigma$:

where $\Delta\sigma$ is the applied stress increment and k_i and C_i are the material constants. It is easy to obtain the crack initiation life, N_i, using this relation, if we assume that the crack initiation curve passes the same point (N_{FL}; $\Delta\sigma_{FL}$) as the Wöhler curve, it means at the fatigue limit level the whole fatigue life consists of the crack-initiation period:

$$N_i = N_{FL} \cdot \left(\frac{\Delta\sigma_{FL}}{\Delta\sigma} \right)^{k_i} \quad (4),$$

kjer je N_{FL} število obremenitvenih ponovitev pri trajni dinamični trdnosti $\Delta\sigma_{FL}$ (sl. 1). Na podlagi enake predpostavke lahko določimo eksponent k_i po enačbi:

where N_{FL} is the number of cycles at the knee of the Wöhler curve, see Figure 1. On the basis of the same assumption, the exponent k_i can be obtained as:

$$k_i = \frac{\log(4N_{FL})}{\log(\sigma_U / \Delta\sigma_{FL})} \quad (5),$$

kjer je σ_U natezna trdnost materiala (sl. 1). Enačba (5) kaže dobro ujemanje z razpoložljivimi eksperimentalnimi rezultati [9].

Pri določevanju števila obremenitvenih ponovitev za nastanek razpoke N_i po enačbi (4) je najpomembnejša veličina trajna dinamična trdnost $\Delta\sigma_{FL}$, ki je tipična materialna veličina in jo določimo z ustreznimi preskusi. Pri zobnikih določimo trajno dinamično trdnost običajno z ustreznimi referenčnimi zobniki. Po standardu ISO [1] so to valjasti zobniki z ravnim ozobjem, modulom m_n = 3 do 5 mm, širino zob b = 10 do 50 mm, površinsko hrapavostjo $R_z \approx 10$ µm, faktorjem koncentracije napetosti Y_{ST} = 2,0 itn., ki so obremenjeni z utripno obremenitvijo. Če geometrijska oblika, površinska hrapavost, velikost zobnika in obratovalne razmere zobnikov v praksi odstopajo od veličin pri referenčnih zobnikih, se vrednost trajne dinamične trdnosti $\Delta\sigma_{FL}$ spremeni in jo določimo z ustreznimi vplivnimi koeficienti.

where σ_U is the ultimate strength, see Figure 1. This relation was found to be in good agreement with available experimental results [9].

The most important parameter when determining the crack-initiation life, N_i, according to equation (4), is the fatigue limit $\Delta\sigma_{FL}$, which is a typical material parameter and is determined using an appropriate test specimen. When determining the fatigue limit for gears, the reference test gears are usually used as the test specimens. According to the ISO standard [1], they are spur gears with a normal module m_n = 3 to 5 mm, face width b = 10 to 50 mm, surface roughness $R_z \approx 10$ µm, stress concentration factor Y_{ST} = 2.0, etc, which are loaded with repeated pulsating tooth loading. If the geometry, surface roughness, gear size and loading conditions of the real gears in practice deviate from the reference testing, the previously determined fatigue limit $\Delta\sigma_{FL}$ must be modified by the appropriate correlation factors.

2 ŠIRJENJE UTRUJENOSTNE RAZPOKE

Pri analizi širjenja utrujenostne razpoke z uporabo linearno elastične mehanike loma (LELM) je hitrost širjenja razpoke da/dN funkcija faktorja intenzivnosti napetosti pri utrujanju $\Delta K=K_{max}-K_{min}$, kjer sta a dolžina razpoke in N število obremenitvenih ponovitev. V prispevku je za analizo širjenja razpoke uporabljen Parisov zakon [10]:

$$\frac{\mathrm{d}\,a}{\mathrm{d}\,N} = C\left[\Delta K(a)\right]^m \tag{6},$$

kjer sta C in m materialni veličini. Z integracijo enačbe (6) sledi ob upoštevanju potrebnega števila ponovitev za širjenje razpoke N_p po enačbi (1):

$$\int_0^{N_p} \mathrm{d}\,N = \frac{1}{C}\cdot\int_{a_o}^{a_c}\frac{\mathrm{d}\,a}{\left[\Delta K(a)\right]^m} \tag{7}.$$

Enačba (7) pove, da lahko eksplicitno določimo potrebno število obremenitvenih ponovitev N_p za razširitev razpoke od začetne dolžine a_o do kritične dolžine a_c, če so znane veličine C, m in $\Delta K(a)$. C in m sta materialni veličini in ju določimo eksperimentalno, običajno s tritočkovnimi preskušanci po standardu ASTM E 399-80 [11]. Odvisnost med faktorjem intenzivnosti napetosti in dolžino razpoke $K = \mathrm{f}(a)$ lahko za preproste primere razpok določimo po postopkih, navedenih v [10] in [11], pri zahtevnejših geometrijskih oblikah elementov in obremenitvenih primerih pa moramo uporabiti druge metode. V tem prispevku je za analizo širjenja utrujenostne razpoke uporabljena metoda končnih elementov v okviru programskega paketa FRANC2D [12]. Z uporabo te metode je določitev faktorja intenzivnosti napetosti zasnovana na načelu odvisnosti pomikov z uporabo singularnih četrtinskih končnih elementov (sl. 2). Za ravninsko deformacijsko stanje in kombinirano obremenitev sledita faktorja intenzivnosti napetosti:

$$K_I = \frac{2G}{(3-4\nu)+1}\cdot\sqrt{\frac{\pi}{2L}}\cdot\left[4v_d - v_e - 4v_b + v_c\right]$$
$$K_{II} = \frac{2G}{(3-4\nu)+1}\cdot\sqrt{\frac{\pi}{2L}}\cdot\left[4u_d - u_e - 4u_b + u_c\right] \tag{8},$$

kjer so G strižni modul materiala, ν Poisonovo število, L dolžina končnih elementov okrog razpoke ter u in v vozliščni pomiki elementov okrog razpoke. Skupni faktor intenzivni napetosti je potem:

$$K = \sqrt{\left(K_I^{\,2} + K_{II}^{\,2}\right)\cdot(1-\nu^2)} \tag{9}.$$

Opisan računski postopek temelji na majhnih prirastkih razpoke, pri katerih je velikost prirastka v posameznem koraku vnaprej predpisana. Za določitev smeri širjenja razpoke je uporabljen kriterij največjih nateznih napetosti. Pri tem je predpostavljeno, da se razpoka razširi radialno glede na vrh razpoke v ravnini, ki je pravokotna na smer

2 FATIGUE CRACK PROPAGATION

The application of linear elastic fracture mechanics (LEFM) to fatigue is based upon the assumption that the fatigue-crack growth rate, da/dN, is a function of the stress intensity range $\Delta K=K_{max}-K_{min}$, where a is the crack length and N is the number of load cycles. In this study the simple Paris equation is used to describe of the crack growth rate [10]:

where C and m are the material parameters. In respect to the crack propagation period, N_p, according to eq. (1), and with the integration of eq. (6) one can obtain:

Equation (7) indicates that the required number of loading cycles, N_p, for a crack to propagate from the initial length a_o to the critical crack length a_c can be explicitly determined if C, m and $\Delta K(a)$ are known. C and m are material parameters and can be obtained experimentally, usually by means of a three-point bending test, in accordance with the standard procedure ASTM E 399-80 [11]. For simple cases the dependence between the stress-intensity factor and the crack length $K = \mathrm{f}(a)$ can be determined using the methodology given in [10] and [11]. For more complicated geometry and loading cases it is necessary to use alternative methods. In this paper the finite-element method in the framework of the programme package FRANC2D [12] was used for the simulation of the fatigue crack growth. In this paper the determination of the stress-intensity factor is based on the displacement-correlation method using singular quarter-point elements, Figure 2. The stress-intensity factor in the mixed-mode plane-strain condition can then be determined as:

where G is the shear modulus of the material, ν is the Poisson ratio, L is the finite-element length on the crack face, and u and v are displacements of the crack-tip elements. The combined stress-intensity factor is then:

The computational procedure is based on incremental crack extensions, where the size of the crack increment is prescribed in advance. In order to predict the crack extension angle the maximum tensile stress criterion (MTS) is used. In this criterion it is proposed that the crack propagates from the crack tip in a radial direction in the plane per-

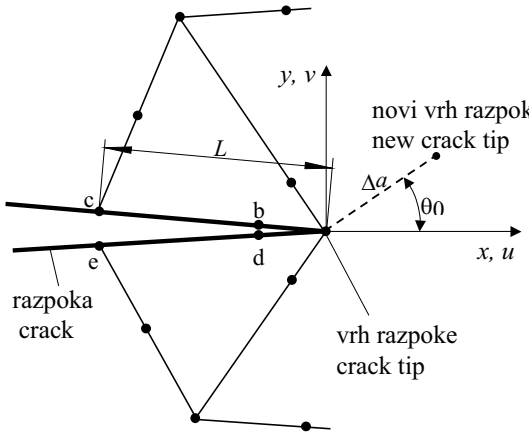

Sl. 2. *Trikotni četrtinski elementi okrog vrha razpoke*
Fig. 2. *Triangular quarter-point elements around crack tip*

največjih nateznih napetosti. Kot širjenja razpoke lahko na temelju te predpostavke izračunamo po enačbi (sl. 2):

pendicular to the direction of greatest tension. The predicted crack-propagation angle can be calculated by, see Figure 2:

$$\theta_0 = 2\tan^{-1}\left[\frac{1}{4}\cdot\frac{K_I}{K_{II}} \pm \sqrt{\left(\frac{K_I}{K_{II}}\right)^2 + 8}\right] \quad (10).$$

Za vsak korak je treba okrog novega vrha razpoke načrtovati novo mrežo končnih elementov. Postopek ponavljamo toliko časa, dokler faktor intenzivnosti napetosti ne doseže kritične vrednosti K_c, ko se pojavi tudi zlom zoba v korenu. Na ta način lahko določimo funkcijsko odvisnost $K = f(a)$.

A new local remeshing around the new crack tip is then required. The procedure is repeated until the stress-intensity factor reaches the critical value K_c, when the complete tooth fracture is expected. Following the above procedure, one can numerically determine the functional relationship $K = f(a)$.

3 PRAKTIČNI PRIMER

Predstavljen model je uporabljen za določitev dobe trajanja dejanskega zobnika z ravnim ozobjem in osnovnimi podatki iz preglednice 1. Material zobnika je zelo trdno legirano jeklo 42CrMo4 (0,43 %C, 0,22 %Si, 0,59 %Mn, 1,04 %Cr, 0,17 %Mo) z modulom elastičnosti E=2,1·10^5 MPa in Poissonovim številom ν = 0,3. Toplotna obdelava zobnika je naslednja: segrevanje na 810°C; 2 min, kaljeno v olju; 3 min in popuščano na 180°C; 2 h.

3 PRACTICAL EXAMPLE

The presented model has been used for the computational determination of the service life of a real spur gear with the complete data set given in Table 1. The gear is made of high-strength alloy steel 42CrMo4 (0.43 %C, 0.22 %Si, 0.59 %Mn, 1.04 %Cr, 0.17 %Mo) with a Young's modulus E = 2.1·10^5 MPa and a Poison's ratio ν = 0.3. The gear material is thermally treated as follows: flame heated at 810°C, 2 min; hardened in oil, 3 min, and tempered at 180°C, 2 h.

Preglednica 1. *Poglavitni podatki obravnavanega zobnika z ravnim ozobjem*
Table 1. *Basic data of a treated spur gear*

modul module	m_n = 4,5 mm
število zob number of teeth	z = 39
ubirni kot na razdelnem krogu pressure angle on pitch circle	α_n = 24°
koeficient profilne premaknitve coefficient of profile displacement	x = 0,06
širina zoba face width	b = 28 mm
material zobnika gear material	42CrMo4
površinska hrapavost surface roughness	R_z = 10 μm

3.1 Nastanek utrujenostne razpoke

Računski postopek, opisan v poglavju 1 je uporabljen za določitev števila obremenitvenih ponovitev N_i za nastanek utrujenostne razpoke. Natezna trdnost σ_u=1100 MPa, trajna trdnost $\Delta\sigma_{FL}$=550 MPa in število obremenitvenih ponovitev na pregibu Wöhlerjeve krivulje $N_{FL}=3\cdot10^6$ so uporabljeni iz virov [1], [13] in [14] za enak material kakor je material obravnavanega zobnika. Izračuni so izvedeni za različne vrednosti normalne utripne obremenitve F, ki deluje v zunanji točki enojnega ubiranja zobnika (sl. 3). Največja glavna napetost v zobnem korenu $\Delta\sigma$ kot posledica delovanja obremenitve F je izračunana numerično po metodi končnih elementov, pri čemer je uporabljen numerični model na sliki 3. Rezultati izračunov so prikazani v preglednici 2.

3.2 Širjenje utrujenostne razpoke

Za analizo širjenja utrujenostne razpoke je uporabljena metoda končnih elementov v okviru programskega paketa FRANC2D (poglavje 2). Začetna razpoka je locirana pravokotno na površino na mestu največje glavne napetosti na natezni strani zobnega korena (sl. 4).

3.1 Fatigue crack initiation

The procedure as described in Section 1 has been used to determine the number of stress cycles, N_i, required for the fatigue crack initiation. The ultimate tensile strength σ_u=1100 MPa, fatigue limit $\Delta\sigma_{FL}$=550 MPa and number of cycles at the knee of the Wöhler curve $N_{FL}=3\cdot10^6$ have been taken from [1], [13] and [14] for the same material as used in this paper. The computational analysis was done for different values of the normal pulsating force F, which is acting at the outer point of the single-tooth contact, see Figure 3. As a consequence of F the maximum principal stress $\Delta\sigma$ in a gear-tooth root has been determined numerically with the finite-element method, where the FE model shown in Figure 3 has been used. The results are summarised in Table 2.

3.2 Fatigue crack propagation

The FEM programme package FRANC2D as described in Section 2 was used for the numerical simulation of the fatigue crack growth. The initial crack was located perpendicular to the surface at the point of the maximum principal stress on the tensile side of the gear tooth, see Figure 4.

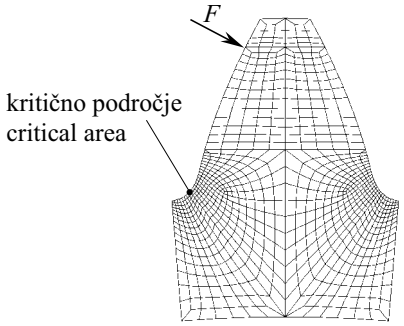

Sl. 3. *Model končnih elementov*
Fig. 3. *Finite element model*

Preglednica 2. *Računski rezultati nastanka utrujenostne razpoke*
Table 2. *Computational results for the fatigue crack initiation*

Obremenitev Loading F N/mm	Največja glavna napetost v zobnem korenu zobnika Maximum principal stress in a gear tooth root σ MPa	Število ponovitev Number of cycles N_i
800	527	$8{,}192.10^6$
900	593	$5{,}109.10^5$
1000	659	$4{,}271.10^4$
1100	725	$4{,}526.10^3$
1200	790	$6{,}010.10^2$
1300	857	$8{,}861.10^1$
1400	922	$1{,}588.10^1$
1500	988	$3{,}087.10^0$

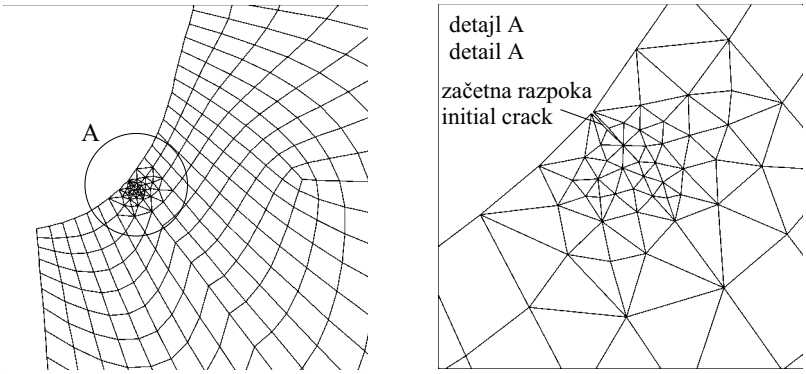

Sl. 4. *Mreža končnih elementov okrog začetne razpoke v korenu zoba*
Fig. 4. *Finite element mesh around initial crack in a gear tooth root*

Pri numeričnih izračunih je predpostavljeno, da ustreza dolžina začetne razpoke a_o mejni dolžini a_{th}, pod katero ne moremo uporabiti zakonitosti LELM. Mejno dolžino razpoke lahko približno določimo po enačbi [15]:

In numerical computations it was assumed that the initial crack, a_o, corresponds to the threshold crack length, a_{th}, below which LEFM is not valid. The threshold crack length may be estimated approximately as [15]:

$$a_{th} \approx \frac{1}{\pi}\left(\frac{\Delta K_{th}}{\Delta \sigma_{FL}}\right)^2 \qquad (11),$$

kjer je $\Delta\sigma_{FL}$ trajna dinamična trdnost in ΔK_{th} mejni faktor intenzivnosti napetosti pri utrujanju. V strokovni literaturi najdemo širok spekter vrednosti za a_{th}, ki pa so za jekla običajno med 0,05 in 1 mm, pri čemer se manjše vrednosti nanašajo na zelo trdna jekla. Z upoštevanjem materialnih veličin $\Delta\sigma_{FL} \approx 550$ MPa in $K_{th} \approx 269$ MPa$\sqrt{\text{mm}}$, vzetih iz virov [13] in [14], znaša mejna dolžina razpoke za obravnavani primer $a_{th} \approx 0{,}1$ mm. Lomna žilavost $K_{Ic} \approx 2620$ MPa$\sqrt{\text{mm}}$ in materialni veličini $C = 3{,}31 \cdot 10^{-17}$ mm/ponov/(MPa$\sqrt{\text{mm}}$)^m in $m = 4{,}16$ so bile za tukaj uporabljen material določene poprej s tritočkovnimi upogibnimi preskušanci po ASTM E 399-80 [14].

Pri analizi širjenja utrujenostne razpoke je upoštevana enaka obremenitev kakor pri nastanku (poglavje 3.1). Pri numeričnih analizah je znašal prirastek razpoke $\Delta a = 0{,}2$ mm do dolžine razpoke $a = 4$ mm, in nato $\Delta a = 0{,}4$ mm do kritične dolžine razpoke a_c, (sl. 2). Za določitev potrebnega števila obremenitvenih ponovitev N_p za razširitev razpoke od začetne dolžine a_{th} do kritične dolžine a_c po enačbi (7), je treba poznati funkcijsko odvisnost $\Delta K = f(a)$. Slika 5 prikazuje funkcijsko odvisnost med skupnim faktorjem intenzivnosti napetosti K in dolžino razpoke a, kjer je K izračunan po enačbi (9) na podlagi numerično izračunanih vrednosti za K_I in K_{II}. Numerični izračuni kažejo, da je faktor intenzivnosti napetosti K_I prevladujoč v primerjavi s K_{II} (K_{II} znaša manj ko 5 % K_I za vse obremenitvene primere in vse dolžine razpok). To dejansko pomeni, da lahko upoštevamo lomno žilavost K_{Ic} kot kritično vrednost faktorja intenzivnosti napetosti K, pripadajočo dolžino razpoke pa za kritično dolžino razpoke a_c. Potrebno število obremenitvenih ponovitev N_p za

where $\Delta\sigma_{FL}$ is the fatigue limit and ΔK_{th} is the threshold stress-intensity range. However, a wider range of values was selected for a_{th} in the literature, usually between 0.05 and 1 mm for steels, where high-strength steels take the smallest values. Considering the material parameters $\Delta\sigma_{FL} \approx 550$ MPa and $K_{th} \approx 269$ MPa$\sqrt{\text{mm}}$ available in [13] and [14] the threshold crack length is equal to $a_{th} \approx 0.1$ mm. The fracture toughness $K_{Ic} \approx 2620$ MPa$\sqrt{\text{mm}}$, and the material parameters $C = 3.31 \cdot 10^{-17}$ mm/cycl/(MPa$\sqrt{\text{mm}}$)^m and $m = 4.16$ were determined previously using three-point bending samples according to the ASTM E 399-80 standard and for the same material as used in this paper[14].

The tooth loading was equal to the computational analysis of the fatigue crack initiation, see Section 3.1. During numerical simulations the crack increment size, Δa, was 0.2 mm, up to the crack length $a = 4$ mm, and after this, 0.4 mm up to the critical crack length a_c, see Figure 2. To be able to determine the number of loading cycles, N_p, required for the crack to propagate from the initial crack length, a_{th}, to the critical crack length, a_c, according to equation (7), it is necessary to determine the dependence $\Delta K = f(a)$ first. Figure 5 shows the functional relationship between the combined stress-intensity factor, K, and crack length, a, where K is obtained with equation (9) using numerically determined values of K_I and K_{II}. Numerical analysis has shown that the K_I stress-intensity factor is much higher than K_{II} (K_{II} was less than 5 % of K_I for all load cases and crack lengths). Therefore, the fracture toughness, K_{Ic}, can be considered as the critical value of K and the appropriate crack length can be taken as the critical crack length, a_c. The loading cycles, N_p, for the crack propagation to the critical crack length can

razširitev razpoke do kritične dolžine potem izračunamo po enačbi (7), (preglednica 3). Slika 6 prikazuje pot širjenja razpoke v korenu zoba.

then be estimated using equation (7), see Table 3. Figure 6 shows the numerically determined crack-propagation path in a gear-tooth root.

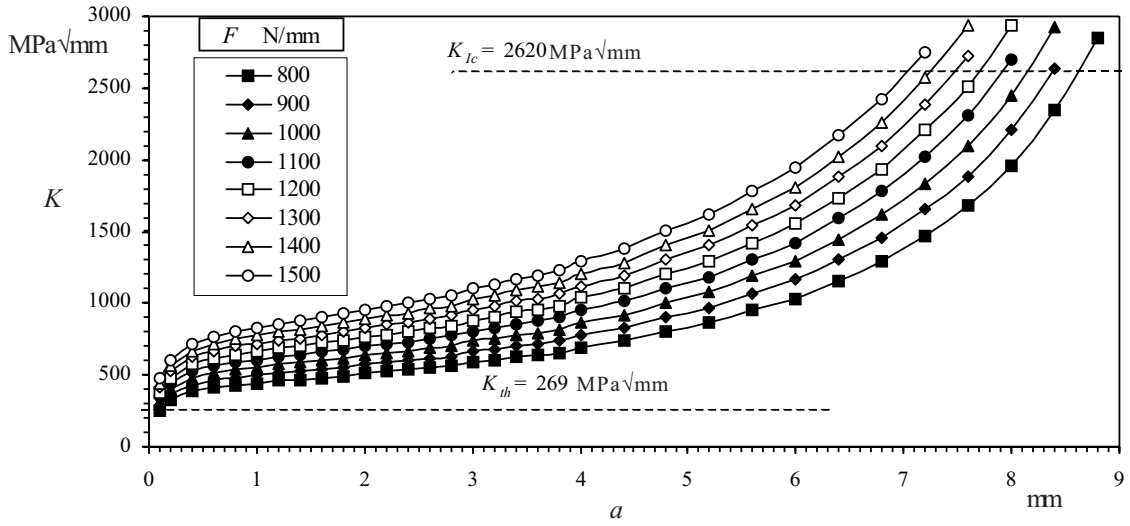

Sl. 5. *Funkcijska odvisnost med faktorjem intenzivnosti napetosti in dolžino razpoke*
Fig. 5. *Functional relationship between the stress intensity factor and crack length*

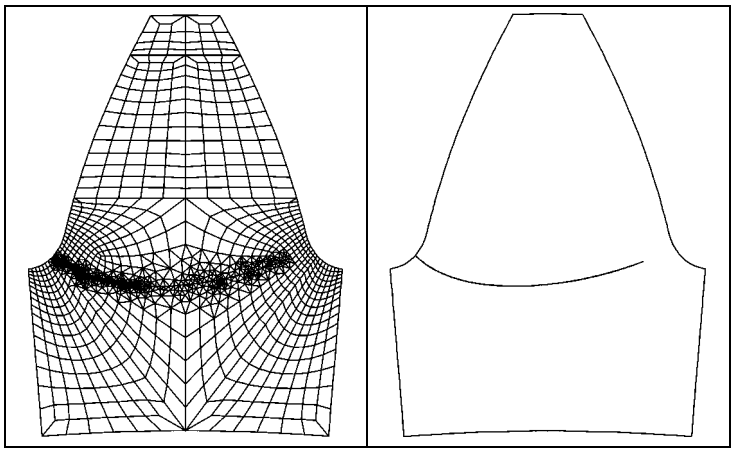

Sl. 6. *Pot širjenja razpoke v zobnem korenu zobnika*
Fig. 6. *Crack propagation path in a gear tooth root*

Preglednica 3. *Računski rezultati širjenja utrujenostne razpoke*
Table 3. *Computational results for the fatigue crack propagation*

Obremenitev Loading *F* N/mm	Kritična dolžina razpoke Critical crack length a_c mm	Število ponovitev Number of cycles N_p
800	8,6	$9{,}473.10^5$
900	8,4	$5{,}845.10^5$
1000	8,2	$3{,}768.10^5$
1100	7,9	$2{,}534.10^5$
1200	7,7	$1{,}773.10^5$
1300	7,5	$1{,}264.10^5$
1400	7,3	$9{,}322.10^4$
1500	7,1	$6{,}993.10^4$

Na temelju dobljenih rezultatov za nastanek razpoke (N_i) in širjenje razpoke (N_p) iz preglednic 2 in 3 lahko določimo skupno dobo trajanja zoba zobnika po enačbi (1) (sl. 7). S slike 7 je razvidno, da je razmerje med fazo nastanka razpoke in koncem širjenja razpoke (zlomom zoba) odvisno od ravni napetosti v korenu zoba. Pri majhnih napetostih blizu trajne trdnosti pomeni faza nastanka razpoke skoraj celotno dobo trajanja zobnika, pri večjih napetostih je zelo pomembna predvsem faza širjenja razpoke. Dobljeni računski rezultati dobe trajanja kažejo dobro ujemanje z razpoložljivimi eksperimentalnimi rezultati, uporabljenimi iz vira [13].

On the basis of the computational results for the crack-initiation (N_i) and crack-propagation (N_p) periods in Tables 2 and 3 the total service life of the gear-tooth root can be obtained according to equation (1), see Figure 7. It is clear from Figure 7 that the ratio among the periods of initiation and of the end of propagation (i.e. final breakage) depends on the stress level. At low stress levels almost all the service life is spent in crack initiation, but at high stress levels a significant part of the life is spent in the crack propagation. The computational results for total service life are in a good agreement with the available experimental results, which are taken from [13].

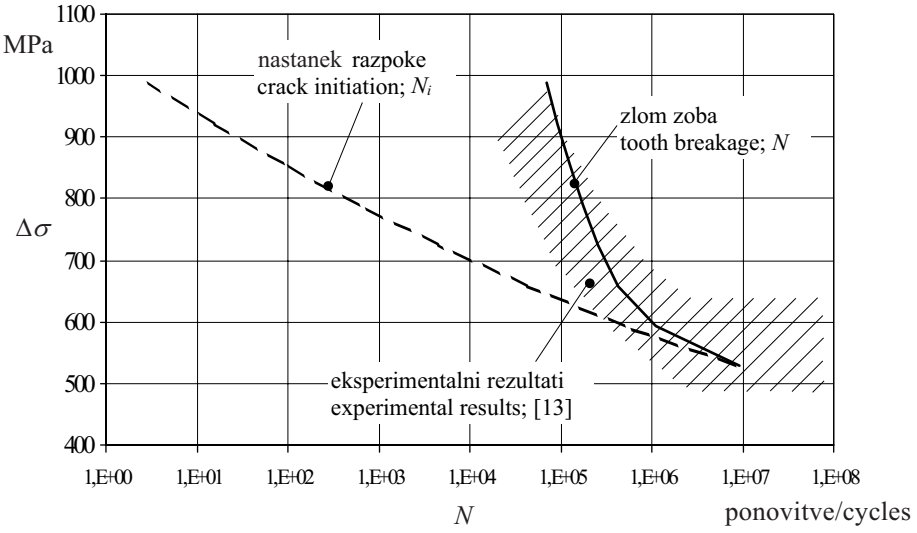

Sl. 7. *Izračun dobe trajanja obravnavanega zobnika*
Fig. 7. *The computed service life of treated gear*

4 SKLEPI

V prispeveku je predstavljen računski model za določitev dobe trajanja zobnikov glede na trdnost v zobnem korenu. Potek utrujanja zobnika, ki vodi do končnega zloma zoba v korenu, je razdeljen v fazo nastanka razpoke (N_i) in fazo širjenja razpoke (N_p). Skupna doba trajanja zobnika je definirana kot $N = N_i+N_p$. Za izračun števila ponovitev za nastanek razpoke N_i je uporabljena preprosta Basquinova enačba. V modelu je predpostavljeno, da je začetna razpoka na mestu največje glavne napetosti v korenu zoba, ki je določena numerično z MKE. Funkcijska odvisnost med faktorjem intenzivnosti napetosti in dolžino razpoke $K = f(a)$, potrebna za analizo širjenja razpoke in določitev števila ponovitev N_p, je določena numerično z metodo odvisnosti pomikov v okviru metode končnih elementov.

Predstavljen model je uporabljen za določitev dobe trajanja realnega zobnika iz zelo trdnega legiranega jekla 42CrMo4. Rezultate računskih analiz prikazuje slika 7, kjer sta predstavljeni dve krivulji: krivulja nastanka razpoke in krivulja zloma zoba, ki hkrati pomeni skupno dobo trajanja zobnika. Rezultati kažejo, da pomeni faza

4 CONCLUSIONS

This paper presents a computational model for determining the service life of gears in regard to bending fatigue in a gear-tooth root. The fatigue process leading to tooth breakage in a tooth root is divided into the crack-initiation (N_i) and crack-propagation (N_p) periods, which enables the determination of total service life as $N = N_i+N_p$. The simple Basquin equation is used to determine the number of stress cycles, N_i. In the model it is assumed that the crack is initiated at the point of the maximum principal stress in a gear-tooth root, which is calculated numerically using the FEM. The displacement-correlation method is then used for the numerical determination of the functional relationship between the stress-intensity factor and crack length $K = f(a)$, which is necessary for a subsequent analysis of fatigue crack growth, i.e. determination of the stress cycles N_p.

The model is used to determine the complete service life of a spur gear made from high-strength alloy steel 42CrMo4. The final results of the computational analysis are shown in Figure 7, where two curves are presented: the crack-initiation curve and the curve of tooth breakage, which at the same time represents the

nastanka razpoke pri majhnih napetostih blizu trajne trdnosti skoraj celotno dobo trajanja zobnika. To je zelo pomembna ugotovitev pri izračunavanju dobe trajanja zobniških dvojic v praksi, ki v večini primerov dejansko obratujejo v obremenitvenih razmerah blizu trajne dinamične trdnosti.

Dobljeni računski rezultati za skupno dobo trajanja zobnika se dobro ujemajo z razpoložljivimi eksperimentalnimi rezultati. Kljub temu velja model v prihodnje še izboljšati na področju teoretičnih spoznanj in numeričnih analiz, prav tako pa bodo potrebne dodatne eksperimentalne raziskave za določitev potrebnih materialnih veličin.

total service life. The results show that at low stress levels near the fatigue limit, almost all service life is spent in crack initiation. It is a very important knowledge for the determination of the service life of real gear drives in practice, because the majority of them really operate with loading conditions close to the fatigue limit.

The computational results for total service life are in a good agreement with the available experimental results. However, the model can be further improved with additional theoretical and numerical research, although additional experimental results will be required to provide the required material parameters.

5 LITERATURA
5 REFERENCES

[1] ISO 6336, Calculation of load capacity of spur and helical gears, *International Standard*, 1993

[2] Shang, D.G., W.X. Yao, D.J. Wang (1998) A new approach to the determination of fatigue crack initiation size, *Int. J. Fatigue*, 20, 683-687.

[3] Glodež, S., J. Flašker, Z. Ren (1997) A new model for the numerical determination of pitting resistance of gear teeth flanks, *Fatigue Fract. Engng Mater. Struct.*, 71-83.

[4] Glodež, S., H. Winter, H.P. Stüwe (1997) A fracture mechanics model for the wear of gear flanks by pitting, *Wear*, 208, 177-183.

[5] Cheng, W., H. S. Cheng, T. Mura, L. M. Keer (1994) Micromechanics modeling of crack initiation under contact fatigue, *ASME J. Tribology*, 116, 2-8.

[6] Manson, S. (1953) "Proc.Heat Transfer Symp.", Univ. Michigan, Eng. Res. Inst., 9-75.

[7] Tavernelli, J.F., L. F. Coffin (1959) A compilation and interpretation of cyclic strain fatigue tests on metals, *Trans. Amer. Soc. of Metals,* 51, 438-450.

[8] Nicholas, T. J. R., J. R. Zuiker (1996) On the use of the Goodman diagram for high cycle fatigue design, *Int. J. Fracture,* 80, 219-235

[9] Jelaska, D. (2000) Crack initiation life at combined HCF/LCF loading, *Proc. Int. Conf. Life Assessment and Management for Structural Components*, Kiev 2000, 239-246.

[10] Ewalds, H.L., R.J. Wanhill (1989) Fracture Mechanics, *Edward Arnold Publication*, London.

[11] ASTM E 399-80, American standard.

[12] FRANC2D, User's Guide, Version 2.7, Cornell University.

[13] Niemann, G., H. Winter (1983) Maschinenelemente - Band II, *Springer Verlag*.

[14] Aberšek, B. (1993) Analysis of short fatigue crack on gear teeth, Ph.D. thesis, University of Maribor, Faculty of Mechanical Engineering, Maribor.

[15] Bhattacharya, B., B. Ellingwood (1998) Continuum damage mechanics analysis of fatigue crack initiation, *Int. J. Fatigue*, 20, 631-639.

Naslova avtorjev: prof. dr. Srečko Glodež
prof. dr. Jože Flašker
dr. Janez Kramberger
Fakulteta za strojništvo
Univerza v Mariboru
Smetanova 17
2000 Maribor
joze.flasker@uni-mb.si
jkramberger@uni-mb.si

prof. dr. Damir Jelaska
Fakulteta za elektrotehniko,
strojništvo in ladjarstvo
Univerza v Splitu
R. Boškovića b.b.
21000 Split, Hrvaška
damir.jelaska@fesb.hr

Authors' Addresses: Prof. Dr. Srečko Glodež
Prof. Dr. Jože Flašker
Dr. Janez Kramberger
Faculty of Mechanical Eng.
University of Maribor
Smetanova 17
2000 Maribor, Slovenia
joze.flasker@uni-mb.si
jkramberger@uni-mb.si

Prof. Dr. Damir Jelaska
Faculty of Electrical Eng.,
Mech. Eng. and Naval Architecture
University of Split
R. Boškovića b.b.
21000 Split, Croatia
damir.jelaska@fesb.hr

Prejeto: 13.12.2001
Received:

Sprejeto: 23.5.2002
Accepted:

© Strojniški vestnik 48(2002)5,267-282
ISSN 0039-2480
UDK 621.867.8:531.36/.38:681.51/.52
Izvirni znanstveni članek (1.01)
© Journal of Mechanical Engineering 48(2002)5,267-282
ISSN 0039-2480
UDC 621.867.8:531.36/.38:681.51/.52
Original scientific paper (1.01)

Naprava s pnevmatično aktivno površino: Tehnike krmiljenja lege togih objektov s povratno zvezo in brez nje

A Pneumatic Active-Surface Device: Open- and Closed-loop Control-Positioning Techniques for Rigid Objects

Suzana Uran - Riko Šafarič

Pomanjkanje proizvodnih tehnik za premikanje in spreminjanje usmerjenosti velikega števila majhnih predmetov je tehnološka ovira za tržni uspeh na različnih področjih mikro elektromehanskih sistemov (MEMS). V prispevku je predstavljen bistveno nov postopek avtomatizacije množičnega sočasnega rokovanja z majhnimi predmeti. Raziskana je naprava s pnevmatično aktivno površino (NPAP). Ustrezna izbira sile, ki jo povzroča pihanje ali sesanje zraka skozi cevke naprave z aktivno pnevmatično površino, povzroča želeno premikanje predmetov na aktivni površini naprave. Naprava omogoča veliko prilagodljivost in hitrost in jo lahko uporabimo za pozicioniranje, orientiranje, identifikacijo, sortiranje, podajanje in sestavljanje predmetov. Dodatno k temu lahko vodimo mnogo predmetov hkrati. Prispevek opisuje eksperimentalno delo, opravljeno na prototipu naprave s pnevmatično aktivno površino, posebej tehnike krmiljenja (s povratno zvezo in brez nje) lege togih objektov, manjših od 1 mm.

(Ključne besede: deli mali, manipulacija predmetov, naprave pnevmatične, zaznavanje predmetov, regulacija lege)

The current lack of manufacturing techniques for handling very high volumes of small objects presents a technology barrier to commercial success in various fields like micro-electromechanical systems (MEMS). A fundamentally new approach to automated, massive, parallel manipulation of small-sized parts is explored in this paper: the pneumatic active surface device (PASD). With the appropriate choice of force – caused by blowing or sucking air-flow through the tubes of the pneumatic active surface device – objects placed on the array can be moved in useful ways. Such a device offers great flexibility and speed and can be employed to position, orient, identify, sort, feed, and assemble parts or objects. Another advantage is that several objects can be controlled simultaneously. This paper describes experimental work on a prototype pneumatic active surface device, in particular an open-loop and closed-loop positioning control techniques for sub-millimeter rigid objects.

(Keywords: small parts, objects manipulation, pneumatic control equipment, position control)

0 UVOD

Množična proizvodnja miniaturnih komponent kakor so integrirana vezja, mikro elektromehanski sistemi (MEMS) ipd. terjajo bistvene izboljšave na področju rokovanja predmetov. Te komponente so izdelane na podlagi procesa mikroproizvodnje, ki izvira iz tehnologije zelo visoke integracije (ZVI - VLSI). Le ta omogoča proizvodnjo tisočev ali milijonov komponent hkrati. Naprava s pnevmatično aktivno površino (NPAP) uporablja nov postopek avtomatiziranega rokovanja predmetov. Namesto rokovanja posameznih

0 INTRODUCTION

The mass production of miniature components such as integrated circuits, micro-electromechanical systems (MEMS), etc. requires fundamental innovations in the handling of parts. These components are built using microfabrication processes derived from VLSI technology, which allows the manufacture of thousands or millions of components in parallel. A pneumatic active surface device (PASD) uses a new approach to automated manipulation of objects (parts): instead of handling a

predmetov (npr. z robotskim prijemalom [12]) z uporabo naprave s pnevmatično aktivno površino premikamo mnoge predmete hkrati. Naprava s pnevmatično aktivno površino omogoča vzporedno in porazdeljeno zaznavanje in proženje in je še posebno primerna za rokovanje serijsko mikroproizvedenih predmetov, katerih majhne izmere (manj ko milimeter) in veliko število ne omogočajo konvencionalnega rokovanja (poberi in odloži) z robotskimi prijemali. V zadnjem času so bile razvite mnoge podobne naprave:

1. Programljivo polje sil je matrika velikega števila programljivih točk mikrogibanja ([1] in [5]). Pri krmiljenju gibanja predmetov po programljivem polju sil je uporabljena strategija »ožajočih se vzorcev« ([1], [2] in [7]) ob uporabi analize ravnotežnega stanja ([1] do [3]). Naprava je opisana v [1] in [2] in ima pomembne lastnosti, to so: občutljiva je na poškodbe in nima vgrajenih zaznaval. Zato za premikanje predmetov po njej ni mogoča izvedba krmiljenja s povratno zvezo. Naš postopek uporablja zaznavala tlaka, ki se uporabljajo za zaznavanje predmeta na NPAP, zato omogoča zaznavanje predmeta na osnovi njegove ploskve, s katero se dotika pnevmatično aktivne površine. Zato naš postopek omogoča izvedbo tehnik krmiljenja s povratno zvezo.
2. Navidezno vozilo [4] je zgrajeno iz celic, ki predstavljajo mehanizem z dvema prostostnima stopnjama. Za krmiljenje vsake izmed celic je uporabljen zapleten postopek krmiljenja, saj je za krmiljenje vsake celice potreben mikroprocesor (MC68HC11). Vsaka celica je informacijsko povezana z drugimi celicami s pomočjo serijske povezave RS232. Nemogoče si je predstavljati, koliko komunikacijske in računalniške pomoči bi bilo treba za izvedbo matrike z nekaj stotisočimi celicami, ki bi premikale mikroskopsko majhen predmet. Osnovna celica naše naprave (cevka in zazanavalo tlaka), ki je načrtovana za premikanje mikroskopsko majhnih delcev, je izvedena preprosteje, zato bi bil potreben en mikroprocesor (MC68000) za krmiljenje prek deset tisoč celic.
3. Prve mikroproizvedene celice in matrike na podlagi zračnega toka so bile predstavljene v [6], toda za njih ni poročil o uporabljenih strategijah krmiljenja predmetov po matriki. Naše tehnike krmiljenja omogočajo od oblike predmeta neodvisno krmiljenje osnovnih premikov in usmeritev s povratno zvezo in brez nje (translacija, rotacija) za toge in elastične predmete. Nekatera poročila o krmiljenju in rokovanju predmetov na programljivem polju sil so v [1] do [3] in [7] in so delno vplivala na razvoj naših tehnik krmiljenja.
4. Mnoge skupine raziskovalcev MEMS so zgradile aktuatorske matrike za mikromanipulacijo, ki so običajno zgrajene iz 'gibalnih točk'. Naprave so zgradili prej omenjeni avtorji ([1], [4] do [6] in v [8] do [11]).

single object directly, for example, with a robot gripper [12], a PASD can be used to move multiple objects simultaneously. This new automation device permits both parallel and distributed forms of sensing and actuation, and is particularly attractive for handling batch microfabricated objects, whose small dimensions (sub-millimeter) and large numbers do not allow conventional pick-and-place operations with robot grippers. Recently, several similar devices have been invented:

1. Programmable force field (massive parallel array of programmable micromotion pixels ([1] and [5])) uses a control strategy called "squeeze patterns" ([1], [2] and [7]) using equilibrium analysis ([1] to [3]). The device described in [1] and [2] has an important drawback because it is susceptible to damage and has no integrated sensors. Therefore closed-loop position control methods cannot be used for moving objects on a surface with programmable force fields. Our approach uses pressure sensors that sense an object on the surface of the PASD and allow the use of object recognition from the footprint of the object sensed by pressure sensors and also the use of closed-loop position techniques.
2. The Virtual Vehicle [4] uses a complicated control technique for each cell, this requires complete microprocessor (MC68HC11) control of a two-degree-of-freedom mechanical mechanism. Each cell is informationally linked to the other cells with a RS232 serial link. It is impossible to imagine how much communication and computer power would be needed in the case of an array of a few hundred thousand micromachined actuators (cells) for carrying near-microscopic objects. The basic cell (a tube and a pressure sensor) of our device, which is designed for carrying near-microscopic objects, is controlled in a simpler way, with only one microprocessor (MC68000) needed to control over ten thousand cells.
3. The first airflow-based micromachined cells and arrays were presented in [6]; however they did not publish any control strategy for moving the objects on the array. Our control techniques allow basic open-loop and closed-loop, rigid and flexible, object movements – translation, rotation, and flip – that are independent of the object's shape. Some reports of control and manipulation of the objects on programmable force fields are reported in [1], [2], [3] and [7] and have been partly influential on the development of our control techniques.
4. Several groups of MEMS researchers have designed and built actuator arrays for micromanipulation, which usually consist of "motion pixels". Devices were built by the previously mentioned authors [1], [4], [5], [6] and also by [8], [9], [10] and [11].

Opis celotnega prototipa NPAP in analiza stabilnosti togega objekta na površini naprave po Ljapunovovi metodi sta predstavljena v [13]. V tem prispevku, ki je drugi objavljen prispevek od treh na temo NPAP v Strojniškem vestniku, so opisane tehnike krmiljenja lege s povratno zvezo in brez nje za translacijo, rotacijo in obračanje togega objekta, manjšega od 1 mm na pnevmatični aktivni površini, podrobno opisani v [13]. Tehnike krmiljenja lege s povratno zvezo in brez povratne zveze za gibljive objekte pa bo objavljena v tretjem prispevku.

1 KRMILJENJE BREZ POVRATNE ZVEZE

1.1 Krmiljenje translacije

Najbolj robustno in uporabno translacijsko tehniko brez povratne zveze smo poimenovali "konvergenčni valovi". Ta tehnika temelji na metodi krmiljenja brez povratne zveze za mehanični aktuator MEMS [1]. Omenjeno tehniko smo testirali za majhne objekte velikosti od 1 do 15 (3 krat 5) ploščine cevke s premerom 0,4 mm. Slika 1 prikazuje postopek delovanja "konvergenčnih valov".

Ponavljajoči se krogi oziroma kvadrati sesajočih cevk ("valovi") se pomikajo (konvergirajo) proti cevki, kjer je želena končna lega objekta. Vsi objekti, ki so znotraj področja, pokritega z valovi, se pomaknejo do želene cevke (lege). Iz vseh drugih cevk, ki niso v želeni legi ali znotraj konvergenčnega vala, piha. Ponavljajoči se konvergenčni valovi povzročijo tako silo kakor vibracije, ki so potrebne, da premikajo objekt na površini. Frekvenco valov lahko spreminjamo. Če je frekvenca previsoka, tedaj se objekt premika prehitro, kar povzroči, da se želena lega doseže s prenihajem. Frekvenca ponavljajočih se valov je odvisna od medsebojne dinamike objekta in površine (trenje med objektom in površino, višina objekta). Razdalja med dvema zaporednima konvergentnima valoma mora biti dolga vsaj toliko, kolikor je dolg objekt. Vzrok za to je v tem, da objekt stoji na mestu in se sploh ne premika, če pokriva sesajoče cevke dveh ali več zaporednih valov. Pogoj za premikanje objekta je, da je samo ena sesajoča cevka pokrita z objektom. Na drugi strani pa velja, da objekt pogosto odpihne s površine, če so vse cevke, ki jih pokriva objekt, postavljene na pihanje. Za večje objekte (npr. 5 krat 5 površin cevk) ena sesajoča cevka ni dovolj, da bi zadržala objekt na površini. Verjetno je treba povečati število sesajočih cevk pod takim večjim objektom; res pa je, da tega še nismo testirali.

Metoda krmiljenja translacije s konvergenčnimi valovi ima to pomanjkljivost, da lega objekta na površini ni merjena. Tako se lahko zgodi, da se objekt zatakne nekje na površini in ne doseže želene lege.

The complete prototype design of our PASD and a Lyapunov stability analysis of an object on the device was presented in [13]. The open-loop and closed-loop position control techniques for translating, rotating and flipping rigid, sub-millimeter objects are described in this paper, which is the second of three papers published in Journal of Mechanical Engineering on the subject of PASDs. Open-loop and closed-loop position control techniques for flexible objects on a PASD will be described in the third paper.

1 OPEN-LOOP CONTROL

1.1 Open-loop translation

The most robust and generally applicable method for the open-loop translation of objects is called "converging waves". It is based on a method originally developed for a MEMS mechanical actuator array [1]. It has been tested and used for smaller objects, from 1 square pixel to 15 square pixels (3-by-5 pixels). The scheme of the converging waves procedure is shown in Figure 1.

Repetitive circles or squares of tubes sucking ("waves") converge towards the tube ("pixel") where the center of the object should land. All objects, which can be found within the area covered by the waves move towards the center tube (desired pixel) and stop in this position. All tubes except the center tube and the pixels of the converging sucking waves are set to blow. The repetitive converging waves generate both a force and a vibration, which are needed to move the object on the surface. The frequency of the waves can be changed. If the frequency is too high the object can move too quickly and this can result in overshooting the desired end-position. In fact the frequency of the value should be dependent on the dynamics of the object and the surface (friction between the surface and the object, the height of the object etc…). The distance between two successive converging waves must be at least as large as the length of the object. This is because if the object on the surface covers more sucking tubes in two successive waves at the same time then the element becomes locked into position and will not move at all. A condition for moving an element is that only one of the tubes covered by the object is set to suck. On the other hand, if all tubes below the object are set to blow then the element is easily blown away from the surface. For larger objects (for example 5-by-5 pixels) one sucking tube is not enough to prevent the object from being blown away. It is probably necessary to increase the number of sucking tubes in the case of larger objects on the surface; however, this has not yet been tested.

The open-loop translation converging wave method has a problem in that the position of the object is not sensed, so in the event that the object is stuck somewhere on the surface the object may not reach the desired destination.

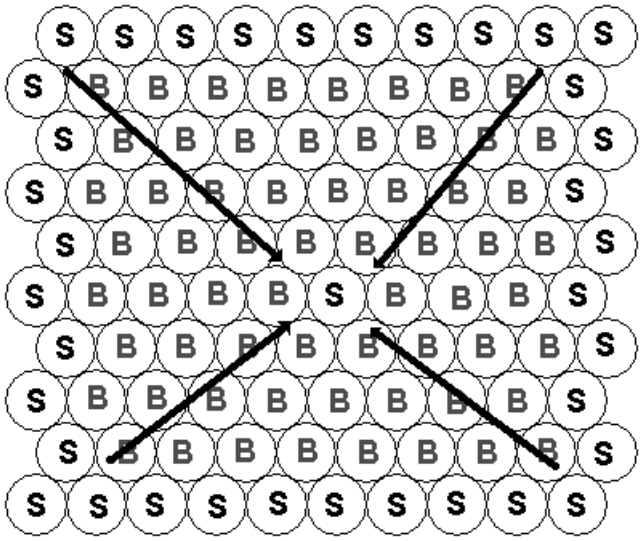

Sl. 1. *Postopek "konvergenčnih valov" (S-sesanje, B-pihanje)*
Fig. 1. *"Converge waves" procedure (S-suck, B-blow)*

1.2 Krmiljenje vrtenja

Ta metoda se imenuje tudi "premikanje črte sesanja". Objekt vrtimo v ravnini NPAP okoli osrednje točke, ki jo definira uporabnik takole: operater izbere osrednjo točko, ki je v enem izmed vogalov objekta, nato izbere še želeno točko, ki je hkrati tudi konvergentni center za konvergentne valove. Črta med tema dvema točkama je nova želena lega roba objekta. Želena točka mora biti izbrana blizu enega izmed vogalov objekta, ki je čim dalje od osrednje točke. Želena točka mora biti izbrana v smeri želene rotacije. Med vrtenjem objekta vse cevke pihajo, razen tistih, ki tvorijo črto med osrednjo in želeno točko. Če je katera izmed cevk, ki sestavljajo omenjeno črto, pokrita z objektom, tedaj mora tudi ta cevka izvrševati ukaz pihanja. Če se to ne bi zgodilo, tedaj bi objekt miroval prisesan na površino. Seveda sta tako želena kakor osrednja točka vedno točki sesanja. Obenem se uporabijo ponavljajoči se konvergenčni valovi za nastanek vibracij na površini NPAP, ki se ožijo v smeri proti želeni točki. Te vibracije so pomembne zato, da preprečijo objektu z ostrimi robovi, da bi se zataknil v vdolbinah med vrstami cevk. Metoda je opisana in prikazana na sliki 2. Črta med cevkama osrednje in želene (konvergentno središče) točke pomeni črto sesanja. Krivulja na nasprotni smeri od osrednje točke sukanja objekta v smeri želene točke pomeni smer vrtenja okoli osrednje točke.

1.3 Krmiljenje preobračanja

Preobračanje objekta pomeni, da je stran objekta, na kateri je pred obračanjem ležal objekt, potem obrnjena kvišku. Preobračanje tako pomeni gibanje, ki je zunaj ravnine aktivne površine in je zaradi

1.2 Open-loop rotation

This method is called "a moving sucking line". The procedure for rotating the object about a user-defined center point is as follows. First, the operator chooses the center point, which is on one of the corners of the object. The user also selects a desired point (converge center). The line between these two points is the new desired position for the edge of the object. The desired point has to be chosen close to (or in a neighborhood of) one of the corners of the object that is far away from the center point. The desired point also has to be in the direction of the desired rotation. During the rotation of the object all the tubes are set to blow except those forming a line between the center point and the desired point. If any of the tubes forming this line, other than the center of rotation, are covered by the object they must also be set to blow. If they do not blow they will lock the object down preventing it from moving as desired. Of course, both the center and the desired points have to be set to suck. In order to induce the required vibration there are also repetitive waves of sucking tubes converging towards the desired point. The vibrations are needed to prevent an object with sharp edges from getting stuck in gaps between the rows of tubes. The method described is illustrated in figure 2. The line between the center point (tube) and the desired point (converge center or the desired tube) represents the sucking line. The curve from the opposite side of the center point of the object to the direction of desired point shows the direction of rotation about the center point of the object.

1.3. Open-loop flipping

Flipping an object consists of turning an object around so that the side originally facing the active surface will be facing away from the surface. This involves motion out of the plane of the active

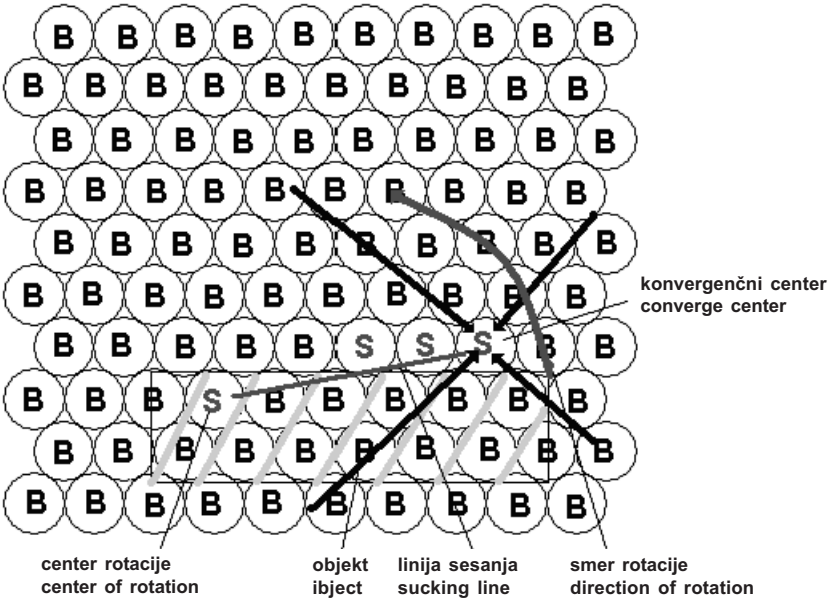

Sl. 2. *Krmiljenje vrtenja z metodo "premikajoče se črte sesanja" (B-pihanje, S-sesanje) (objekt je predstavljen s pravokotnikom, ki je pobarvan s sivimi črtami)*
Fig. 2. *Open-loop rotation about the center with "moving sucking line" method (B-blow, S-suck). The object is represented by the rectangle with gray strips*.

tega mnogo bolj zahtevna, kakor sta vrtenje in premik objekta na sami ravnini. Vdolbine med cevkami po navadi povzročajo težave pri tehnikah krmiljenja brez povratne zveze, ker objekt ne more gladko drseti po površini in se zaradi tega pogosto zatakne na njej. Zato smo pri poprej opisanih metodah uporabljali konvergentne valove in s tem vibracije, da bi preprečili zatikanje ostrih robov objektov v vdolbinah aktivne površine. V primeru preobračanja objekta pa so prav te vdolbine potrebne. V samem začetku preobračanja se mora oster in relativno raven rob objekta poravnati z vdolbino med cevkami, vse cevke vzdolž roba objekta pa izpolnjujejo ukaz sesaj. Nato se izvede ukaz "pihaj" na vse cevke, ki jih pokriva objekt. Ta ukaz povzroči, da se objekt dvigne kvišku za 90 stopinj in obmiruje na svojem ostrem robu, zataknjenem v vdolbini. Po tem dvigu objekta kvišku se izpolni ukaz "sesaj na vseh cevkah na drugi strani objekta", kar povzroči, da se objekt prevrže in obleži na aktivni površini na drugi strani objekta. Preobračanje objekta kaže slika 3.

Naslednji postopek natančno opisuje preobračanje objekta vzdolž črte sesanja:

- Korak 1: prisesaj objekt na površino in začni sesati na črti sesanja (sl. 3)
- Korak 2: začni pihati skozi cevke, najprej v tretji, nato v drugi vrsti pod objektom. Objekt bo počasi začel drseti proti vdolbini med črto sesanja in prvo vrsto, ki jo pokriva objekt. Po tej aktivnosti se bo oster rob objekta zataknil v vdolbini in se nekoliko dvignil, kakor je prikazano na sliki 4.
- Korak 3: prva vrsta cevk je v tem trenutku izpolnila ukaz, "pihaj". Objekt se dvigne na svoj oster rob vzdolž črte sesanja, tako da

surface and is therefore more challenging than rotation and translation within the plane. The gaps between the tubes are usually a complicating factor in the open-loop translation and rotation control techniques because an object cannot slide smoothly and often gets stuck at the edges or in the gaps. Vibration techniques such as converge waves have been used to prevent objects from sticking with their sharp edges in the gaps. In the case of a flipping operation the grooves are desired or even required. Before initiating the flip a sharp (and relatively straight) edge of the object is aligned with a groove in the surface and the tubes along this edge are set to suck. Then the object is lifted up to approximately 90 degrees by blowing through all the tubes that were covered by the object and were sucking the object a moment before. After the object has been lifted up to 90 degrees and rests on the sharp edge suction is initiated on this other side of the sucking line so the object is laid down on the other side. The flipping of the object is shown in Figure 3.

The step-by-step procedure for how to flip an object along a line of sucking tubes is as follows:

- Step 1: suck the object and then set to suck on the sucking line (Figure 3).
- Step 2: set to blow, first to the third and then to the second row, of the object. The object slowly slides towards the gap between the sucking line and the first row covered with the object. After this step the sharp edge of the object is stuck in the gap once the object is lifted up a little as shown in Figure 4.
- Step 3: the first row covered by the object is immediately set to blow. The object is lifted up on the sharp edge on along the sucking line so the

oklepa s površino kot okoli 90 stopinj. Pihajoči zračni tokovi ob obeh straneh objekta pomagajo stabilizirati objekt v pokončni legi (sl. 4).

- Korak 4: cevke na drugi strani linije sesanja spremenijo smer iz pihanja v sesanje, kar povzroči prisesanje objekta na površino (sl. 4).

object makes an angle of approximately 90 degrees with the surface. The air streams (blowing out) on each side of the object may assist in stabilizing the object in this position (Figure 4).

- Step 4: the tubes on the other side of the sucking line are changed from blowing to sucking and the object is sucked down onto the surface (Figure 4).

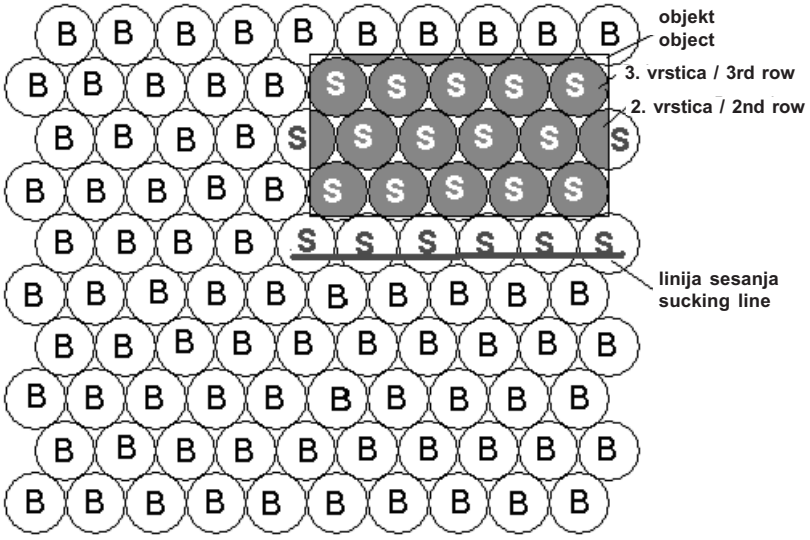

Sl. 3. *Začetna lega pri obračanju (B-pihanje, S-sesanje)*
Fig. 3. *A starting position for the flipping of the object (B-blow, S-suck)*

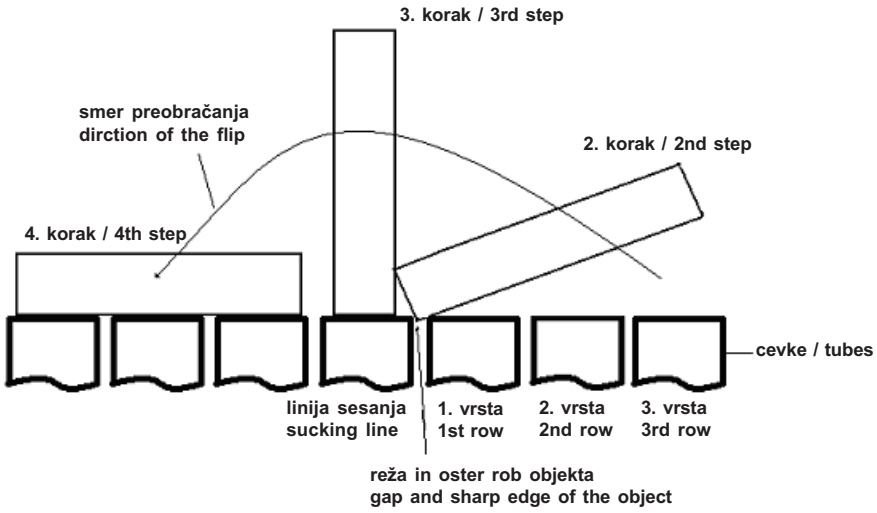

Sl. 4. *Preobračanje objekta*
Fig. 4. *The flipping of the object*

2 KRMILJENJE S POVRATNO ZVEZO

2.1 Krmiljenje premika s povratno zvezo

Da bi preprečili nenadzorovano zatikanje objekta na površini NPAP, kakor je to pogost primer pri tehnikah krmiljenja brez povratne zveze, smo v samo krmiljenje vključili informacijo o dejanski legi objekta. Osnovni koraki krmiljenja premika s povratno zvezo so:

2 CLOSED-LOOP CONTROL

2.1 Closed-loop translation

It is desirable to incorporate feedback information regarding the position of the object to prevent the object from getting stuck on the PASD, as is often the case when open-loop control techniques are used. The basic steps of the closed-loop translation control are:

- Korak 1: uporabnik definira želeno oziroma končno lego (cilj).
- Korak 2: meritev lege objekta.
- Korak 3: načrtovanje in izvedba premika objekta v novo lego.
- Korak 4: meritev nove lege.
- Korak 5: koraka 3 in 4 je treba ponoviti, če objekt ni dosegel želene lege, sicer se postopek ustavi.

V koraku 1 uporabnik določi želeno lego z uporabo miške na zaslonu osebnega računalnika, ki je uporabljen za komunikacijski vmesnik človek - stroj. Želena lega se preračuna v številko cevke, uporabljene za končno točko premika krmiljenja s povratno zvezo.

Korak 2 in 4 opravljata enako delo, to je meritev lege objekta na NPAP in določata dolžino objekta v smeri X in Y.

Korak 3 računa napake lege v smeri X in Y. Nato določi dolžino črte sesanja, ki je uporabljena kot prožilna sila za drsenje objekta proti želeni legi. Dolžina linije sesanja za premik v smeri Y je enaka pravokotni projekciji objekta na os X NPAP. Podobno velja za premik objekta v smeri X, kjer je dolžina črte sesanja enaka pravokotni projekciji objekta na os Y NPAP.

Korak 5 izvaja odločitev na podlagi izračuna položajnega odstopka (razlike med želeno in dejansko vrednostjo) v smeri X in Y. Če sta oba položajna odstopka v smeri X in Y enaka nič, tedaj je objekt dosegel želen položaj in postopek se s tem konča. Če želena lega ni dosežena, tedaj se ponovijo koraki 3, 4 in 5.

Razvili smo dve tehniki premika s povratno zvezo, ki se razlikujeta zgolj v koraku 3:

- običajni premik s povratno zvezo (OPPZ) in
- premik z navidezno povratno zvezo (PNPZ).

2.1.1. Tehnika krmiljenja običajnega premika s povratno zvezo (OPPZ)

Pri tej tehniki se objekt premika samo za eno črto naenkrat v smer X ali Y, dokler se ne doseže želena lega. Prvi korak 3 se izvede s proženjem črte sesanja v smeri X, kar povzroči, da se objekt premakne v smer X za eno črto (vrsto). Takoj za tem se izvedeta koraka 4 in 5, šele po tem pa se spet izvede korak 3, vendar tokrat v smeri Y za eno črto sesanja (sl.5a). Opisan vrstni red izvajanja posameznih korakov se izvaja, dokler želen položaj ni dosežen. Če je, npr. želena lega v smeri X dosežena prej kakor pa v smeri Y, tedaj se postopek nadaljuje samo za premike v smeri Y. Med izvajanjem črte sesanja v koraku 3 se izvajajo tudi konvergenčni valovi (gl. 1.1), da bi se preprečilo zatikanje objekta na površini NPAP. Konvergenčni valovi so osrednjeni v tisto izmed

- Step 1: user defines the desired end-position (target).
- Step 2: the position of the object is measured.
- Step 3: motion is planned and actuation is used to move the object.
- Step 4: the new position is measured.
- Step 5: if the object has not reached the desired position steps 3 and 4 are repeated, otherwise the process is stopped.

In step 1 the user clicks with a mouse on a desired position on the screen of the PC, which is used as a man-machine communication interface. The position of the mouse is translated into the tube number, which is used as an end point of the closed-loop translation.

Steps 2 and 4 are the same. They sense the position of the object on the PASD and calculate the length of the object in X and Y direction of the PASD.

Step 3 calculates a position error in the X and Y directions. It also calculates the direction and length of the "sucking line", which is used as an actuating force to slide the object towards the desired position. The length of the sucking line for a movement in the Y direction is the same as the rectangular projection of the object onto the X axis of the PASD. It is similar for a movement in the X direction, where the length of the sucking line is equal to a rectangular projection of the object onto the Y axis of the PASD.

Step 5 is used as a decision statement. It calculates the X- and Y-position errors: the differences between the actual and desired positions in both X and Y directions. If both X- and Y-direction errors are equal to zero the object has reached, the desired position and the procedure finishes. If the desired position is not reached, then steps 3, 4 and 5 are repeated.

The two closed-loop translating techniques according to two types of actuating procedures in step 3 were developed:

- a regular closed-loop translation (RCLT),
- a quasi closed-loop translation (QCLT).

2.1.1. Regular closed-loop translation (RCLT) technique

In this technique the object is moved one line at a time in either the X or the Y direction until the desired destination has been reached. First, step 3 is executed by sucking one line in the X direction resulting in the object sliding in the X direction by one line. Next, step 4 and 5 are executed. After that step 3 is executed again, but only for one sucking line, this time in the Y direction (see Figure 5a). The described procedure is repeated until the destination is reached. If, for example, the desired X position is reached before the desired Y position, then each of the following steps will only move the object in the Y direction. Converge waves (described in subsection 1.1) are also executed to prevent the object from getting stuck during the execution of the sucking line steps (step 3). The converging waves are centered on the end point of the sucking line with a greater

obeh končnih točk črte sesanja z večjo razdaljo do roba objekta. Hitrost premikanja objekta ob uporabi OPPZ je sorazmerno majhna, ker je po vsakem umeščanju s črto sesanja treba izvesti meritev lege objekta.

Slike 6a do 6e prikazujejo premikanje objekta (1,5mm × 0,9mm) od začetne do želene lege na stvarni NPAP z OPPZ. Slike (6f do 6j) kažejo meritve lege z mikroračunalnikom, ki so prikazane v istih trenutkih, kakor jih prikazuje zgornja vrsta slike 6. S slike 6 je razvidno, da meritve lege vedno ne ustrezajo dejanskim legam objekta na NPAP. Razlog za napačni merilni podatek je ta, da robovi objekta niso ostri, kakor tudi spodnja stran objekta ni ravna ploskev, kar povzroči, da nekatere cevke NPAP niso tesno pokrite z objektom. S slik 6c in 6d lahko razberemo, da se je objekt začasno zataknil na površini. Razrešitev tega problema je prikazana na sliki 6e, kjer so konvergenčni valovi poskrbeli za dovolj vibracij, kakor je opisano v prejšnjem odstavku.

2.1.2. Tehnika krmiljenja premika z navidezno povratno zvezo (PNPZ)

Tehnika PNPZ je bila razvita, da bi povečali hitrosti premikanja objekta na NPAP. Računanje in izvajanje črte sesanja (korak 3) v smereh X in Y se nadaljuje brez merjenja lege objekta na NPAP med črtami sesanja. Dve črti sesanja (ena v X, druga v smeri Y) sta generirani izmenoma in premikata objekt proti želeni legi (sl. 5b). Šele ko pričakujemo, da objekt doseže želeno lokacijo, izmerimo dejansko lego objekta. Če želena lega ni dosežena, se izračunajo in izvedejo nove črte sesanja v smeri proti želeni legi v eni ali obeh smereh. Tehnika PNPZ je krmiljenje brez povratne zveze na časovnem koraku med obema meritvama lege. Vsaka črta sesanja izvaja tudi konvergentne vibracije (gl. 1.1), da bi se preprečilo zatikanje objekta na površini NPAP. Konvergenčni valovi vzbujalnih vibracij imajo začetni premer izmere treh cevk, kakor je to bilo izvedeno pri OPPZ. Dosedanje izkušnje so pokazale, da se objekt sploh ni zatikal na površini. Mnogokrat pa se je zgodilo, da se je objekt nenadzorovano preobrnil na površini ob zatikanju, medtem ko se je izvajal postopek premika krmiljenja brez povratne zveze med dvema zaporednima meritvama dejanske lege objekta, nato pa je preprosto nadaljeval pot do želene vrednosti. Število nenadzorovanih obračanj se lahko močno zmanjša, če nekoliko znižamo nadtlak pihanja zraka skozi cevke.

Hitrost premikanja objekta ob uporabi PONPZ je bila približno 1cm/s, kar je desetkrat hitreje kakor v primeru uporabe OPPZ. Hitrost premikanja objekta je odvisna od dinamične interakcije med NPAP in objektom. S povečevanjem razlike nadtlaka pihanja

distance to the edge of the PASD than the other end point of the same sucking line. The movement of objects using the RCLT method is slow because after each sucking line operation (step 3) a complete position measurement is required.

Figures 6a–6e show the movement of an object (1.5mm × 0.9mm) from the start position to the desired position on a real PASD with RCLT. Figures (6f–6j) in the lower row show the measurement of position with a microcomputer and are presented on the screen of the computer at the same time as the real object position is shown in the upper row of Figure 6. From Figure 6 we can see that the measurement positions do not always match the real positions of the object on the PASD. This is because either the edges of the object are not sharp or the bottom side of the object is not a regular plane, which means that some tubes on the PASD are not tightly covered with the object. Figures 6c and 6d show that the lower left corner of the object got temporarily stuck. The problem is solved as in Figure 6e with the use of converge waves described above.

2.1.2. Quasi closed-loop translation (QCLT) technique

The QCLT technique was developed with the aim of increasing the speed of the object on the PASD. The calculation and execution of the sucking line (step 3) in the X and Y directions continues without measuring the object position on the PASD in between waves. In fact, two sucking waves (one in the X direction, another in the Y direction) are created simultaneously and they move the object towards the desired position (see Figure 5b). Once the object should have reached the desired location the position is measured and compared to the desired position. If the desired position is not reached a new set of waves are calculated and executed in one or two directions, as needed. The QCLT technique is an open-loop translating procedure during the time interval between two position measurements. To prevent the objects from getting stuck somewhere on the PASD every sucking line also has its own converging excitation (see subsection 1.1). The convergewave has a starting diameter of 3 pixels, as was the case for the RCLT technique. Experience has shown that objects do not get stuck at all; it is more likely that the object flips uncontrollably if it gets stuck for a moment during the open-loop-translating procedure between two position measurements and then continues on the path demanded by the sucking line waves. The number of uncontrolled flips can be decreased if the blow pressure is slightly reduced.

The speed of the object movement using the QCLT technique is approximately 1 cm/sec, which is a tenfold improvement over the RCLT technique. The speed of the object movement depends on the dynamic interaction between the PASD and the object.

in podtlaka sesanja v cevkah lahko povečamo hitrost premikanja objekta po površini. Hitrost pa se zmanjša, če je objekt težji, oziroma površina objekta ali NPAP bolj hrapava, ker je v obeh primerih večje trenje. Če bi črta sesanja potovala prehitro v primerih povečanega trenja med objektom in površino, tedaj bi prišlo do manjšega prenihaja prek želene lege ali pa bi bilo celo mogoče, da bi objekt odpihnilo s površine NPAP, ker objekt ne bi mogel dovolj hitro slediti premikajočim se črtam sesanja.

V splošnem lahko rečemo, da PNPZ omogoča hitrejše premikanje objekta po površini (1 do 1,5cm/s), medtem ko OPPZ omogoča le počasnejše (0,1 do 0,15 cm/s), vendar natančnejše pozicioniranje objekta na površini NPAP.

Increasing the difference between positive (blow) and negative (suck) pressures can increase the speed of the object's movement. The speed can be reduced if the object is heavier or if the surface is rough; in both cases the friction is higher. If the sucking line waves are travelling to fast in these high-friction situations the objects may slightly overshoot the desired position or it may even be blown off the PASD because the object cannot follow the sucking lines fast enough.

In general the QLCT technique allows enables the faster movement of objects (1–1.5 cm/sec), while the RCLT technique allows slower (0.1–0.15 cm/sec) but more accurate positioning of the object on the PASD.

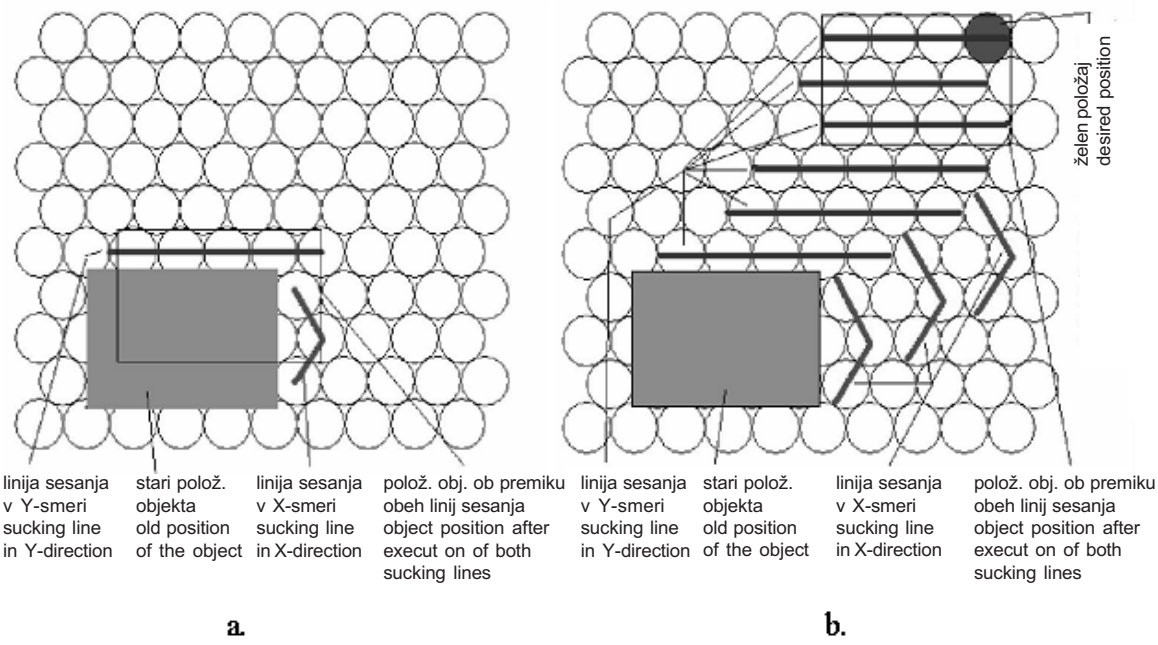

Sl. 5. *Premik objekta s tehniko OPPZ (a) in PNPZ (b)*
Fig. 5. *Translating the object with the RCLT (a) and QCLT (b) techniques*

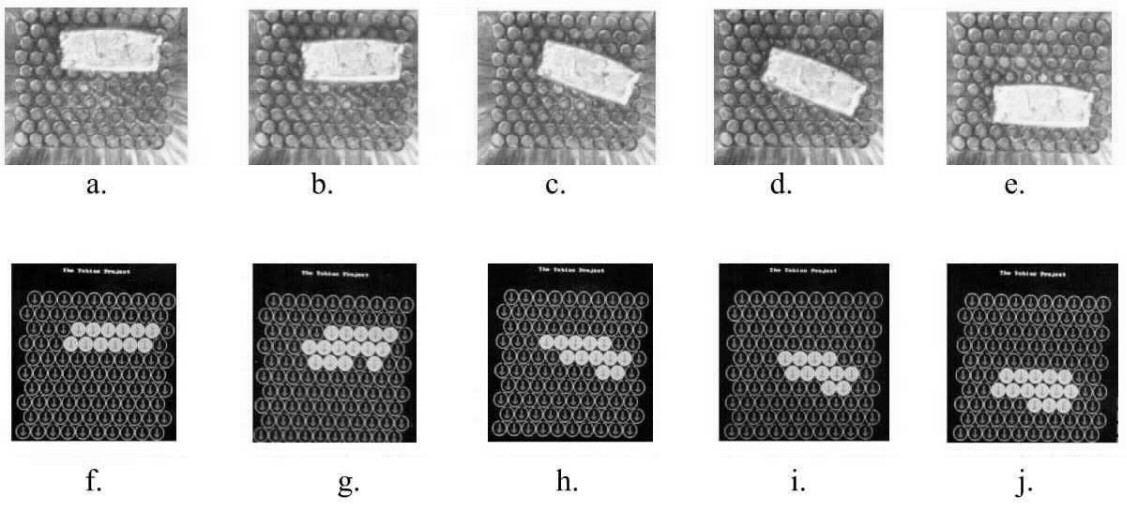

Sl. 6. *Premik objekta na stvarni NPAP z OPPZ*
Fig. 6. *Movement of the object on a real PASD with RCLT*

2.2 Krmiljenje vrtenja s povratno zvezo

Tehnika krmiljenje vrtenja s povratno zvezo je v bistvu razširitev poprej opisane tehnike vrtilnega krmiljenja brez povratne zveze, predstavljene v podpoglavju 1.2. Osnovni koraki postopka izvajanja krmiljenje vrtenja s povratno zvezo so naslednji:

- Korak 1: uporabnik poda želeni kot zasuka vrtenja.
- Korak 2: meritev lege objekta.
- Korak 3: prožilno polje cevk premakne objekt do želenega kota vrtenja.
- Korak 4: meritev nove lege objekta.
- Korak 5: postopek se konča, razen če objekt ni opravil predpisanega kota zasuka. Takrat se morata koraka 3 in 4 ponoviti.

Uporabnik določi dve točki: vrtilno središče, ki je blizu enega izmed koncev objekta, in novo želeno lego drugega konca objekta. To se opravi s pritiskom na miško na mesto na zaslonu, kjer se prikazuje lokacija objekta, izmerjena v koraku 1. Nato računalniški algoritem izračuna želeni kot zasuka. Dejanski kot se izračuna iz črte, narejene med obema koncema objekta v koraku 1. Računalniški algoritmi izmerijo in izračunajo tri točke: želeno vrtilno središče, dejanski konec objekta in želeni konec objekta v korakih 2 in 4 (sl. 7). Nato sledi v koraku 4 izvedba proženja, ki vrti objekt za želeni kot zasuka. Če se objekt ni zasukal za želeni kot zasuka ali zasedel točko želene lege, se koraka 3 in 4 ponovita, ampak tokrat z novim želenim kotom zasuka. Algoritem konstruira novo želeno črto, ki sloni na prvotni želeni točki, povečani za en premer cevke v smeri stran od dejanske črte. Ponavljanje korakov 3 in 4 z novo želeno črto, ki je nekoliko stran od premikanega objekta, je treba v

2.2 Closed-loop rotation

The closed-loop rotation technique is an extension of the previously described open-loop rotation technique from subsection 1.2. The basic steps of closed-loop rotation are:

- Step 1: user gives the desired angle of rotation.
- Step 2: the position of the object is measured.
- Step 3: the actuators are used to move the object to the desired angle of rotation.
- Step 4: the new position of the object is measured.
- Step 5: if the object has not reached the desired angle of rotation then steps 3 and 4 are repeated, otherwise the procedure is stopped.

A user has to define two points: the center of rotation (located near one end of the object) and the new, desired location of the other end of the object. This is done by clicking with the mouse on a screen showing the object sensed in step 1. Based on this a computer algorithm calculates the desired angle. The actual angle is calculated from the line drawn between both ends of the objects as observed in step 1. The computer algorithm measures and calculates all three points (an actual or desired center of rotation, an actual end of the object and a desired end of the object) in steps 2 and 4 (see figure 7). An actuation is executed to move the object from the actual angle to the desired angle (step 4). If the object has not reached the desired angle or occupied the desired position point the algorithm repeats steps 3 and 4, but with a new, desired angle of rotation. The algorithm constructs a new, desired line based on the originally desired end point that is increased by one pixel away from the actual line. Repeating steps 3 and 4 with a new, desired angle that is a little further away from the controlled object is frequently required when the object does not

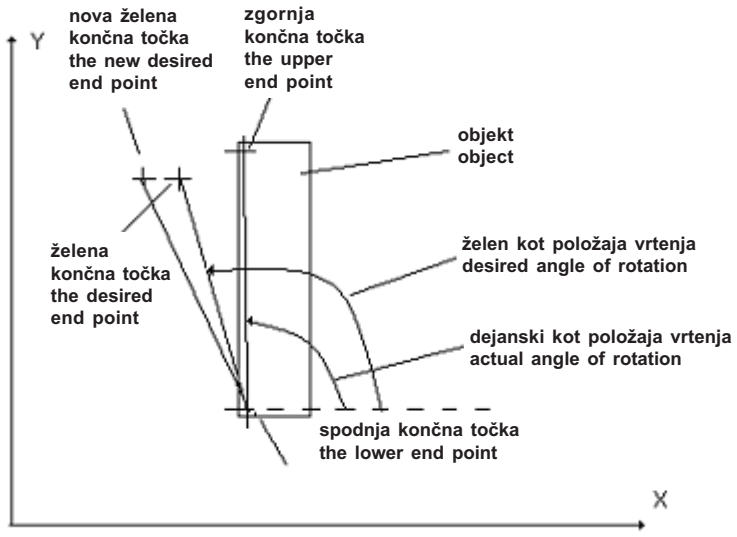

Sl. 7. *Definicije kotov vrtenja*
Fig. 7. *The definition of rotation angles*

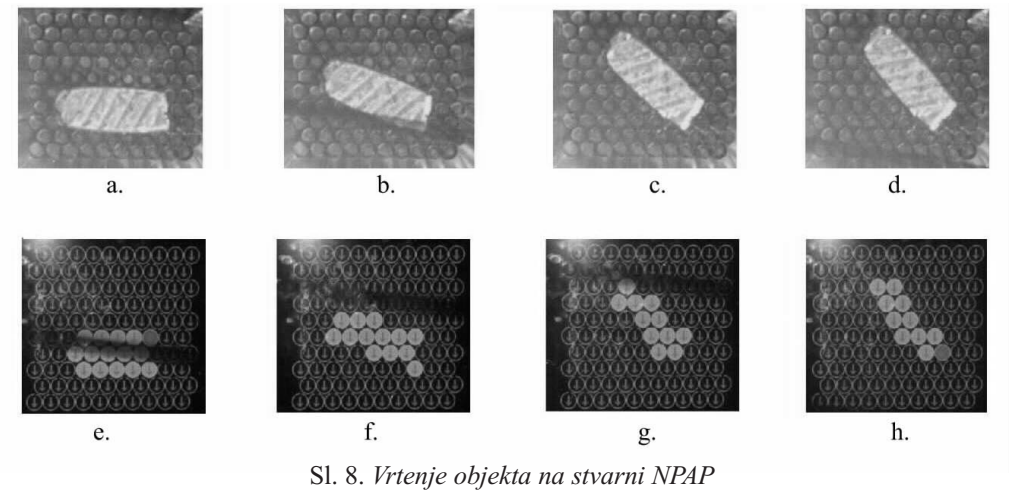

Sl. 8. *Vrtenje objekta na stvarni NPAP*
Fig. 8. *Rotation movement of the object on the real PASD*

primeru, ko objekt nima ravne spodnje površine. Če sta želeni kot zasuka ali želena točka dosežena, naprava konča postopek v koraku 5. Konvergenčni valovi, opisani v podpoglavju 1.1 se ves čas izvajajo med krmiljenjem vrtenja objekta s povratno zvezo, da bi preprečili zatikanje objekta z ostrimi robovi na površini. Konvergenčni valovi so usmerjeni v želeno točko črte sesanja.

Slike 8a do 8j kažejo vrtenje objekta okoli njegovega spodnjega desnega vogala za 60 ločnih stopinj na dejanski NPAP. S slik 8h in 8j vidimo, da se je središče vrtenja premaknilo za en premer cevke v smer Y. Razlog za to je v tem, da robovi v bližini spodnjega levega vogala niso ostri, tako da nekatere cevke NPAP pod objektom niso tesno pokrite.

2.3 Krmiljenje preobračanja s povratno zvezo

Tehnika obračanja objekta na površini NPAP z krmiljenjem s povratno zvezo sloni na tehniki, opisani v podpoglavju 1.3. Razlika med obema tehnikama je v tem, da računalniški algoritem posredno določi, ali se je objekt obrnil ali pa ne. Potreben pogoj za preobračanje objekta na površini pri obeh tehnikah je: oster rob objekta in obstoj vdolbine med cevkami na površini NPAP. Ker nekateri robovi objektov niso dovolj ostri ali vdolbine med cevkami na površini niso dovolj globoke ali pa kombinacija obeh omenjenih razlogov, se zgodi, da v okoli 25 % primerov tehnika krmiljenja brez povratne zveze ne deluje. Tako postane zelo pomembna identifikacija, ali je bila zadana naloga obračanja objekta opravljena ali ne. Uporabili smo metodo za posredno določevanje, ali se je objekt preobrnil na površini NPAP.

- Korak 1: določitev objekta z meritvijo v njegovi prvotni legi.
- Korak 2: poskus obračanja objekta ob uporabi tehnike obračanja s krmiljenjem brez povratne zveze.
- Korak 3: določitev objekta na novi lokaciji z meritvami.
- Korak 4: Nova in stara lega objekta se primerja: če sta legi narazen za več ko tri vrste, tedaj se je

have a flat bottom. If the desired angle or desired position has been reached the algorithm finishes the procedure in step 5. Converge waves (described in subsection 1.1) are also executed to prevent the object (particularly objects with sharp edges) from getting stuck during the execution. The converge waves are centered on the desired end-point of the sucking line.

Figures 8a–8j show the rotation of the object about the lower right corner by 60 degrees on the real PASD. Figures 8h and 8j show that the measured center of rotation is moved slightly (by 1 pixel) in the Y direction. The reason for this is that the edges of the object close to the lower right-hand corner are not sharp, so the tubes of the PASD under the object are not tightly covered.

2.3 Closed-loop flipping

The closed-loop flipping technique uses the same basis as the open-loop flipping technique described in section 1.3. The only difference between them is that a computer algorithm is used to determine whether the object is flipped or not. The necessary conditions for flipping are the same in both techniques: a sharp edge of the object and an existing gap between tubes on the PASD. Because some of the edges on the object are not sharp enough or some of the gaps between the tubes are not deep enough, or a combination of both reasons, it happens in approximately 25% of cases that the open-loop flipping technique does not work. Therefore, it becomes important to identify whether or not the task has been completed successfully. An indirect method is used to determine if the object has actually been flipped:

- Step 1: the object is sensed in its original position.
- Step 2: an attempt is made to flip the object using the open-loop flipping technique.
- Step 3: the object is sensed in its new position.
- Step 4: the new and old positions are compared: if they differ by more than three rows the object

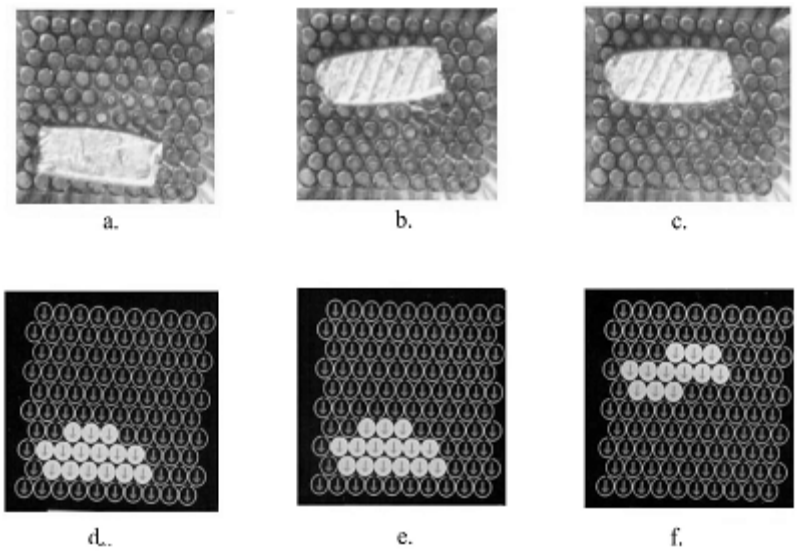

Sl. 9. *Krmiljenje preobračanja objekta s povratno zvezo na dejanski NPAP*
Fig. 9. *A closed-loop flipping of the object on a real PASD*

objekt obrnil pravilno (nadaljevanje s korakom 5), če ne, algoritem ponovi celotni postopek od koraka 1 do 4.

- Korak 5: konec.

S povečevanjem nadtlaka pihanja lahko povečamo odstotek uspešno izvedenih poskusov obračanja brez povratne zveze. Vendar se moramo zavedati, če preveč povečamo nadtlak pihanja skozi cevke, se poveča tudi število neuspelih poskusov obračanja zaradi tega, ker se objekt odpihne s površine NPAP.

Slike 9a do 9f kažejo obračanje objekta s krmiljenjem s povratno zvezo na dejanski NPAP. Sliki 9a in 9d kažeta lego objekta pred obračanjem. Sliki 9b in 9e kažeta lego objekta trenutek po tem, ko se je izvedlo obračanje, preden se je novo izmerjena lega prikazala na zaslonu. Sliki 9c in 9f kažeta lego objekta po končanem obračanju objekta s krmiljenjem s povratno zvezo.

3 UPORABA ORODIJ NA NPAP

Orodja so objekti, ki jih postavimo na NPAP zato, da bi povečali učinkovitost delovanja z objekti. Na primer, obe uporabljeni tehniki krmiljenja togih objektov s povratno zvezo in brez nje imata nekaj pomanjkljivosti, posebej sorazmerno počasen premik objekta po površini, pa tudi razpoznavanje objekta je omejeno zgolj na pravokotno projekcijo objekta na površini NPAP; torej višine objekta ne moremo izmeriti. Z uporabo posebej načrtovanih orodij se lahko tema dvema problemoma izognemo, kakor je pojasnjeno v nadaljevanju.

3.1 Povečanje hitrosti pomika objekta na NPAP

Na začetku poglavja 2 smo omenili, da trenje med objektom in površino NPAP omejuje hitrost pomika togega objekta na površini. Torej hitrost pomika objekta na površini lahko povečamo, če

has flipped correctly (continue with step 5), if not then the algorithm repeats the whole procedure from step 1 to step 4.

- Step 5: the end.

Using a higher positive (blowing) pressure can increase the percentage of successfully completed open-loop flipping attempts. Unfortunately, however, the number of cases where the object is blown off the surface is also increased when the pressure is increased too much.

Figures 9a–9f show closed-loop flipping on a real PASD. Figures 9a and 9d show the position of the object before the flipping. Figures 9b and 9e show the position of the object a moment after the flipping, prior to measuring the position with the computer. Figures 9c and 9f show the position after the closed-loop flipping of the object.

3 USING TOOLS ON PASD

Tools are objects, other than the parts being handled, which can be placed on the PASD. They are used to improve the handling or processing of the parts. For example, both open-loop and closed-loop position-control techniques for rigid objects have some disadvantages: movement of the part is relatively slow, and recognition of the part's size is limited to the footprint, which means the third dimension (height) cannot be observed. With the use of specially designed tools it is possible to overcome these two problems as explained below.

3.1 Increasing the speed of a movement on the PASD

As mentioned at the start of section 2, it is mainly the frictional force between the object and the PASD that limits the speed of an object moving on the PASD. So, if the frictional force can be reduced the speed of

nam uspe zmanjšati trenje med njima. Zmanjševanje hrapavosti površine je ena izmed možnosti, ki pa po drugi strani preprečuje izvajanje obračanja objekta na taki površini (gl. 1.3). Uspešna rešitev tega problema je, da uporabimo namensko orodje, ki zelo zmanjša hrapavost površine NPAP in posledično zmanjša tudi trenje med površino NPAP in objektom. To namensko orodje je preprost gibljiv plastični trak, ki se uporabi za pot med trenutno in želeno lego objekta. Plastični trak mora biti zelo tanek in gibljiv. Naslednji koraki algoritma opisujejo postopek za povečanje hitrosti objekta na NPAP (sl. 10):

- Korak 1: Postavi gibljiv trak PVC primerne izmere na mesto med trenutnim in želenim položajem objekta. Trak je mogoče premikati po površini NPAP z uporabo posebnih tehnik, razvitih za pomik gibljivih objektov, ki bodo razložene v naslednjem prispevku.
- Korak 2: Izmeri lego traku in postavi vse cevke pod trakom na sesanje, kar povzroči, da je trak utrjen na mestu v naslednjih korakih.
- Korak 3: Vse preostale cevke okoli traku morajo pihati.
- Korak 4: Objekt se odlepi in oddrsi s trenutne lege proti želeni legi zato, ker pod objektom začne pihati iz cevk, na želeni legi na drugi strani traku pa hkrati cevke sesajo.
- Korak 5: Objekt prepotuje oziroma drsi z ene strani na drugo stran traku v kanalu pihajočega zraka na vsaki strani traku, ki objektu omogoča potovanje zgolj po traku v "trenutku".

Hitrost pomikanja togega objekta na NPAP z gibljivim trakom PVC je okoli 10 do 15 cm/s, kar je

motion can be increased. Lowering the friction of the whole surface is not an option, as this will prevent operations like the flipping of objects (see subsection 1.3). A successful solution to this problem is the use of a special tool that can dramatically reduce the roughness of the PASD and, therefore, the frictional forces between the PASD and the object during the movement. This special tool is a simple flexible plastic band, which is used as a path between an actual position and a desired position of the object on the PASD. The plastic band has to be very thin and flexible. The method of increasing the speed of the movement on the PASD is described in the next steps (see figure 10):

- Step 1: Place the flexible PVC band of proper dimensions between the actual and desired positions of the object. It is possible to move it from one place on the PASD to another place using special techniques developed for handling flexible objects.
- Step 2: Detect the position of the band and set all the covered tubes of the PASD on suck, so the band is fixed during the next steps.
- Step 3: All other tubes on both sides of the band have to be set to blow.
- Step 4: The object is released from its current position by switching to blow in the tubes that were covered by the object, and setting to suck the tubes of the desired position on the other side of the PVC band at the same time.
- Step 5: The object travels (slides) from one side to another side of the band practically instantaneously.

The speed of the movement using the described method is approximately 10–15 cm/sec,

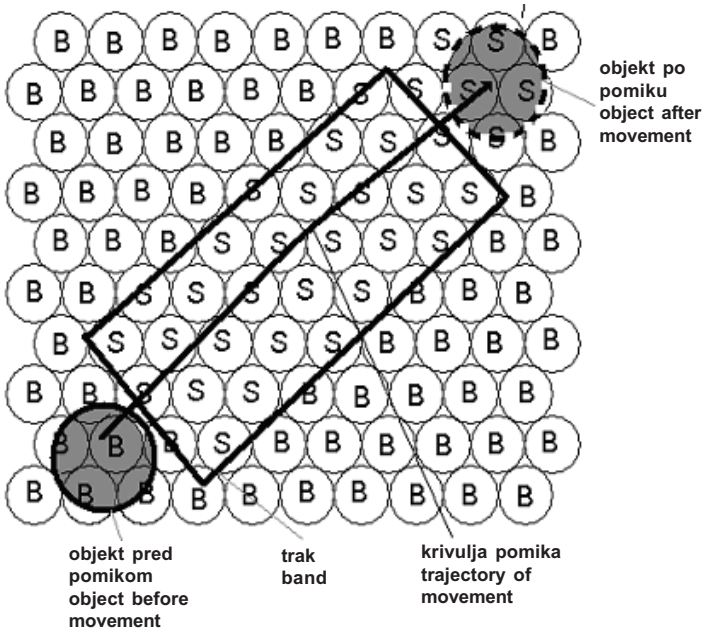

Sl. 10. *Povečanje hitrosti pomika objekta na NPAP z uporabo traku*
Fig. 10. *Increasing the speed of the object on the PASD with the band*

desetkrat hitreje od do sedaj opisane najhitrejše PNPZ, opisane v podpoglavju 2.1.2. Opravili smo teste s plastičnim trakom dolžine 6 mm, ker smo bili omejeni s površino NPAP (5 mm × 5 mm). Menimo, da bi lahko trak podaljšali za večkrat ob zadovoljivih rezultatih premikanja objekta.

3.2 Nastavljanje lege objekta na gibljivem traku

V postopku, opisanem v prejšnjem podpoglavju, smo uporabili trak kot drsno površino na NPAP za hiter pomik objekta prek traku. Gibljiv trak z gladko površino se lahko uporabi tudi za nastavljanje lege objekta na traku. Predlagana metoda je krmiljenje premikanja togega objekta brez povratne zveze na vrhu traka PVC. Majhno trenje med objektom in trakom, ki leži na površini NPAP, omogoča delovanje postopka. Slika 11 prikazuje delovanje prej omenjenega postopka:

- Korak 1: Gibljiv plastični trak postavimo na NPAP in objekt postavimo na trak.
- Korak 2: Cevke sesajo na mestu želene lege (približno na sredini traku), drugod pa cevke pihajo.
- Korak 3: Objekt potuje (drsi) z višje lege traku, ki ga sestavljajo pihajoče cevke pod trakom v smeri depresije na traku, ki jo sestavljajo sesajoče cevke zaradi kombinacije gravitacijske sile in majhne sile trenja.
- Korak 4: Če se depresija na traku premika, se z njo premika tudi objekt.

Hitrost pomika objekta s tem postopkom je okoli 1 do 1,5 cm/s. Seveda je ta metoda krmiljenje brez povratne zveze po legi, kar lahko povzroči neljube zaplete, objekt ne sledi depresiji zaradi različnih razlogov.

which is 10 times greater than the QCLT method described in subsection 2.1.2. Tests were made with a 6-mm length of the plastic band because of the limitations of the square area (5 × 5 mm) of the PASD. But we believe that the length of the band could be several times longer than that used in these tests.

3.2 Positioning of an object on a flexible band

In the previous method the band was used as a "sliding" surface on the PASD to bring the object from one end to the other in a short period of time. A flexible low-friction surface can also be used to position an object within the surface or the band, as described in this section. The proposed method is an open-loop control technique for moving an object on the top of the flexible plastic surface. A low frictional force between the object and the band lying on the PASD is essential. Figure 11 shows how this control technique works:

- Step 1: The flexible material is placed on the PASD, and the object is placed on top of the flexible material or the band.
- Step 2: The valves are set to suck somewhere in the middle of the band (where the object should be going to) and set to blow on each side of the sucking region.
- Step 3: The object travels from the "hills" above the blowing tubes to the depression made by the sucking tubes because of the gravitational force combined with the low friction between the object and the flexible band.
- Step 4: If the depression on the band is moving the object follows it on the top of the band.

The speed of movement with this method is approximately 1–1.5 cm/sec. Of course this kind of method is open-loop control technique so it could happen that the object does not always slide to the depression on the band generated by the sucking tubes.

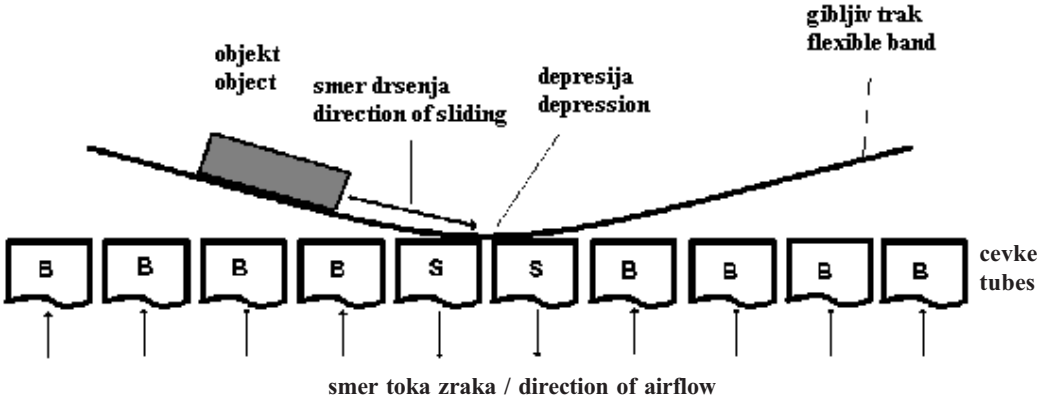

Sl. 11. *Nastavljanje lege objekta na traku*
Fig. 11. *Positioning of the object on the band*

3.3 Mostično orodje

Na NPAP je mogoče izmeriti z zaznavali pritiska zgolj pravokotno projekcijo objekta na površino. Tako lahko določimo zgolj dvoizmerno sliko objekta na površini, medtem ko tretja izmera (višina) ostane nepoznana. Mostično orodje se uporabi za določitev višine objekta. Če lahko objekt drsi pod mostom, lahko ocenimo, da je višina objekta nižja od razdalje med površino in nižjim spodnjim delom mostičnega orodja. Na ta način se da grobo določiti višino objekta. Če uporabimo več različnih mostičnih orodij zaporedoma, lahko določimo višino objekta dokaj natančno. Slika 12 prikazuje uporabo mostičnega orodja.

3.3 A "bridge" tool

It is only possible to measure the footprint of an object on the PASD with pressure sensors. It is, therefore, only possible to obtain a two-dimensional picture of the object on the surface; the third dimension (height) remains unknown. A bridge tool is used for determining the height of objects. If an object can go under the bridge we know that the height of the object is smaller than the distance between the surface and the lower part of the bridge tool. In this way it is possible to roughly determine the height of an object. It is of course necessary to have several different bridge tools to be able to distinguish between different height groups. Figure 12 shows the use of the bridge tool.

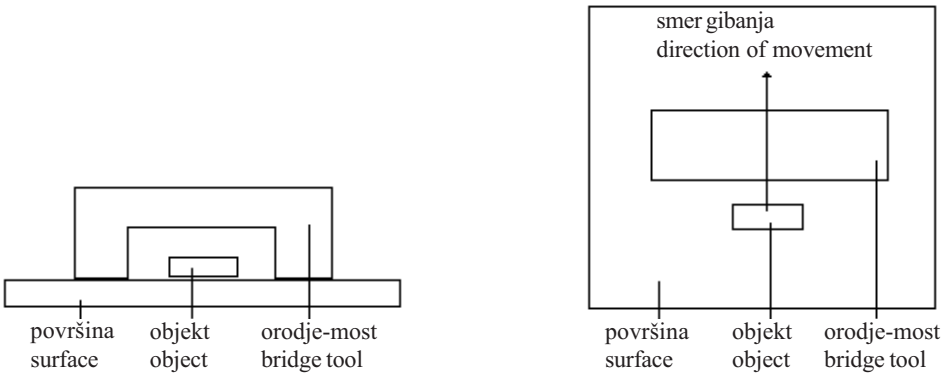

Sl. 12. *Uporaba mostičnega orodja za določitev višine*
Fig. 12. *Use of the bridge tool to determine the object's height*

4 SKLEP

Ta prispevek prikazuje najprej preskuse tehnik krmiljenja brez povratne zveze po legi, utemeljene na konvergenčnih valovih za premik, vrtenje in obračanje togega objekta, manjšega od 1 mm na prototipu NPAP. Ker so omenjene tehnike imele težave pri krmiljenju, kar je bila posledica pogostih zatikanj objektov na površini NPAP, smo v krmiljenje brez povratne zveze vključili informacijo o legi objekta. Drugi del prispevka tako opisuje krmiljenje s povratno zvezo lege za premik, vrtenje in obračanje togega objekta na površini NPAP. Obe tehniki krmiljenja objekta po legi na NPAP, predstavljeni v prvih dveh delih prispevka, imata naslednji pomanjkljivosti: relativno počasno premikanje objekta in razpoznavanje velikosti in oblike objekta iz odtisa (dotikalne površine med objektom in površino NPAP), tako da tretje izmere (višine) objekta ni bilo mogoče določiti. Zato zadnji del prispevka opisuje uporabo posebnih "orodij" (prilagodljivi trak in gibljivi"most"), ki zaobideta omenjena problema.

Naslednji prispevek na temo NPAP v naslednji številki Strojniškega vestnika bo prikazal natančen opis tehnik krmiljenja brez povratne zveze in krmiljenje s povratno zvezo lege za gibljive objekte na NPAP.

4 CONCLUSION

This paper first presents the prototype design and experiments of the open-loop position-control techniques based on converging waves for translating, rotating and flipping rigid sub-millimeter objects on a PASD. It is also desirable to incorporate the feedback information regarding the position of the rigid object to prevent the object getting stuck on the PASD as it is often the case when open-loop control techniques are used. The next part of the paper shows closed-loop position-control techniques developed for translating, rotating and flipping rigid parts on the PASD. The open-loop and closed-loop position-control techniques for rigid objects have some drawbacks: relatively slow movement of the part and a limited ability to recognise the size of the part; so the third dimension cannot be determined. The last part of the paper describes the use of specially designed tools – a flexible band and a bridge tool – to overcome these two problems.

Open-loop and closed-loop position-control techniques for flexible objects will be described in the next issue of Journal of Mechanical Engineering.

Zahvala

Projekt razvoja prototipne naprave NPAP je bil med drugim financiran tudi iz programa Fulbright-ovih štipendij in je bil izveden v laboratorijih Centra za tehniko avtomatizacije Središča za napredne tehnologije države new York na Politehničnem inštitutu v Resselaer-u. Avtorji prispevka bi se radi posebej zahvalili vsemu osebju, ki je karkoli prispevalo k razvoju NPAP v Središču za napredne tehnologije, posebej prof. Hary-ju Stephanou, Tobias-u Winther-ju in Ben-u Potsaid-u.

Acknowledgment

This project was funded by the Fulbright Scholar Program and was accomplished in the Laboratories of the Center for Automation Technologies, A New York State Center for Advanced Technology, Rensselaer Polytechnic Institute. The authors of the paper would like to thank all the personnel involved in the Center for Automation Technologies, especially to Harry Stephanou, Tobias Winther and Ben Potsaid.

5 LITERATURA
5 REFERENCES

[1] Böhringer, K.-F., B.R. Donald, N.C. MacDonald (1999) Programmable force fields for distributed manipulation, with applications to MEMS actuator arrays and vibratory parts feeders, *The International Journal of Robotics Research*, vol. 18, No. 2, 168-200.

[2] Böhringer, K-F., K. Goldberg, M. Cohn, R. Howe (1988) Parallel microassembly with electrostatic force fields, *Proceedings of the 1998 IEEE*, International Conference on Robotics & Automation, Lueven, Belgium, 1204-1211.

[3] Kavraki, L. E. (1997) Part orientation with programmable vector fields: two stable equilibria for most parts, *Proceedings of the 1997 IEEE*, International Conference on Robotics and Automation, Albuquerque, New Mexico, 2446-2451.

[4] Luntz, J. E., W. Messner, H. Choset (1997) Parcel manipulation and dynamics with a distributed actuator array: the virtual vehicle, *Proceedings of the 1997 IEEE*, International Conference on Robotics and Automation, Albuquerque, New Mexico, 2446-2451.

[5] Akiyama, T., D. Collard, H. Fujita (1997) Scratch drive actuator with mechanical links for self-assembly of three-dimensional MEMS, *Journal of Microelectromechanical Systems,* Vol. 6, No. 1, 10-17.

[6] Konishi, S., H. Fujita (1994) A conveyance system using air flow based on the concept of distributed micro motion system, *Journal of Microelectromechanical Systems*, Vol. 3, No. 2, 54-58.

[7] Wenheng, L., P. Will (1995) Parts manipulation on an intelligent motion surface, *Proceeding of IROS'95*, 399-404.

[8] Pister, K. S. J., R. Fearing, R. Howe (1990) A planar air levitated electrostatic actuator system, *Proceedings IEEE Workshop on MEMS*, Napa Valley, California, 67-71.

[9] Fujita, H. (1993) Group work of microactuators, *International Advanced Robot Program Workshop on Micromachined Technologies and Systems*, Tokyo, Japan, 24-31.

[10] Storment, C. W., D.A. Borkholder, V. Westerlind, J.W. Suh, N.I. Maluf, G.T.A. Kovacs (1994) flexible, dry-released process for aluminum electrostatic actuators, *Journals of Microelectromechanical Systems,* 3(3), 90-96.

[11] Liu, C., T. Tsao, P. Will, Y. Tai, W. Liu (1995) A micro-machined magnetic actuator array for micro-robotics assembly systems, *Transducers-Digest Int. Conf. On Solid-State Sensors and Actuator*s, Stockholm, Sweden, 34-38.

[12] Vikramaditya, B., B.J. Nelson (1999) Visually servoed micropositioning for robotics micromanipulation, *Microcomputer Application*, Vol. 18, No. 1, 64-72.

[13] Uran, S., R. Šafariè, T. Winther (2002) Pneumatic active surface device: prototype design and lyapunov stability analysis, *Strojniški vestnik*, 48(2002)4, 218-233.

Naslovi avtorjev: dr. Suzana Uran
prof. dr. Riko Šafarič
Fakulteta za elektrotehniko,
računalništvo in informatiko
Univerza v Mariboru
Smetanova 17
2000 Maribor
suzana.uran@uni-mb.si
riko.safaric@uni-mb.si

Authors' Addresses: Dr. Suzana Uran
Prof. Dr. Riko Šafarič
Faculty of Electrical Eng. and
Computer Sciences
University of Maribor
Smetanova 17
2000 Maribor, Slovenia
suzana.uran@uni-mb.si
riko.safaric@uni-mb.si

Prejeto: 8.5.2001
Received:

Sprejeto: 23.5.2002
Accepted:

© Strojniški vestnik 48(2002)5,283-294
ISSN 0039-2480
UDK 62-25:621.983.4:621.753.5
Pregledni znanstveni članek (1.02)

© Journal of Mechanical Engineering 48(2002)5,283-294
ISSN 0039-2480
UDC 62-25:621.983.4:621.753.5
Review scientific paper (1.02)

Prispevek k obvladovanju neuravnoteženosti krempljastih polov alternatorjev

A Contribution to the Unbalance Control of Claw Poles for Automotive Alternators

Miha Nastran - Vid Krušič - Miha Boltežar

Krempljasti poli so še vedno največji in najtežji sestavni del rotorja alternatorjev, ki bo vsaj še nekaj časa ustvarjal električno energijo v motornih vozilih. Zaradi visokih vrtljajev, ki jih alternator med delovanjem doseže, je masna uravnoteženost rotorja bistvenega pomena za dobo trajanja ležajev, majhen hrup in miren tek. Prispevek obravnava izdelavo krempljastih polov s hladnim preoblikovanjem, pri čemer je poudarek na zmanjšanju njihove neuravnoteženosti, s čimer bi bistveno pripomogli k pospešitvi avtomatskega uravnoteženja rotorjev. V začetku je na kratko orisan problem ter samo načelo uravnoteženja. V nadaljevnju sledi eksperimentalna analiza sedanje proizvodnje, z uporabo metode končnih elementov pa razložimo vzroke za pojav neuravnoteženosti. Poudarek je dan raziskavam v smeri izboljšav sedanjega orodnega sistema za doseganje majhne neuravnoteženosti krempljastih polov.

(Ključne besede: rotorji alternatorjev, uravnoteženost mas, sistemi orodni, metode numerične)

The claw pole still represents the largest and the heaviest part of an alternator's rotor; and it is expected that alternators will continue to be used for electric power generation in motor vehicles for at least a decade. Due to the high speeds of the rotor during operation its mass centricity is very important for the service life of the bearings, low noise and smooth running. This paper presents the production of claw poles using cold-forming technology, and a focus on reducing the eccentricity. Achieving this aim will mean a step towards shortening the time needed for automated balancing. We start with the problem of production and principle of balancing, this is followed by an experimental analysis of current production and a FEM analysis, which helps to describe the reasons why unbalance occurs. Emphasis is placed on work towards improving the tooling system for achieving well-balanced claw poles after cold forming.

(Keywords: alternator rotors, mass centricity, tool systems, numerical methods)

0 UVOD

Geometrijska natančnost polizdelkov je še vedno eden glavnih problemov v tehnologiji hladnega preoblikovanja. Pri tem ima pomembno vlogo preoblikovalno orodje, ki s svojimi značilnostmi prispeva h kakovosti izdelka [1]. Način, s katerim se rešuje problem merske nenatančnosti polizdelkov, je navadno odvisen od geometrijskih značilnosti polizdelka. Zmanjšanja preoblikovalnega odpora z načelom sprostitvenih osi na mestih z največjo napetostjo se je lotil že Kondo ([2] do [4]). Podobna metoda je bila uporabljena tudi za hladno kovanje zobnikov ([5] in [6]). V prispevku je prikazan problem natančne izdelave krempljastega pola s hladnim preoblikovanjem (sl.1) ter podane smernice za ustrezne poprave orodja.

0 INTRODUCTION

The geometrical accuracy of products is still one of the major problems facing cold-forming technology. The forming tool and its characteristics have an important affect on the quality of the finished part [1]. The principle used for controlling geometrical errors depends mainly on the geometrical properties of the product being produced. Lowering the forming resistance by the principle of relief axis at the points with the highest pressure is one of the methods that has been used already by Kondo ([2] to [4]). A similar method has been used in the cold forming of gears ([5] and [6]). The problem of geometrically accurate production of the claw pole by using cold-forming technology is presented in the paper (Fig.1), and some advice relating too an improved forming tool is given.

Sl. 1. *Platina in izdelani krempljasti pol alternatorja*
Fig. 1. *Blank and finished claw pole for alternators*

Med obratovanjem doseže rotor alternatorja do 18.000 vrtljajev v minuti. Ena bistvenih zahtev, ki jih je treba izpolnjevati, je majhna masna neuravnoteženost celotnega sklopa rotorja. Problem se rešuje z uravnoteženjem rotorja pred vgradnjo v celoten sklop alternatorja. V proizvodnji se to navadno doseže z odvzemanjem materiala v dveh ravninah, kar je lahko v primeru velike neuravnoteženosti zelo zamuden proces. Zaradi slabih sestavnih delov se lahko zgodi, da rotorja ni mogoče primerno uravnotežiti in postane izmet. Na tem mestu se pojavi težnja po čimbolj natančno izdelanih polizdelkih (v prikazanem primeru je to krempljasti pol), ki so sestavni del končnega izdelka.

During operation the rotor of an alternator is moving at high speeds (up to 18,000 rpm), thus one of the important demands is to keep the rotor unbalance as low as possible. Balancing the rotor before its final assembly into the alternator solves the problem. In the production this is normally achieved by drilling holes in two planes, which is often a time-consuming process if the rotor is very unbalanced. In some cases it is impossible to achieve the prescribed tolerance. Thus the need for the cold-formed parts, in this case the claw pole, to be as precise as possible is clear.

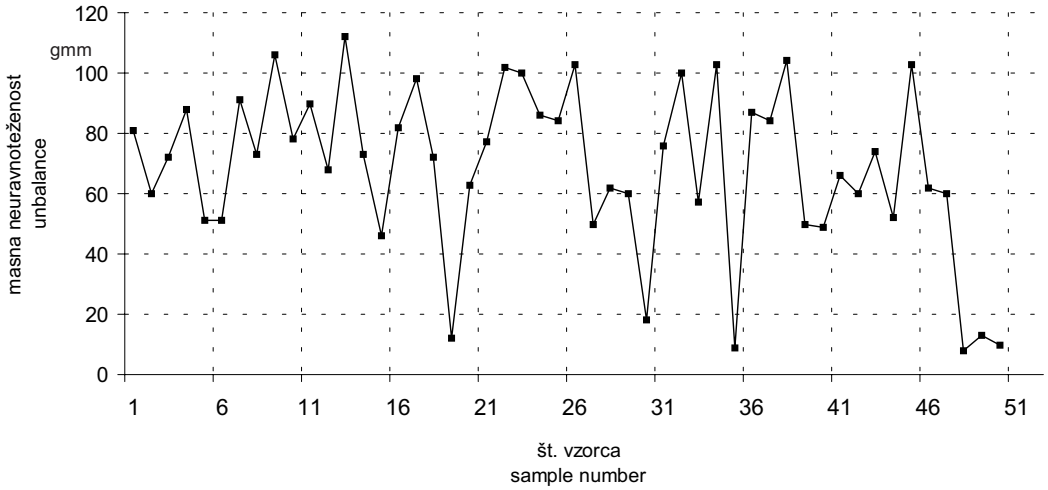

Sl. 2. *Meritve masne neuravnoteženosti krempljastega pola na 50 vzorcih*
Fig. 2. *Unbalance measurements of the claw pole for 50 samples*

Krempljasti pol je najtežji sestavni del rotorja, zato se je primerno posvetiti njegovi izdelavi v smeri majhne neuravnoteženosti. Analiza trenutnega stanja v proizvodnji krempljastih polov pokaže na veliko neuravnoteženost (sl.2), saj merjeni rezultati presegajo dovoljeno mejo 80 gmm (velikost se navadno podaja v gmm, kar pomeni določeno maso materiala na določeni ročici). Zmanjšanje masne neuravnoteženosti krempljastih polov je zato eno ključnih vprašanj.

The claw pole is the heaviest part of the rotor so it is worth spending time to reduce its unbalance. An analysis of the current production shows a large degree of unbalance (Fig.2). The measured values exceed the upper limit of 80 gmm, (it is normally measured in gmm which represents a certain amount of material on a given radius). Reducing this unbalance is therefore one of the main tasks.

1 NAMEN URAVNOTEŽENJA

Uravnoteženje delimo na uravnoteženje togih ter prožnih rotorjev ([7] in [8]). Pri prožnih rotorjih

1 THE PURPOSE OF BALANCING

Balancing is basically divided onto the balancing of rigid and elastic rotors ([7] and [8]).

moramo izvajati modalno uravnoteženje, pri katerem je treba upoštevati upogibne deformacije gredi. S tem se v našem prispevku ne bomo ukvarjali.

Pri uravnoteženju togih rotorjev poznamo uravnoteženje v eni (statično) in več (dinamično) ravninah. Pri uravnoteženju v eni ravnini za počasi tekoče rotorje poskušamo odpraviti njihovo izsrednost oz. uravnotežiti momente mase. Pri balansiranju v dveh ali več ravninah pri hitrotekočih rotorjih pa poskušamo odpraviti masne deviacijske momente glede na par pravokotnih osi, od katerih je ena vedno os vrtenja. Z drugimi besedami, želimo odpraviti momente centrifugalnih sil pri vrtenju.

Uravnoteženje se lahko izvaja terensko, pri čemer se rotor vrti v svojih ležajih, ali pa na uravnotežnih napravah, kjer rotor namestimo na napravo ter ga testno zavrtimo za ugotovitev neuravnoteženosti. Slednja možnost se uporablja tudi pri velikoserijski izdelavi alternatorjev na avtomatiziranih balansirnih napravah

Kupci alternatorjev predpisujejo največjo masno neuravnoteženost, ki jo morajo rotorji dosegati. Pri uravnotežanju z odvzemanjem materiala, ki je v navadi pri množični proizvodnji rotorjev alternatorjev, se pojavijo omejitve pri možni količini odvzetega materiala. Preveliko odvzemanje lahko povzroči celo dodatne neprijetne učinke, npr. pojav magnetne neuravnoteženosti pri uravnoteženju rotorjev elektromotorjev [9].

Ker namen prispevka ni poglobljeno obravnavanje uravnotežnega sistema temveč raziskava možnosti za izboljšanje polizdelkov, bomo v nadaljevanju predstavili tehnološki postopek izdelave krempljastega pola.

2 TEHNOLOŠKI POSTOPEK IZDELAVE

Izhodiščni material za izdelavo krempljastega pola s hladnim preoblikovanjem je debela pločevina, navita na kolute, iz katere se najprej izsekajo platine v obliki zvezd (sl.1). Debelina platin je odvisna od tipa krempljastega pola in se giblje med 10 in 13 mm. Sledi hladno preoblikovanje v sedmih stopnjah na prenosnem orodju, pri čemer se postopoma pride do končne oblike. Po hladnem preoblikovanju sledi še žarjenje za izboljšanje magnetnih lastnosti materiala.

Z vidika masne neuravnoteženosti izdelanega krempljastega pola je zlasti pomembna prva operacija na prenosnem orodju, ko se s tehnologijo finega reza prebije luknja. Centriranje platine v prvi stopnji je prikazano na sliki 3. Funkcionalno je luknja namenjena pritrditvi pola na gred rotorja, med postopkom izdelave v naslednjih šestih stopnjah orodja pa je uporabljena za pozicioniranje platine v orodju.

Centričnost izdelane luknje glede na pozicionirne trne je 0,032 mm, to pomeni, da bi v primeru popolnoma geometrijsko pravilno izdelane platine masna neuravnoteženost izdelanega krempljastega pola nihala za ± 13 gmm. V primerjavi s skupno izsrednostjo

Modal balancing is necessary for elastic rotors, where bending deformations of the shaft need to be taken into account. This topic will not be discussed in the paper.

Single-plane (static) and multiplane (dynamic) balancing are used with rigid rotors. Single-plane balancing is needed for slow-running rotors where gravity moments need to be eliminated. During dynamic balancing the aim is to reduce the mass-deviation moments with regard to two perpendicular axes, one of which is the axis of revolution. In other words, the centrifugal moments during rotating should be removed.

Two different balancing principles are used in practise. The first case is when the rotor is rotating in his own bearings. In the second case, special balancing machinery is used to test and correct the rotor. This latter method is also used in the mass production of alternators.

The highest mass unbalance of the rotors is prescribed by the customer. The balancing principle in mass production normally involves removal of the material by drilling. There are certain limitations relating to the amount of material that can be removed. If too much material has to be removed in order to keep the rotor in the tolerance field some other effects can appear. For example, magnetic unbalance during the balancing of rotors for electric motors [9].

The aim of our paper is not to discuss the theoretical principle of balancing but to improve the mass balance of a cold-formed claw pole. Therefore, the technological process of claw-pole production will be presented in the next section.

2 TECHNOLOGICAL PROCESS

The material used for claw-pole production in cold-forming technology is thick sheet metal bound in coils. Blanks are made first by free blanking. The thickness depends on the type of claw pole and ranges between 10 and 13 mm. Next, the blanks are formed to their final shape on a mechanical press using a seven-step transfer die. Finally, the claw poles are annealed to improve their magnetic properties.

Flow piercing of the hole (first transfer die) is a forming step that has a major affect on the final claw-pole unbalance. Positioning of the blank in the first transfer die is shown in Fig.3. The hole is used for mounting the claw pole onto the rotor shaft. It is also used for positioning the blank during forming in subsequent operations.

The manufacturing tolerance field of the piercing punch with regard to the positioning pins is 0.032 mm. If the blanks were produced in a geometrically precise way, the maximum theoretical unbalance would be 13 gmm. This is a negligable

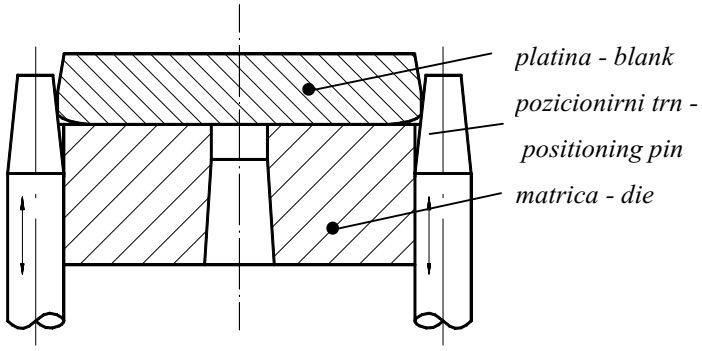

Sl. 3. *Pozicioniranje platine pri prebijanju luknje*
Fig. 3. *Centering of the blank during piercing*

izdelanega krempljastega pola je to zanemarljivo, saj se ta giblje pri vrednosti 80 gmm. Iz povedanega smemo za neuravnotežje izdelanih krempljastih polov sumiti prvo tehnološko operacijo (prosto rezanje), pri kateri ne izdelamo geometrijsko pravilne oblike platine. Ta nepravilna oblika je bistvena za vnos neuravnotežja v polizdelek, ki se nato prenese v končni izdelek.

3 VZROKI ZA NASTANEK NEURAVNOTEŽJA PRI PROSTEM REZANJU

Želja po čim boljšem izkoristku materiala narekuje čim gostejšo postavitev platin na trak. Izkazalo se je, da je le to ključnega pomena za nastanek masne neuravnoteženosti. Z namenom, da bi ugotovili vpliv velikosti mostička med dvema platinama, smo dva pestiča vzeli iz orodja in povečevali razmik izrezanih platin.

Rezultati so prikazani na sliki 4, kjer se vidi, da se je ob večanju razmika med platinama masna neuravnoteženost izdelanega krempljastega pola zmanjšala. Glavni vzrok za izsrednost izdelanega krempljastega pola je izsredena obremenitev stiskalnice in nesimetričen rez, ki je posledica neenakomerne porazdelitve materiala okrog rezilnega pestiča. Pri gibu orodja navzdol nastanejo poleg glavne rezalne sile v smeri giba orodja še stranske rezalne sile, ki pa med seboj niso v ravnotežju (sl.8).

amount compared to the total claw-pole unbalance, which is around 80 gmm. Therefore, we can conclude that the first operation, the free blanking of the blanks, is essential for the accuracy of the finished product, where a geometrically imperfect blank is made. This nonsymmetrical geometry of the blank is essential for the unbalance of the finished product.

3 REASONS FOR NONSYMMETRICAL FREE BLANKING

In order to save on the material costs it is necessary to arrange the blanks to be as close together as possible. However, many problems occur for this reason, a fact that was experimentally verified. In order to determine the influence of the web width, two punches were taken out of the tool and the feed was increased.

The results are presented in Fig.4. We can conclude that when the web width is increased the unbalance of the finished claw pole becomes proportionally lower. The major reason for the unbalance of the finished claw pole is a non-symmetrical blanking, which is the reason for the non-uniform distribution of the material surrounding the blanking punch. Apart from the major blanking force there are side forces that emerge when the tool closes (Fig.8). These side forces are not symmetrical due to

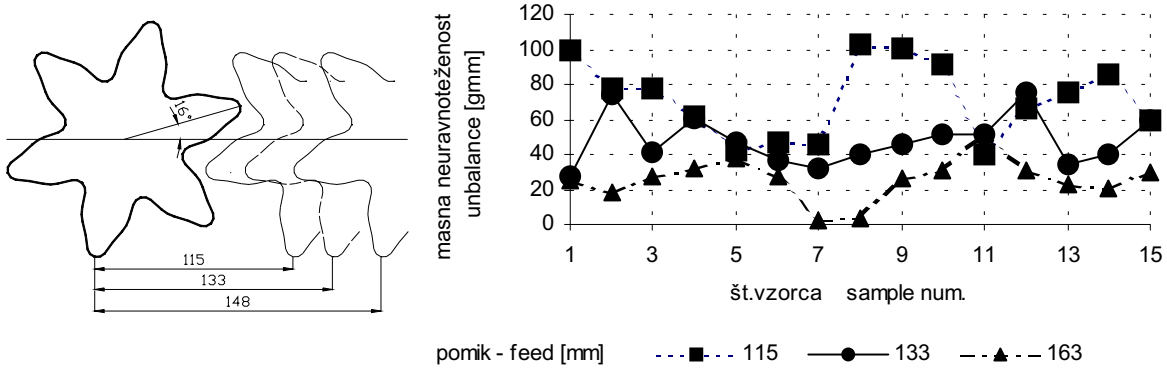

Sl. 4. *Vpliv razmika platin na izsredenost*
Fig. 4. *Influence of the blank scatter on the eccentricity*

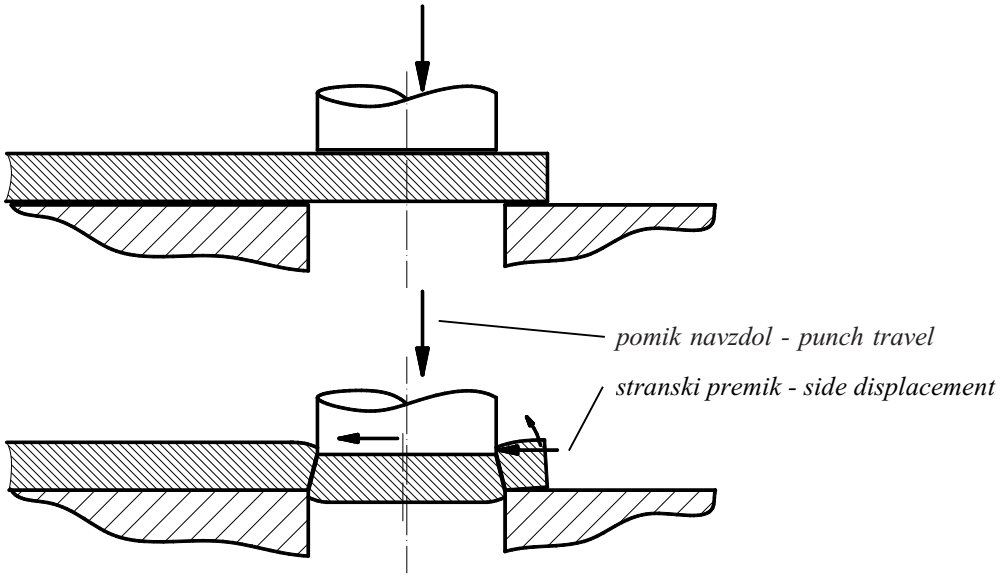

Sl. 5. *Vodoravni premik rezilnega pestiča proti matrici*
Fig. 5. *Horizontal shift of the punch relative to the die*

Zaradi zračnosti v vodilih orodja in stiskalnice povzročajo stranski premik pestiča v primerjavi z matrico (sl.5).

Za potrditev domneve o pojavu nesimetričnih stranskih sil na pestič med postopkom rezanja je bilo narejeno numerično simuliranje začetne faze rezanja. Skušali smo napovedati dogajanje po obodu enega zoba pestiča. Problem je v tem, da je zaradi poprej izrezane platine na eni strani zoba pestiča bistveno več materiala kakor na drugi strani (sl. 8). Posledica tega je razvoj bočnih sil na zob pestiča, ki nista v medsebojnem ravnovesju in povzročata vodoravni premik pestiča.

Z dvema numeričnima simuliranjima začetne faze rezanja, pri čemer je bilo v prvem primeru okoli pestiča manj materiala v drugem pa več, smo domnevo potrdili (sl. 6 in 7). Primerjava deformacij platine v obeh primerih pokaže, da ima v primeru, ko je na zunanji

the different size of the web. Because of the clearing in the tool and press guiding system these side forces cause a punch shift relative to the die (Fig. 5).

In order to confirm our assumption about the development of side forces on the punch we made a numerical simulation of the beginning of the cutting process. The circumstances on one side of the blanking teeth were predicted. The problem is a nonuniform distribution of the material surrounding the punch, due to the blank cut in the previous step (Fig. 8). A consequence is the development of side forces on the punch, which causes a horizontal shift of the punch.

The assumption was confirmed by performing two numerical simulations of the initial cutting phase. In the first case less material was used surrounding the punch, in the second case more material was used (Fig. 6 and 7). Comparing the deformation in the first

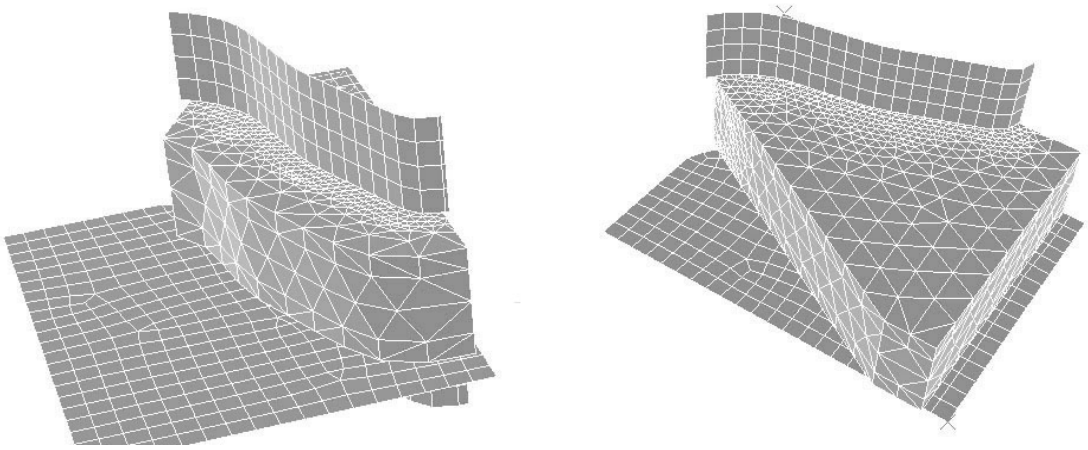

a) b)

Sl. 6. *Model zoba pri rezanju platine a) manj materiala b) več materiala*
Fig. 6. *FE Model during blanking a) less material b) more material*

strani pestiča manj materiala, le-ta veliko večjo težnjo po gibanju navzgor in s tem proti pestiču. Deformacija zgornjega dela platine je v prvem primeru 0,045mm v drugem pa 0,01mm. Prav tako je potrjena domneva o neenakomernem razvoju prečnih sil na pestič, kar ima za posledico pritiskanje zoba pestiča v stran.

Potek sil v ravnini pestiča je prikazan na sliki 8. V primeru večje količine materiala na zunanji strani pestiča je bočna pritisna sila manjša. Komponenta sile v smeri zoba zaradi deformacije ni problematična, ker je po obodu celotnega pestiča nameščenih šest zob, katerih sile se med seboj izničijo. Problematična je rezultanta sile prečno na zob, katere velikost je glede na rezultate simuliranja približno 1,5 % celotne preoblikovalne sile. Z upoštevanjem dejstva, da je potrebna sila za rezanje ene platine 2000 kN, pomeni to 27 kN bočne sile na zobe, ki povzročajo torzijo pestiča in s tem neenakomeren potek kota lomne cone na platini.

Odpravljati vzroke premika rezalnih pestičev na orodju in stiskalnici bi bilo ekonomsko neupravičeno, saj bi pomenilo bistvene posege v stroj in orodje. Povečanje

and second case shows that when there is less material near the punch it has a much higher tendency to move upwards and towards the punch. Vertical deformation of the blank in the first case is 0.045 mm, and in the second case it is 0.01 mm. The assumption of the nonsymmetrical side forces was confirmed as well, these forces cause a sideways movement of the punch.

The forces acting on the punch are presented in Fig. 8. In the case when we have more material outside the punch the side force is lower than with less material. The force component acting parallel to the punch tooth is not problematic since there are six teeth arranged circumferentially and the forces disappear. The most problematic component acts perpendicularly to the tooth. Its magnitude is 1.5% of the total blanking force, according to the simulation. Taking the 2000 kN that is needed for one blank into account, it means 27 kN of side force. These forces are the reason for the torsional punch displacement, which causes a nonuniform distribution of the angle of the fracture zone.

Solving the problem of the horizontal punch displacement would mean large investments in the tool and press, which may not be the correct economic decision. Increasing the web width between the blanks

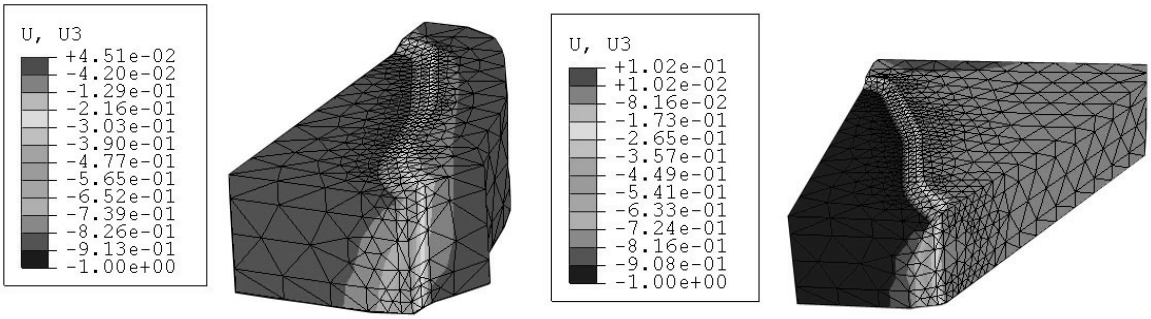

Sl. 7. *Deformacija platine v prvem in drugem primeru*
Fig. 7. *Blank deformation in the first and second cases*

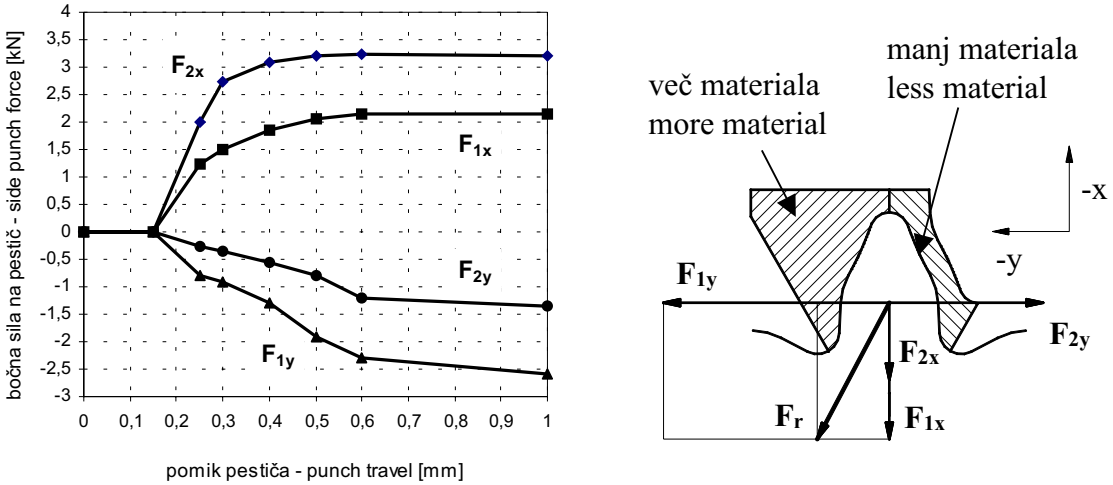

Sl. 8. *Komponenti rezalne sile na pestič v ravnini platine*
Fig. 8. *Blanking force components in the blank plane*

razmika med pestiči pa bi hkrati pomenilo tudi manjši izkoristek materiala ter povsem novo orodje za rezanje. Zaradi povedanega se bomo osredotočili na prvo operacijo v prenosnem orodju - fino rezanje luknje.

4 TEORETIČEN IZRAČUN NEURAVNOTEŽENOSTI

Da bi potrdili domnevo o glavnem vplivu nesimetričnega odreza platine na masno neuravnoteženost izdelanega krempljastega pola, je bila masna neuravnoteženost tudi teoretično izračunana na podlagi meritev premika pestiča pri rezanju platin.

V primeru morebitnega ujemanja izračunanih rezultatov ter rezultatov meritev neuravnotežja izdelanega krempljastega pola, je jasno, da preoblikovanje na prenosnem orodju ne vpliva bistveno na končno neuravnoteženost izdelka. V ta namen je bilo iz serije vzetih 25 platin, na katerih smo merili kot preloma materiala med rezanjem (sl. 9).

would mean higher material costs, which is again not a profitable solution. Apart from that, a completely new blanking tool will be required. Because of this, further discussion will be focused on the flow piercing of the hole, which is the first operation in the transfer die.

4 THEORETICAL CALCULATION OF THE ECCENTRICITY

In order to confirm the assumption about the major affect of the blanking tool on the claw-pole unbalance we made a theoretical calculation of the unbalance. It was based on the punch shift during blanking, which was measured by examining the blanks.

When the results obtained theoretically by inspecting the blanks are identical to those measured on the finished claw poles we can conclude that the forming on the transfer tool does not have any affect on the overall unbalance. In order to perform this calculation, 25 blanks were taken from production. The angle of the fracture zone was measured at six positions on the blank (Fig.9).

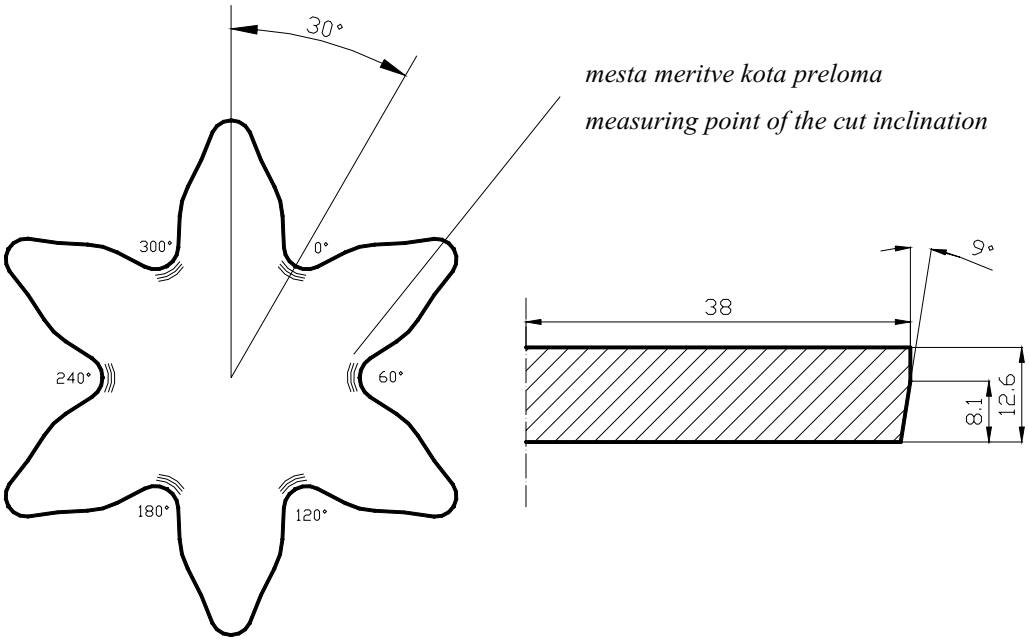

Sl. 9. *Meritev kota preloma materiala na platini*
Fig. 9. *Measuring the cutting angle on the blank*

Iz šestih meritev kota preloma materiala sta bili ocenjeni smer ter velikost premika pestiča proti matrici, iz tega pa izračunana masna neuravnoteženost platine:

The direction and amplitude of the punch shift were calculated based on six measurements of the angle, the theoretical unbalance was also calculated:

$$\Delta_0 = t \cdot \left[\tan\left(\frac{\varphi_0 + \varphi_{180}}{2} \right) - \tan \varphi_0 \right]$$

$$\Delta_{60} = t \cdot \left[\tan\left(\frac{\varphi_{60} + \varphi_{240}}{2} \right) - \tan \varphi_{60} \right] \qquad (1).$$

$$\Delta_{120} = t \cdot \left[\tan\left(\frac{\varphi_{120} + \varphi_{300}}{2} \right) - \tan \varphi_{120} \right]$$

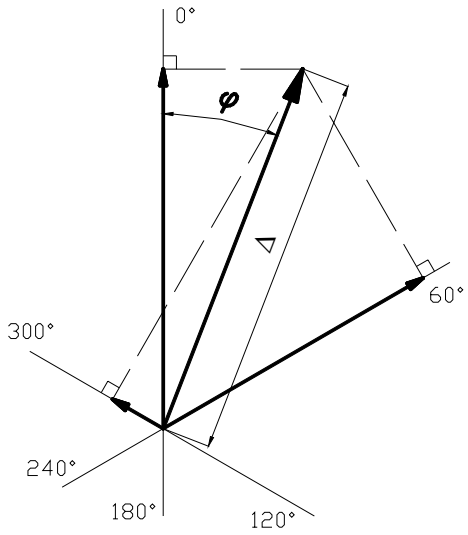

Sl. 10. *Izračun premika pestiča proti matrici*
Fig. 10. *Calculation of the punch shift*

Oznake v enačbah so glede na sliko 9:
φ_i - kot preloma pri kotu *i* v vodoravni ravnini v °,
t - debelina lomne cone v mm,
Δ_i -velikost premika pestiča v smeri *i* v vodoravni ravnini v mm.

Zaradi napak pri merjenju pa je rezultanto premika primerno določiti po metodi najmanjših kvadratov.

In Fig.9 the following notation is used:
φ_i - fracture angle at an angle in the horizontal plane,
t - fracture-zone thickness,
Δ_i - punch shift in the i-th direction in the horizontal plane [mm].

Because of the measurement errors the punch shift calculation was based on three measurements using the least-square method.

$$G = \left[\Delta \cdot \cos\varphi - \Delta_0\right]^2 + \left[\Delta \cdot \cos\left(\varphi - 60^0\right) - \Delta_{60}\right]^2 + \left[\Delta \cdot \cos\left(\varphi - 120^0\right) - \Delta_{120}\right]^2 \quad (2).$$

Pri čemer je Δ absolutna vrednost premika pestiča, φ pa smer, v kateri se premakne (sl.10). Z minimiziranjem funkcije G pridemo do končnega rezultata. V ta namen parcialno odvajamo po Δ in φ:

Where Δ is an absolute punch displacement, φ is the displacement direction (fig.10). By minimizing the function G a final result is obtained by partial differentiation in Δ and φ:

$$\frac{\partial G}{\partial \varphi} = 0 \quad \frac{\partial G}{\partial \Delta} = 0 \quad (3),$$

$$\tan\varphi = \frac{\sqrt{3}\left(\Delta_{60} + \Delta_{120}\right)}{2\cdot\Delta_0 + \Delta_{60} - \Delta_{120}} \quad (4),$$

$$\Delta = \frac{\sqrt{3}}{3}\left(\Delta_{60} + \Delta_{120}\right)\cdot\sin\varphi + \frac{1}{3}\left(2\cdot\Delta_0 + \Delta_{60} - \Delta_{120}\right)\cdot\cos\varphi \quad (5).$$

Dobljeni sta smer in velikost premaknitve pestiča, iz česar se nato po enačbi (6) izračuna še teoretična neuravnoteženost platine:

Based on the direction and the amplitude of the punch shift, a theoretical unbalance of the claw pole is finally calculated according to:

$$U = \left|\frac{\Delta}{2}\cdot\frac{t}{s}\cdot m\right| \quad (6).$$

Posamezne oznake so:
U - masna neuravnoteženost v gmm,
D - premika pestiča v mm,
s - debelina materiala v mm,
m - masa platine v g

Na vzorčnih platinah je bila označena izračunana smer premika pestiča proti matrici, nato pa so bile prenesene v prenosno orodje, kjer je bila

Notation:
U - eccentricity [gmm],
Δ - punch shift [mm],
s - material thickness [mm],
m - blank mass [g]

The calculated direction of the eccentricity of the blanks was marked before being put into the transfer die. A sample charge of claw poles was

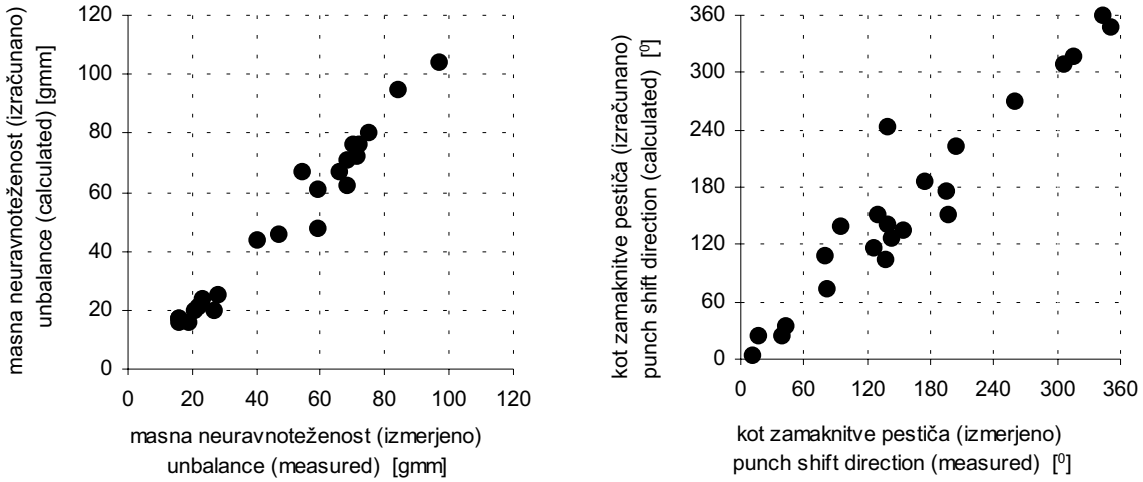

Sl. 11. *Primerjava izračunov in meritev*
Fig. 11. *Comparison between calculated and measured values*

izdelana končna oblika krempljastega pola. Po končani izdelavi krempljastih polov je bila na njih izmerjena končna masna neuravnoteženost ter smer, v kateri neuravnoteženost leži.

Primerjava med izmerjenimi vrednostmi neuravnoteženosti krempljastega pola in izračunanimi vrednostmi neuravnoteženosti platin je prikazana na sliki 11. Izmerjene in izračunane vrednosti so praktično enake, kar pomeni, da je neuravnoteženost vnesena že v prvi preoblikovalni operaciji (rezanje platin). Izboljšanje rezilnega orodja je težko izvedljivo, zato bo v nadaljnjem prikazana mogoča sprememba prve stopnje prenosnega orodja (fino rezanje luknje), s čimer bi bistveno zmanjšali končno neuravnoteženost izdelka.

5 PREDLOG REŠITVE

Trenutno je centriranje platine v prvi stopnji prenosnega orodja izvedeno s tremi vzmetenimi pozicionirnimi trni, medsebojno premaknjenimi za kot 120^0. Prerez je prikazan na sliki 3. Problem takšne izvedbe je v tem, da je masno središče platine, kjer bi moralo biti središče luknje, premaknjeno za določeno vrednost (sl.12). Vzrok za to je središčenje platine po spodnji površini, katere središče zaradi nesimetričnega reza ne leži v masnem središču platine. Prednost uporabljenega načela pozicioniranja na spodnjo površino platine je v tem, da je preprosto izvedljiv.

produced. Afterwards a final mass unbalance and its direction was measured and compared to the theoretically obtained values.

The comparison between the calculated values of the blank unbalance and the measured values of the claw-pole eccentricity is presented in Fig.11. Practically, there is no difference between the measured and the calculated values. It confirms the assumption that the eccentricity is already input at the first forming stage (blanking). Improving of the blanking tool is connected with large investments; therefore, the modification of the flow-piercing tool in the first step of the transfer die will be discussed. Much could be done in order to lower the final eccentricity.

5 SOLUTION PROPOSAL

Currently, the positioning of the blank during flow piercing is made by using three positioning pins aligned in a 120^0 scatter. A cross-section is presented in fig.3. The problem of this centering principle is that the mass center where the fine blanked hole should lie in order to have the minimum eccentricity is not positioned in the center of the hole (Fig.12). The reason for this is the centering of the blank on its bottom surface, whose center does not lie in the blank mass center. The advantage of this centering principle using the lower blank surface is that it is relatively simple to perform.

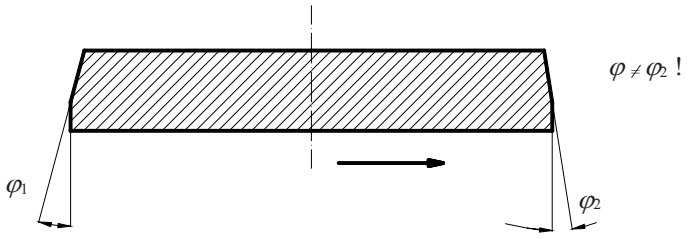

Sl. 12. *Premaknitev masnega središča platine*
Fig. 12. *Shift of the mass center of the blank*

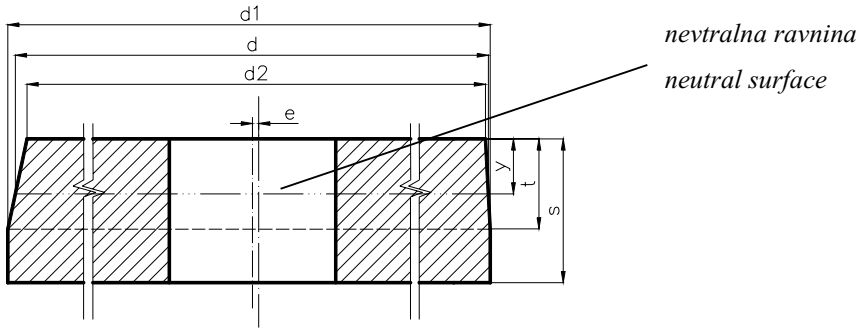

Sl. 13. *Položaj nevtralne ravnine*
Fig. 13. *Position of the neutral surface*

V primeru centriranja na zgornjo površino platine bi prišlo do enakega pojava, saj tudi središče te površine zaradi nesimetričnega reza ne leži v masnem središču platine. Da bi izločili vpliv nesimetričnega reza na neuravnoteženost pola, bi morali pozicionirati v tisti ravnini, ki v svojem središču vsebuje tudi masno središče, ta pa leži nekje med zgornjo in spodnjo površino (sl. 13).

Glede na parametre platine (sl.13), ki so približno nespremenljivi, lahko lego centrirne ravnine izračunamo po enačbi (7). V enačbi se pojavljajo le stalni parametri in je torej tudi lega ravnine približno nespremenljiva. Globina prodora je predvsem odvisna od stanja orodja in je v praksi relativno nespremenljiva za vse platine (*s - t ~ 4,5* mm).

The same problem occurs in the case of centering on the top surface of the blank. Due to the nonsymmetrical cut, the center of this surface does not lie in the blank mass center. In order to eliminate the nonsymmetrical blanking, positioning should take place in the plane, which is symmetrical to the mass center of the blank. This plane lies somewhere between the upper and lower surface of the blank.

According to the blank parameters (Fig.13), which are almost constant, the position of the centering plane can be calculated according to eq.7. The equation is based on constant parameters only; therefore, the position of the surface is constant. Punch penetration is relatively constant for all the blanks and basically depends on the tooling conditions *(s - t ~ 4.5 mm)*.

$$y = t^2 \cdot \left(\frac{d_1 + d_2}{d_1 \cdot (2 \cdot s - t) + d_2 \cdot t} \right) \qquad (7).$$

Oznake:
d_1 - premer platine na spodnji površini v mm,
d_2 - premer platine na zgornji površini v mm,
s - debelina platine v mm,
t - debelina lomne cone platine v mm,
y - oddaljenost središčne ravnine od zgornje površine platine v mm
Za konkretne geometrijske parametre platine:
d_1 = 74,9 mm,
d_2 = 72,3 mm,
s = 12,6 mm,
t = 8,1 mm
je lega nevtralne ravnine y = 5,17 mm.

To pomeni, da leži v središču ploskve, ki je prerez platine in ravnine 5,17 mm pod zgornjo površino, tudi masno središče platine. Lega te ravnine je neodvisna od trenutnega premika pestiča proti matrici, kar pomeni, da jo je primerno uporabiti za usreditveno ravnino.

Predlog nove izvedbe orodja je prikazan na sliki 14. Nad sedanji pozicionirni trn se namesti še drug glavni pozicionirni trn, ki bi ležal na premeru d (sl.13), kakor ga določa nevtralna ravnina:

Notation:
d_1 - blank diameter on bottom surface [mm],
d_2 - blank diameter on top surface [mm],
s - blank thickness [mm],
t - fracture-zone thickness [mm],
y - centering plane distance [mm].
For real blank parameters:
d_1 = 74.9 mm,
d_2 = 72.3 mm,
s = 12.6 mm,
t = 8.1 mm
the position of the neutral surface is y = *5.17 mm*.

This means that the mass center of the blank lies in the center of the surface, which is 5.17 mm below the top surface of the blank. The most important thing is that the position of this plane is independent of the punch shift during blanking. It means that this plane could be used for better centering of the blank during flow piercing.

The tool scheme of the new centering principle is presented in Fig.14. Above the current positioning pin another one (major) is mounted. The position of this pin will be determined by the diameter d (Fig.13) of the neutral plane:

$$d = d_2 + \frac{y}{t}(d_1 - d_2) = 73,9 \ \ mm \qquad (8).$$

Med zapiranjem orodja pritisne glavni pozicionirni trn na sedanji pozicionirni trn, ki je namenjen samo za pozicioniranje v prvi stopnji, ga odmakne in s tem sprosti platino, ki se nato pozicionira glede na nov pozicionirni trn. Ta se platine dotika v prej izračunani razdalji od zgornje ravnine, ki v svojem središču vsebuje masno središče. Podlaga za takšno izvedbo pozicionirnega sistema je predvsem v tem, da je izmera matrice in pestiča med preoblikovanjem konstantna, kar je tudi praktično povsem pravilno, saj je elastična deformacija matrice in pestiča v primerjavi z deformacijo platine minimalna. Prav tako je nespremenljiva debelina materiala ter približno nespremenljiva debelina lomne cone.

During the tool closing the new positioning pin acts on the current positioning pin, which is now used only for centering in the first step. It is pushed down and the blank is released for a moment and allows the upper positioning pin to position the blank in the calculated surface. It touches the blank in the previously calculated distance from the top blank surface. The basic fact for such a tool design is in first case the assumption that there is no elastic deformation of the punch and die during blanking. This is found to be correct in practice. The elastic deformation of the punch compared to the deformation of the blank can be neglected. Material thickness and the height of the punch penetration are held almost constant as well.

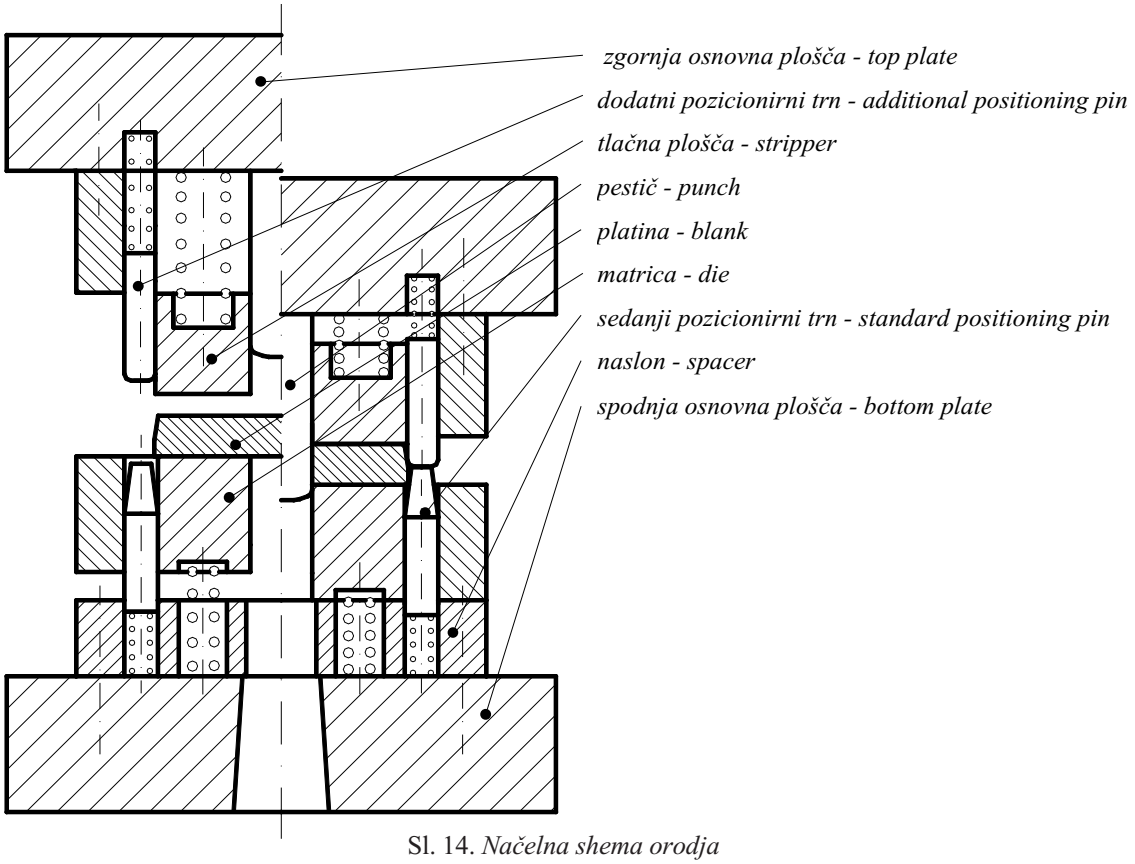

Sl. 14. *Načelna shema orodja*
Fig. 14. *Tool scheme*

6 SKLEP

V prispevku je prikazano sistematično reševanje problema manjšanja masne neuravnoteženosti pri izdelavi krempljastega pola alternatorja. Eksperimentalno delo in teoretična izhodišča so uspešno kombinirana in podprta z numeričnimi metodami. Poudarjen je sistematičen postopek reševanja konkretnih industrijskih problemov na področju občutljivosti in stabilnosti proizvodnih postopkov v velikoserijski proizvodnji, ki so problem tako z vidika stalnosti paramterov postopka kakor primernosti orodij [10]. Na koncu so podane še smernice za ustrezne konstrukcijske spremembe preoblikovalnega orodja, ki bi omogočal bistveno bolj stabilen tehnološki proces.

6 CONCLUSION

A systematic approach to lowering the eccentricity of the claw poles for alternators is presented in the paper. Experimental work and theoretical aspects are combined successfully and supported with modern numerical methods. A systematic approach to solving the real industrial sensitivity and stability problems in the mass series production processes is discussed. They are problematic from the point of view of process parameters and tools [10]. Some solution proposals of constructional tool modifications for more stable and reliable production process are discussed at the end.

7 LITERATURA
7 REFERENCES

[1] Kuzman, K., V. Krušič (1998) Tools-one of the major attributes for the succesfull cold forging, Int. Conf. on Forging Related technologies, *ImechE Conf. Trans* 1998-3 333-340.

[2] Kondo, K. (1999) Improvement of product accuracy in cold die forging, A*dvanced Technology of Plasticity*, Nueremberg, Germany,vol I, 41-48.

[3] Kuzman, K. (2001) Problems of accuracy control in cold forming. *J. mater. process. technol.*. vol. 113, no. 1/3, special issue "5th APCMP, Seoul, Korea", 10-15.

[4] Kuzman, K. (1999) Stability control of cold forming processes. *Advanced technology of plasticity 1999: Proceedings of the 6th International Conference on Technology of Plasticity*, Nuremberg, September 19-24, Berlin [etc.]: *Springer,* vol. II, 805-812.

[5] Ohga, K., F.Murakoshi, H.Ando, K.Miyoshi, K.Kondo (1999) Net shape forging of gear toothed parts utilizing divided flow method, *Advanced Technology of Plasticity,* Nueremberg, Germany, vol II, 793-798.

[6] Kampuš, Z., K. Kuzman (1993) Analysis of geometrical accuracy in ironing. *Advanced technology and plasticity.* Volume I. International Academic, 1005-1010.

[7] Kellenberger, W. (1987) Elastisches Wuchten, *Springer Verlag*.

[8] Federn, K. (1977) Auswuchttechnik, Band1, Band 2, *Springer Verlag*.

[9] Petrič, M. (2001) Primerjava masnega ter magnetnega neuravnoteženja rotorja z ozirom na vibracije enosmernih elektromotorjev. *Fakulteta za strojništvo*, Ljubljana.

[10] Gantar, G., K. Kuzman (2000) Sensitivity analysis of deep drawing production process. *Proceedings of the Workshop: Characterization of Manufacturing Processes: Synergetics and Data Processing Methods*, Ljubljana, May 25 - 26, 2000 , 49-53.

Naslovi avtorjev: Miha Nastran
doc.dr. Miha Boltežar
Fakulteta za strojništvo
Univerza v Ljubljani
Aškerčeva 6
1000 Ljubljana
miha.nastran@fs.uni-lj.si
miha.boltezar@fs.uni-lj.si

Vid Krušič
Iskra Avtoelektrika d.d.
Celovška 91
1000 Ljubljana
vid.krusic@iskra-ae.com

Authors' Addresses: Miha Nastran
Doc. Dr. Miha Boltežar
Faculty of Mechanical Eng.
University of Ljubljana
Aškerčeva 6
1000 Ljubljana, Slovenia
miha.nastran@fs.uni-lj.si
miha.boltezar@fs.uni-lj.si

Vid Krušič
Iskra Avtoelektrika d.d.
Celovška 91
1000 Ljubljana, Slovenia
vid.krusic@iskra-ae.com

Prejeto: 1.2.2002
Received:

Sprejeto: 23.5.2002
Accepted:

Poročila
Reports

FITNET (FITness-for-service NETwork) – pomoč evropski industriji

Napake (kot so razpoke in napake v zvarnih spojih) se lahko pojavijo med proizvodnjo in uporabo kovinskih konstrukcij. Porušitev le ene konstrukcijske komponente zahtevnega objekta (kakor so posode pod tlakom, cevovodi ali deli letal) lahko ogrozi življenja ter povzroči materialno škodo in onesnaži okolje. Iz nekaterih napak v konstrukciji pa se med obratovanjem ne razvijejo vedno razpoke, ki bi povzročile porušitev v celotni obratovalni dobi konstrukcijske komponente. Popravilo takšnih napak, oziroma zamenjava komponent pomeni precejšnji finančni izdatek in je lahko tudi tvegano, ker se lahko med popravilom pojavi več razpok, ki so bolj nevarne od prvotnih.

Postopek za oceno primernosti za uporabo konstrukcije z napako, ki sloni na zakonitostih mehanike loma ter ocene dopustne velikosti in lege napake, omogoča dosledno določitev dobe trajanja ter oceno o primernosti popravila, zamenjave ali nadaljnji uporabi sedanje konstrukcije.

Čeprav že obstaja več postopkov za ocenitev primernosti za uporabo konstrukcije z napako (npr. API 579, BS 7910), bi bilo treba oblikovati Evropski postopek za končno skladen Evropski (CEN) standard.

Prav zaradi podanih razlogov se je pred kratkim začel izvajati projekt FITNET - Evropsko tematsko delo v mreži za oceno primernosti pri uporabi konstrukcije z napako. Tematsko delo v mreži, ki je delno financirano od Evropske zveze, koordinira GKSS raziskovalni center v Nemčiji. Pri projektu sodeluje 40 udeležencev iz evropske industrije, raziskovalnih inštitutov in univerz, ki razvijajo novo tehnologijo znanja v povezavi z drugimi raziskovalnimi programi. FITNET združuje 16 Evropskih držav vključno s tremi državami kandidatkami za razširitev Evropske zveze Poljsko, Slovenijo in Madžarsko. V FITNET so prisrčno vabljeni tudi posamezniki in člani iz drugih organizacij. Projekt se je začel izvajati februarja 2002 in bo tekel do konca februarja 2006. Načrtovane dejavnosti v okviru projekta FITNET vključujejo:

- pregled in preverjanje sedanjih postopkov in raziskovalnih spoznanj pri postokih za oceno primernosti za uporabo konstrukcije z napako,
- oblikovanje delovnih primerov in izobraževalnega gradiva na elektronskih občilih,
- organiziranje in izvajanje javnih seminarjev in delavnic,
- sodelovanje s CEN pri standardizaciji postopka.

Podrobnejši program lahko najdete na domači strani – www.eurofitnet.org.

Nenad Gubeljak

Strokovna literatura
Professional Literature

Iz revij

IZ DOMAČIH REVIJ

EGES, Energetika, gospodarstvo in ekologija skupaj, Ljubljana
2002, 1
Gospodinjski aparati v razredih od A do G in kotli z zahtevanimi izkoristki
Vuk, R.: Evropski standard EN 834
Izgube in izkoristek kotlov
Šijanec Zavrl, M.: Predlog novega predpisa o toplotni zaščiti in učinkoviti rabi energije v stavbah
Zekić, A., Novak, J.: Male hidroelektrarne (MHE), I. del

Elektrotehniški vestnik, Ljubljana
2002, 1
Geršak, G., Humar, J., Fefer, D.: Uporaba računalniškega modeliranja za določevanje konstante in homogenosti magnetnega polja zračne tuljave
Klopčar, N., Lenarčič, J.: Primerjava robotskega ramenskega obroča z ramenskim obročem pri človeku

Les, Ljubljana
2002, 4
Hočevar, M.: Kalkulacija stroškov za določanje prodajnih cen in odnosa s kupci

2002, 5
Torelli, N.: Reakcijski les in njegova mehanika

Livarski vestnik, Ljubljana
2002, 1
Horaček, M.: Tehnologija preciznega litja - tehnologija za novo tisočletje

Materiali in tehnologije, Ljubljana
2002, 1-2
Mišović, M., Tadić, N., Ćulafić, Z. Jelić, M.: Rezidualne napetosti v peskanih pločevinah iz zlitine AlMg4.5Mn
Glogovac, B., Jaklič, A., Torkar, M., Kolenko, T., Končan, I., Kumer, B., Marolt, T.: Merilni pristop za optimizacijo ogrevanja jekel v kontinuirni peči
Tušek, J.: Pojavi pri varjenju z večžično elektrodo za povečanje talilnega učinka

Obzornik za matematiko in fiziko, Ljubljana
2002, 2
Jurišić, A.: Problem Mercedesovega vozla
Strnad, J.: Stefanova sila

Organizacija, Maribor, Kranj
2002, 4
Čižman, M.: Uporaba ABC metod za razporejanje stroškov v javnih zavodih
Papler, A., Leskovar, R., Kljajić, M.: Interaktivno večkriterijsko razporejanje proizvodnje

2002, 5
Rant, Ž.: Ljudje v procesni organizaciji

IZ TUJIH REVIJ

Automatika, Zagreb
2001, 1-2
Somek, B., Dadić, M., Maletić, M.: Active noise control in ducts
Szemes, P., T., Korondi, P., Ando, N. Hashimoto, H.: Friction compensation for micro tele-operation Systems
Klaić, M.: Mjeriteljstvo električnih veličina

2001, 3-4
Matko, D., Geiger, G., Werner, T.: Modelling of the pipeline as a lumped parameter system
Benčić, Z.: Intelektualno vlasništvo, suvremeni resurs za postizanje globalne tehnološke kompetitivnosti
Lebedev, N.: Balansni ventili "IMI" za energetski efikasne grejne sisteme
Coad, W.J.: Sistemi sa promenljivom količinom vazduha za poboljšanje kvaliteta unutrašnjeg vazduha, primenom sistema ventilacije i klimatizacije
Vukoslavčević, P.V., Petrović, D., Wallace, J.M.: O simultanom 3-D merenju turbulentnih vektora brzine i vrtložnosti sondama sa zagrejanim vlaknima

Engineering Review, Rijeka
2000, 20, 1-72
Matika, D., Pavleković, D.: Plovilo kao izvor podvodnog šuma
Obsieger, B.: Formulacija metode rubnih elemenata kod potencijalnog strujanja oko čvrstog tijela
Siminiati, D. Diferencijalna jednadžba gibanja ventila za ograničenje tlaka
Staniša, B., Pomenić, L.: Zasoljenje protočnog dijela parnih turbina

Tehnički vjesnik, Slavonski Brod
2001, 3,4
Grizelj, B., Kenter, I.M., Grizelj, D.: Geometrieeinflussanalyse des Werkstücks im Verfahren Laserstrahlbiegen
Samardžić, I., Kolumbić, Z., Baotić, M.: Doprinos primjeni praškom punjenih žica za zavarivanje MAG postupkom

Scientific Bulletin, Bucharest
2001, 1, Series A
Ducariu, A., Bibac, I., Puscas, N.N.: Characterization of silicon integrated mach-zehnder interferometers AT 1590 NM

2001, 1, Series B
Brânzoi, V., Brânzoi, F., Trîmbitasu, E., Pilan, L.: The electrochemical behaviour of lead electrode in H_2SO_4 concentrated solutions with and without $CoSO_4$ additions
Petrescu, M., Jianu, E., Fecioru, M., Bălută, G.: Development of ultrahigh pressure devices for high-grade diamond synthesis

2001, 2, Series B
Brânzoi, V., Baibarac, M., Brânzoi, F.: The inhibition action of sodium salts of some organic acids on the corrosion of armco iron in H_2SO_4 and HCl solutions
Moldovan, P., Popescu, G.: Influence of melt velocity on the filtration efficiency of aluminium alloys

2001, 1, Series B
Ionită, A.D., Ionescu, T.: State of the art in laboratory computerized systems
Sava, M., Giurea, J.: Numerical methods for thermoaerodynamical computation of wet cooling towers

2001, 2, Series C
Schiopu, P., Schiopu, C.: Dynamic equilibration electronic system

2001, 1, Series D
Camciuc, A., Pastramă, St.D.: A study on circumferentially cracked thick walled tubes
Stanciu, V., Miclescu, A.: Contributions regarding turbojet engine thrust optimisation at fixed point
Rugescu, R.D.: Thrust and drag of variable mass aerospace vehicles

2001, 2, Series D
Olaru, A., Staicu, St.: Theoretical and experimental research dynamic behaviour of the industrial robots
Minciu, C., Constantin, G., Croitoru, S.: On functional geometry of cutting tool active faces
Rugescu, R.D., Codoban, AL.: Optimum lift-off thrust and angle of a small missile for a maximal range

CDA
Condizionamento dell'aria Riscaldamento Refrigerazione, Milano
2002, 2
Della Casa, S., Porro, A.: Impianti elettrici antideflagranti

2002, 3
Corgnati, S., P., Fracastoro, G.V.: Linee guida per la modellazione di grandi serre
Strada, M., Vivianetti, F., Sella, A., Traverso, R.: Il nuovo complesso delle scienze biomediche di bari

2002, 4
Laria, R.: L'acqua per il raffredamento e le pompe di calore

2002, 5
Castellotti, F.: Le superfici vetrate innovative
Laria, R.: L'acqua per gli impianti di umidificazione

HLH
Heizung Lüftung/Klima Haustechnik, Düsseldorf
2002, 3
Hell, F.: Brennwertnutzung in Erdgas- und Heizölfeuerungen
Schnieder, J., Betschart, W., Feist, W.: Raumluftströmungen im Passivhaus: Messung und Simulation
Büdenbender, L.: Eckregulierventile im Visier

2002, 4
Meier-Wiechert, G.: Die Aufwandszahlen in der DIN V 4701 Teil 10
Wildeboer, J., Grübbel, M., Gores, I.: Thermische Anwendungsgrenzen der Verdrängungsströmung

2002, 5
Siepert, H.: Optimaler Radeinlauf von Radialventilatoren
Feurich, H.: Reduzierte WC-Spülung und kleine Rohrweiten senken Kosten

Magdeburger, Magdeburg
2001, 1/2
Tschöke, H., Heinze H.-E.: Einige unkonventionellen Betrachtungen zum Kraftstoffverbrauch von PKW
Gronwald, F., Nitsch, J.: Universeller Zusammenhang: Wie das elektromagnetische Feld die Welt verbindet
Kremling, A., Bettenbrock, K., Stelling, J., Reichl, U., Gilles, E.-D.: Systemorientierte Bioprozesstechnik: Interdisziplinäre Forschung in Biologie, System- und Computerwissenschaften

Osebne vesti
Personal Events

Doktorati, magisteriji, diplome

DOKTORATI

Na Fakulteti za strojništvo Univerze v Ljubljani sta z uspehom zagovarjala svoji doktorski disertaciji, in sicer:

dne 14.maja 2002: mag. **Igor Simonovski,** doktorsko disertacijo z naslovom: "Valčna analiza nelinearnih nestacionarnih nihanj elektromotorja" in

dne 15. maja 2002: mag. **Andrej Lebar,** doktorsko disertacijo z naslovom: "Modeliranje obdelave z abrazivnim vodnim curkom".

S tem sta navedena kandidata dosegla akademsko stopnjo doktorja tehničnih znanosti.

MAGISTERIJI

Na Fakulteti za strojništvo Univerze v Ljubljani sta z uspehom zagovarjala svoji magistrski deli, in sicer:

dne 23. maja 2002: **Maja Rotar**, delo z naslovom: "Numerično modeliranje aero-termodinamskih karakteristik hladilnega stolpa na naravni vlek" in

dne 30. maja 2002: **Stojan Renčelj**, delo z naslovom: "Analiza merilne točnosti konvencioalnega merilnika toplotne energije".

*

Na Fakulteti za strojništvo Univerze v Mariboru so z uspehom zagovarjali svoja magistrska dela, in sicer:

dne 5. maja 2002: **Jožef Predan**, delo z naslovom: "Vpliv zaostalih napetosti na utrujenostno rast razpoke v heterogenih materialih";

dne 17. maja 2002: **Iztok Palčič,** delo z naslovom: "Upravljanje proizvodnje v večprojektnem okolju" in **Mihael Brunčko,** delo z naslovom: "Uporabnost metode meritve ohmske upornosti za spremljanje usmerjenega strjevanja";

dne 21. maja 2002: **Uroš Župerl**, delo z naslovom: "Analiza, napoved in optimiranje rezalnih veličin z nevronskimi mrežami" in **Mirko Ficko**, delo z naslovom: "Model oblikovanja prilagodljivih obdelovalnih sistemov z genetskimi algoritmi";

dne 31. maja 2002: **Simon Eržen**, delo z naslovom: "Konstruiranje bočnega ojačitvenega droga v vratih osebnega vozila z uporabo lahkih materialov"; **Primož Ternik**, delo z naslovom: "Modeliranje toka nenewtonskih disperznih sistemov" in **Dženana Bašić**, delo z naslovom: "Vrtinčne komore v sistemih za odvajanje onesnaženih voda pri velikih padcih".

S tem so navedeni kandidati dosegli akademsko stopnjo magistra tehničnih znanosti.

DIPLOMIRALI SO

Na Fakulteti za strojništvo Univerze v Ljubljani so pridobili naziv univerzitetni diplomirani inženir strojništva:

dne 30. maja 2002: Tomaž CURK, Aleš OBLAK;

dne 3. junija 2002: Janez BENEDIČIČ, Tomaž LEDINEK, Gregorij MRLJAK.

*

Na Fakulteti za strojništvo Univerze v Ljubljani so pridobili naziv diplomirani inženir strojništva:

dne 9. maja 2002: Roman CIGLAR, Robert RADOVAN, Boris SABO, Marko ŠKRJANC, Jurij ZAJC;

dne 10. maja 2002: Roman KOCI, Primož KRISTAN, Damijan MOČNIK, Roman SUŠNIK, Anica ŠKODA;

dne 13. maja 2002: Darko JAGODIC, Marjan KUSTERLE, Bruno KUZMIN, Sandi ROJC.

Na Fakulteti za strojništvo Univerze v Mariboru so pridobili naziv diplomirani inženir strojništva:

dne 30. maja 2002: Jernej ČOKL, Janez HOČEVAR, Marko KAPUN, Jožef KEREC, Boris KNEZ, Boris PUŠNIK, Robert ZOREC.

Navodila avtorjem
Instructions for Authors

Članki morajo vsebovati:
- naslov, povzetek, besedilo članka in podnaslove slik v slovenskem in angleškem jeziku,
- dvojezične preglednice in slike (diagrami, risbe ali fotografije),
- seznam literature in
- podatke o avtorjih.

Strojniški vestnik izhaja od leta 1992 v dveh jezikih, tj. v slovenščini in angleščini, zato je obvezen prevod v angleščino. Obe besedili morata biti strokovno in jezikovno med seboj usklajeni. Članki naj bodo kratki in naj obsegajo približno 8 tipkanih strani. Izjemoma so strokovni članki, na željo avtorja, lahko tudi samo v slovenščini, vsebovati pa morajo angleški povzetek.

Vsebina članka

Članek naj bo napisan v naslednji obliki:
- Naslov, ki primerno opisuje vsebino članka.
- Povzetek, ki naj bo skrajšana oblika članka in naj ne presega 250 besed. Povzetek mora vsebovati osnove, jedro in cilje raziskave, uporabljeno metodologijo dela,povzetek rezulatov in osnovne sklepe.
- Uvod, v katerem naj bo pregled novejšega stanja in zadostne informacije za razumevanje ter pregled rezultatov dela, predstavljenih v članku.
- Teorija.
- Eksperimentalni del, ki naj vsebuje podatke o postavitvi preskusa in metode, uporabljene pri pridobitvi rezultatov.
- Rezultati, ki naj bodo jasno prikazani, po potrebi v obliki slik in preglednic.
- Razprava, v kateri naj bodo prikazane povezave in posplošitve, uporabljene za pridobitev rezultatov. Prikazana naj bo tudi pomembnost rezultatov in primerjava s poprej objavljenimi deli. (Zaradi narave posameznih raziskav so lahko rezultati in razprava, za jasnost in preprostejše bralčevo razumevanje, združeni v eno poglavje.)
- Sklepi, v katerih naj bo prikazan en ali več sklepov, ki izhajajo iz rezultatov in razprave.
- Literatura, ki mora biti v besedilu oštevilčena zaporedno in označena z oglatimi oklepaji [1] ter na koncu članka zbrana v seznamu literature. Vse opombe naj bodo označene z uporabo dvignjene številke[1].

Oblika članka

Besedilo naj bo pisano na listih formata A4, z dvojnim presledkom med vrstami in s 3 cm širokim robom, da je dovolj prostora za popravke lektorjev. Najbolje je, da pripravite besedilo v urejevalnilku Microsoft Word. Hkrati dostavite odtis članka na papirju, vključno z vsemi slikami in preglednicami ter identično kopijo v elektronski obliki.

Prosimo, da ne uporabljate urejevalnika LaTeX, saj program, s katerim pripravljamo Strojniški vestnik, ne uporablja njegovega formata. V urejevalniku LaTeX oblikujte grafe, preglednice in enačbe in jih stiskajte na kakovostnem laserskem tiskalniku, da jih bomo lahko presneli.

Enačbe naj bodo v besedilu postavljene v ločene vrstice in na desnem robu označene s tekočo številko v okroglih oklepajih

Enote in okrajšave

V besedilu, preglednicah in slikah uporabljajte le standardne označbe in okrajšave SI. Simbole fizikalnih veličin v besedilu pišite poševno (kurzivno), (npr. *v, T, n* itn.). Simbole enot, ki sestojijo iz črk, pa pokončno (npr. ms^{-1}, K, min, mm itn.).

Vse okrajšave naj bodo, ko se prvič pojavijo, napisane v celoti v slovenskem jeziku, npr. časovno spremenljiva geometrija (ČSG).

Papers submitted for publication should comprise:
- Title, Abstract, Main Body of Text and Figure Captions in Slovene and English,
- Bilingual Tables and Figures (graphs, drawings or photographs),
- List of references and
- Information about the authors.

Since 1992, the Journal of Mechanical Engineering has been published bilingually, in Slovenian and English. The two texts must be compatible both in terms of technical content and language. Papers should be as short as possible and should on average comprise 8 typed pages. In exceptional cases, at the request of the authors, speciality papers may be written only in Slovene, but must include an English abstract.

The format of the paper

The paper should be written in the following format:
- A Title, which adequately describes the content of the paper.
- An Abstract, which should be viewed as a miniversion of the paper and should not exceed 250 words. The Abstract should state the principal objectives and the scope of the investigation, the methodology employed, summarize the results and state the principal conclusions.
- An Introduction, which should provide a review of recent literature and sufficient background information to allow the results of the paper to be understood and evaluated.
- A Theory
- An Experimental section, which should provide details of the experimental set-up and the methods used for obtaining the results.
- A Results section, which should clearly and concisely present the data using figures and tables where appropriate.
- A Discussion section, which should describe the relationships and generalisations shown by the results and discuss the significance of the results making comparisons with previously published work. (Because of the nature of some studies it may be appropriate to combine the Results and Discussion sections into a single section to improve the clarity and make it easier for the reader.)
- Conclusions, which should present one or more conclusions that have been drawn from the results and subsequent discussion.
- References, which must be numbered consecutively in the text using square brackets [1] and collected together in a reference list at the end of the paper. Any footnotes should be indicated by the use of a superscript[1].

The layout of the text

Texts should be written in A4 format, with double spacing and margins of 3 cm to provide editors with space to write in their corrections. Microsoft Word for Windows is the preferred format for submission. One hard copy, including all figures, tables and illustrations and an identical electronic version of the manuscript must be submitted simultaneously.

Please do not use a LaTeX text editor, since this is not compatible with the publishing procedure of the Journal of Mechanical Engineering. Graphs, tables and equations in LaTeX may be supplied in good quality hard-copy format, so that they can be copied for inclusion in the Journal.

Equations should be on a separate line in the main body of the text and marked on the right-hand side of the page with numbers in round brackets.

Units and abbreviations

Only standard SI symbols and abbreviations should be used in the text, tables and figures. Symbols for physical quantities in the text should be written in Italics (e.g. *v, T, n,* etc.). Symbols for units that consist of letters should be in plain text (e.g. ms^{-1}, K, min, mm, etc.).

All abbreviations should be spelt out in full on first appearance, e.g., variable time geometry (VTG).

Slike

Slike morajo biti zaporedno oštevilčene in označene, v besedilu in podnaslovu, kot sl. 1, sl. 2 itn. Posnete naj bodo v kateremkoli od razširjenih formatov, npr. BMP, JPG, GIF. Za pripravo diagramov in risb priporočamo CDR format (CorelDraw), saj so slike v njem vektorske in jih lahko pri končni obdelavi preprosto povečujemo ali pomanjšujemo.

Pri označevanju osi v diagramih, kadar je le mogoče, uporabite označbe veličin (npr. *t, v, m* itn.), da ni potrebno dvojezično označevanje. V diagramih z več krivuljami, mora biti vsaka krivulja označena. Pomen oznake mora biti pojasnjen v podnapisu slike.

Vse označbe na slikah morajo biti dvojezične.

Za vse slike po fotografskih posnetkih je treba priložiti izvirne fotografije ali kakovostno narejen posnetek. V izjemnih primerih so lahko slike tudi barvne.

Preglednice

Preglednice morajo biti zaporedno oštevilčene in označene, v besedilu in podnaslovu, kot preglednica 1, preglednica 2 itn. V preglednicah ne uporabljajte izpisanih imen veličin, ampak samo ustrezne simbole, da se izognemo dvojezični podvojitvi imen. K fizikalnim veličinam, npr. *t* (pisano poševno), pripišite enote (pisano pokončno) v novo vrsto brez oklepajev.

Vsi podnaslovi preglednic morajo biti dvojezični.

Seznam literature

Vsa literatura mora biti navedena v seznamu na koncu članka v prikazani obliki po vrsti za revije, zbornike in knjige:

[1] Tarng, Y.S., Y.S. Wang (1994) A new adaptive controler for constant turning force. *Int J Adv Manuf Technol* 9(1994) London, pp. 211-216.

[2] Čuš, F., J. Balič (1996) Rationale Gestaltung der organisatorischen Abläufe im Werkzeugwesen. *Proceedings of International Conference on Computer Integration Manufacturing,* Zakopane, 14.-17. maj 1996.

[3] Oertli, P.C. (1977) Praktische Wirtschaftskybernetik. *Carl Hanser Verlag,* München.

Podatki o avtorjih

Članku priložite tudi podatke o avtorjih: imena, nazive, popolne poštne naslove, številke telefona in faksa ter naslove elektronske pošte.

Sprejem člankov in avtorske pravice

Uredništvo Strojniškega vestnika si pridržuje pravico do odločanja o sprejemu članka za objavo, strokovno oceno recenzentov in morebitnem predlogu za krajšanje ali izpopolnitev ter terminološke in jezikovne korekture.

Avtor mora predložiti pisno izjavo, da je besedilo njegovo izvirno delo in ni bilo v dani obliki še nikjer objavljeno. Z objavo preidejo avtorske pravice na Strojniški vestnik. Pri morebitnih kasnejših objavah mora biti SV naveden kot vir.

Rokopisi člankov ostanejo v arhivu SV.

Vsa nadaljnja pojasnila daje:

Uredništvo
STROJNIŠKEGA VESTNIKA
p.p. 197/IV
1001 Ljubljana
Telefon: (01) 4771-757
Telefaks: (01) 2518-567
E-mail: strojniski.vestnik@fs.uni-lj.si

Figures

Figures must be cited in consecutive numerical order in the text and referred to in both the text and the caption as Fig. 1, Fig. 2, etc. Figures may be saved in any common format, e.g. BMP, GIF, JPG. However, the use of CDR format (CorelDraw) is recommended for graphs and line drawings, since vector images can be easily reduced or enlarged during final processing of the paper.

When labelling axes, physical quantities, e.g. *t, v, m,* etc. should be used whenever possible to minimise the need to label the axes in two languages. Multi-curve graphs should have individual curves marked with a symbol, the meaning of the symbol should be explained in the figure caption.

All figure captions must be bilingual.

Good quality black-and-white photographs or scanned images should be supplied for illustrations. In certain circumstances, colour figures may be considered.

Tables

Tables must be cited in consecutive numerical order in the text and referred to in both the text and the caption as Table 1, Table 2, etc. The use of names for quantities in tables should be avoided if possible: corresponding symbols are preferred to minimise the need to use both Slovenian and English names. In addition to the physical quantity, e.g. *t* (in Italics), units (normal text), should be added in new line without brackets.

All table captions must be bilingual.

The list of references

References should be collected at the end of the paper in the following styles for journals, proceedings and books, respectively:

[1] Tarng, Y.S., Y.S. Wang (1994) A new adaptive controler for constant turning force. *Int J Adv Manuf Technol* 9(1994) London, pp. 211-216.

[2] Čuš, F., J. Balič (1996) Rationale Gestaltung der organisatorischen Abläufe im Werkzeugwesen. *Proceedings of International Conference on Computer Integration Manufacturing,* Zakopane, 14.-17. maj 1996.

[3] Oertli, P.C. (1977) Praktische Wirtschaftskybernetik. *Carl Hanser Verlag,* München.

Author information

The following information about the authors should be enclosed with the paper: names, complete postal addresses, telephone and fax numbers and E-mail addresses.

Acceptance of papers and copyright

The Editorial Committee of the Journal of Mechanical Engineering reserves the right to decide whether a paper is acceptable for publication, obtain professional reviews for submitted papers, and if necessary, require changes to the content, length or language.

Authors must also enclose a written statement that the paper is original unpublished work, and not under consideration for publication elsewhere. On publication, copyright for the paper shall pass to the Journal of Mechanical Engineering. The JME must be stated as a source in all later publications.

Papers will be kept in the archives of the JME.

You can obtain further information from:

Editorial Board of the
JOURNAL OF MECHANICAL ENGINEERING
P.O.Box 197/IV
1001 Ljubljana, Slovenia
Telephone: +386 (0)1 4771-757
Fax: +386 (0)1 2518-567
E-mail: strojniski.vestnik@fs.uni-lj.si